ABSTRACT

Title of dissertation:     A MICROSCOPIC MODEL FOR
                          QUANTUM OPTOMECHANICS

                          Kanupriya Sinha, Doctor of Philosophy, 2015

Dissertation directed by:  Professor Bei-Lok Hu
                          Department of Physics

We study a microscopic model, the Mirror-Oscillator-Field (MOF) model pro-
posed in [1], for describing optomechanical interactions. In contrast with the con-
ventional approach where the mirror-field interaction is understood as arising from
the radiation pressure of an optical field inducing the motion of the mirror's CoM,
the MOF model incorporates the dynamics of the internal degrees of freedom of the
mirror that couple to the optical field directly. Considering the mirror's internal
and mechanical degrees of freedom as two separate degrees of freedom we derive
the optomechanical properties of the coupled mirror and field system. The major
advantage in this approach is that it provides a self-consistent treatment of the
three relevant subsystems (the mirror's motion, its internal degrees of freedom and
the field) including their back-actions on each other, thereby giving a more accu-
rate account of the coupled internal and external dynamics. The optical and the
mechanical properties of a mirror arising from its dynamical interaction with the
field are obtained without imposing any boundary conditions on the field addition-
ally, as is done in the conventional way. We find that our results agree with those

from the boundary condition approach in the appropriate limits and more generally the model provides a framework within which one can study optomechanical elements with different internal structures and mechanical properties, which makes it suited for studying hybrid systems. Considering the quantum dynamics of the coupled subsystems we look at the entanglement between the mirror's motion and the field, showing that the internal degrees of the mirror, in the appropriate parameter regimes, can act as a means to coherently transfer quantum correlations between the field and the mechanics thus leading to a larger optomechanical entanglement. We then use the MOF model to study the entanglement between the motion of an atom and a field for the setup in [95] and find a larger optomechanical entanglement when the field is closer to the internal resonance. We also study the interaction between two mirrors as described by the MOF model, specifically looking at the entanglement between the motion of their centers of mass.

Conclusively, we see that including the dynamics of the internal degrees of freedom of a mirror, which is the quintessential mediator of interaction between the mirror center of mass and the field, leads to qualitatively different physics, specifically in the quantum regime, thus giving a physically more complete treatment of mirror-field interactions.

# A MICROSCOPIC MODEL FOR
# QUANTUM OPTOMECHANICS

by

Kanupriya Sinha

Dissertation submitted to the Faculty of the Graduate School of the
University of Maryland, College Park in partial fulfillment
of the requirements for the degree of
Doctor of Philosophy
2015

Advisory Committee:
Professor Bei-Lok Hu, Chair/Advisor
Professor Luis Orozco
Professor Steven L. Rolston
Professor Eite Tiesinga
Professor Christopher Jarzynski

# Dedication

To *Amma ji Gaai*, my beloved mother,

hoping this thesis will inspire her 'Quantum Poetry'

# Acknowledgments

First and foremost, I would like to express my deepest gratitude towards my advisor, Prof. Bei-Lok Hu, for being the truly exceptional guide that he is. I thank him for all the values that he inspires, always motivating one to probe deeper and to reach into the internal degrees of freedom at the heart of any issue. I am forever grateful to him for giving me this beautiful problem to study that has come to burgeon into this thesis, for guiding me through the course of the work in truly inspirational ways, and for teaching me to think in terms of the underlying physical issues. I thank him for his patience and kindness beyond all boundary conditions, throughout the past seven years.

Many thanks to Prof. K. Thyagarajan, my undergraduate advisor, for his exemplary teaching that combined rigor and wonder in perfect proportions, which fascinated me beyond repair into pursuing physics. I thank him for his time and patience to answer my incessant stupid questions post every lecture (specially considering the fact that I took five courses with him), and for guiding me through my undergraduate thesis on quantum properties of four wave mixing.

My grad school experience has been exceedingly enriched in all aspects thanks to Yiğit Subaşı, a wonderful friend, an inspiring physicist and the go-to help-desk person for all problems ranging from fixing the calculation at hand to organizing my 'Ideas folder'. While Yiğit's many thorough cross-examinations of my sloppy calculations have meant that I had to do the whole thing all over again, I remain eternally grateful for his knack of bursting my scientific bubble, all the insightful

of toy models. I also thank Darrick and Prof. H. J. Kimble for ever so graciously hosting my visits at Caltech and ICFO.

I thank my committee members Prof. Luis Orozco, Prof. Steve Rolston, Prof. Eite Tiesinga and Prof. Chris Jarzynski, for taking the time to be on my thesis committee and for their very thorough and thoughtful reading of this thesis.

I would like to say 'some wonderful things' to express my gratitude towards my phenomenal roommates and friends, the fellow residents of the International House of Physicists (IHoP), who have been an endless source of inspiration, fun, food, caffeine, and emergency physics discussions. Thanks galore to Juraj, Dalia, Paco, Ana, Marko, Prateek, Kevin, Wrick and Jupe. Many thanks to Sid, my roommate and butler-in-chief for the past year, for his gourmet cooking that fueled much of this work. I would also like to thank Aastha, Rahul and Kaushik for their invaluable friendships.

Finally, an insurmountable deal of gratitude to my family for their unconditional love and unwavering support, sans any fluctuations and dissipation, for their dedication towards my education, and most of all for putting up with my obstinacy all these years.

# Contents

List of Tables

# List of Figures

# Chapter 1: Introduction

Optomechanics describes the interaction of light with mechanical systems. Historically, the concept that light can exert a mechanical force dates back to Johannes Kepler in 1619, when he put forward the concept of radiation pressure in order to explain the tails of comets pointing away from the sun. To quote Kepler [2] –

*"The direct rays of the Sun strike upon it [the comet], draw away with them a portion of this matter, and issue thence to form the track of light we call the tail. In this manner the comet is consumed by breathing out, so to speak, its own tail."*

Since Kepler the cometary dust has evolved into a diverse assortment of optomechanical systems – ranging from the massive kg scale mirrors at the Laser Interferometer Gravitational-Wave Observatory (LIGO), down to single atoms and ions – upon which much light has been shed.

The first theoretical formulation of the mechanical effects of radiation was due to Maxwell in 1862. Maxwell predicted that all electromagnetic waves carry momentum and when reflected off of a surface exert a mechanical force on the surface that goes as $\sim IA/c$, with $I$ being the intensity of radiation and $A$ being the surface area. The experimental demonstrations of the effect by Nichols and Hull [3] and independently by Lebedew [4] in 1901, for the first time confirmed Maxwell's

predictions. Given that the radiation pressure forces are typically very small, these experiments, quite challenging for their time, were able to delineate the pressure from radiation from that exerted by the thermal gases in the radiometer setup. To get some idea of the magnitude of the radiation pressure force one can estimate that the solar radiation pressure on earth is about $10\mu$Pa, which is roughly about the pressure exerted by a housefly sitting on an elephant. It is this smallness of the radiation pressure forces that makes optical cavities much befitting candidate systems to study optomechanical phenomena, since a cavity allows the light intensity to build up by a factor of the number of round trips a single photon makes before leaking out. Thus, rightfully, cavity optomechanics has garnered a lot of interest over the past few decades.

The first studies in cavity optomechanics can be attributed to Braginsky and others in the late 1960s. Working with microwave Fabry-Perot cavities, they showed that the dynamical backaction of the radiation pressure on the suspended end-mirror of the cavity can experience a(n) (anti-)damping force depending on the detuning of the resonator [5,6]. Later these studies led to the prediction of the standard quantum limit (SQL) [7] and paved way for the design of interferometers for gravitational-wave detection [8,9]. The first demonstration of cavity-optomechanical effects in the optical domain was by Dorsel *et al* [10], wherein they showed a radiation pressure induced optical bistability in the transmission of a Fabry-Perot interferometer.

At a somewhat disparate end of the parameter regime, in 1970 Arthur Ashkin used radiation forces to trap micron-sized dielectric spheres, later proposing the idea for laser cooling of atoms in 1978 [11, 12]. In 1975, Hansch and Schawlow [13],

and Wineland and Dehmelt [14] independently proposed the idea of using the non-conservative nature of radiation forces to cool atoms. The ability to cool and trap single particles at the atomic scale has since led to tremendous advances in atomic, molecular and optical (AMO) physics, making the quantum regime readily accessible to the (small enough) masses.

Meanwhile for the larger masses, there have been significant experimental developments in the field of cavity quantum optomechanics over the last decade that have allowed us to bring to reality the gedankenexperiments of the early 20th century and more. To give a sense of the accomplishments of the field, the experiments today can access ground states of macroscopic mechanical oscillators [15, 16], achieve quantum-coherent coupling between a mechanical oscillator and an optical field mode [21], observe squeezing of the optical field via non-linear interaction with mechanical motion [22, 23], exhibit quantum coherent state transfer in micro- and electro-mechanical systems [15, 24], entangle microwaves with a micro-mechanical oscillator [25] and much recently squeeze the motion of a mechanical oscillator [26], among other astounding feats. Indeed the incredible experimental progress has been made possible both due to innovative theoretical proposals and ingeniously designed optomechanical setups ranging from Fabry-Perot cavities that come in a variety of sizes [27]– [32], to photonic crystals [16, 33, 34], microtoroidal resonators [35]– [41], superconducting microwave circuits [42]– [44], levitated nanospheres, to cold atoms [45]– [52]. As a thorough account of all the developments is beyond the scope of this thesis, we point the reader to some of the review articles written on the subject [17–20]. However, as the experimental setups have grown to span a vast range

of mass and length scales, we remark that the existing theoretical models fall short in accessing the potential physical effects realizable with these systems. We discuss these limitations and motivate the need for a microscopic theory for optomechanics further in the following section.

## 1.1   Motivation for a Microscopic model for Optomechanics

When an optical field interacts with a mechanical object there is a redistribution of the photon momentum upon reflection. At the microscopic level this interaction results from the coupling of the EM field with the surface charges or the internal degrees of freedom of the mechanical object, such as the electrons in an atom. For instance, take a simplistic case from classical electromagnetism wherein a field incident on a perfect conductor induces surface charge currents on the surface of a mirror, which in turn experience a Lorentz force in the presence of the magnetic field. This Lorentz force is the radiation pressure force on the mirror center of mass (CoM). Upon time-averaging, it can be equivalently expressed in terms of photon momentum imparted by the field on the mirror, thereby leading to the semi-classical picture of radiation pressure as the transfer of momentum from the photons to the mechanical element in consideration. While for a perfect conductor the response of these surface charges to the applied field is instantaneous, more generally, the internal degrees of freedom respond with a lag, which can be accounted for via the reflection and transmission coefficients of the optomechanical element in consideration. However, allowing for the CoM to move, as the retarded response

4

of its internal degrees gets convoluted with the mirror's CoM motion one can no longer use the reflection and transmission coefficients as an exact description for the coupled optical and mechanical dynamics of the mirror. This necessitates an explicit inclusion of the mirror's internal dynamics. In the following we list a few issues that help illustrate the relevance of including the internal degrees of freedom of a mirror –

*Time scale issues* – It can be seen that as the center of mass moves, the surface charges observe a Doppler shifted field and respond according to their velocity dependent reflection properties, an effect that is typically not accounted for. Specially as one probes closer to an internal resonance of the mirror, the retardation effect becomes more pronounced and hence there is an increased discrepancy between the boundary condition approach and what one would find from a proper account of the coupled internal and external dynamics of the mirror. In other words, with the slow internal dynamics being comparable to the timescales of the mirror motion one can no longer adiabatically eliminate the internal degrees of freedom and use the effective reflection and transmission coefficients to describe the dynamics of the system. Still, the conventional approach towards studying optomechanical interactions only considers the effective boundary conditions for the optical field at the position of the mirror's CoM that arise from the microscopic picture in the limit where the internal dynamics has reached a steady-state. This implicitly assumes that the internal degrees of the mirror are strongly damped, which is typically a valid assumption for most of the optomechanical systems. However, for systems that have well-isolated internal degrees of freedom this condition no longer holds

true, rendering the boundary condition approach as inaccurate.

*Novel "mirrors"* – While the role of these internal degrees of freedom is universally acknowledged in the case of atom-field interactions when describing the mechanical effects of a field on an atom [53, 54], their relevance in determining the optomechanical properties of larger systems is seldom discussed. Among the limited examples, it has been shown in some recent works that the internal degrees of freedom of a mirror can play a decisive role when it comes to optomechanical cooling in a variety of physical setups ranging from photonic crystals wherein the strong frequency dependence of the reflectivity coming from the internal structure of the mirror can allow for efficient Doppler cooling [55], to semiconductor nano-membranes where the intrinsic bandgap of the semiconductor can lead to an innovative photothermal cooling mechanism [56]– [58]. One can see that the Doppler effect would become prominent for the case of photonic crystals – or for that matter any "mirror" with a sharp internal resonance – since the internal degrees of a moving mirror observe a different field frequency than that in the laboratory frame. As a consequence they exhibit a velocity dependent reflectivity which in turn leads to a Doppler friction force. Such a force becomes particularly strong near the photonic band gaps of a photonic crystal. Similarly, for the case of semiconductor membranes, one can leverage the fact that the internal degrees of the mirror are coupled to a bath that can be at a lower temperature than the mechanical bath, thus an appropriate coupling of the mechanics to the internal dynamics could potentially lead to an improved cooling limit. These are just a few examples that demonstrate how the internal structure of an optomechanical element can be used to develop new

schemes for the purposes of optomechanical cooling.

*Quantum correlations and entanglement* – To systematically account for all the quantum correlations between the individual subsystems, for example the quantum entanglement between the mirror and the field [17]– [64], one needs to take into consideration the full quantum nature of the macroscopic object including the dynamics of its quantal internal degrees of freedom. Such a treatment becomes one of a practical necessity when studying the optomechanical entanglement for well-isolated systems whose internal degrees preserve coherences for longer time scales, for example when considering the quantum entanglement between the motion of atoms or atomic ensembles and a field. Furthermore, acounting for the quantum fluctuations of the internal degree of freedom one can properly describe all three-body processes involving the field, the internal degree of freedom and the center of mass motion, such as, say, an internal excitation splitting into a field photon and a mirror phonon. This is similar to the case of an external field driving the blue-detuned mechanical sideband of the cavity resonance in a typical cavity optomechanical setup [17]. In the resolved sideband limit, the radiation pressure coupling between the drive, cavity mode and the mirror motion leads to a process where a blue-detuned drive photon splits into a cavity photon and a mirror phonon thereby entangling the cavity mode and the mirror motion [63]. We elaborate on this issue further in chapter 2. More generally, we remark that one can draw an analogy with the usual concepts from cavity optomechanics, likening the cavity resonance to the internal resonance of the mirror itself and use the intuition from the existing cavity optomechanical schemes as a guide to illustrate new effects coming from the internal structure of the mirror.

*Hybrid systems* – It is well-established that for a single atom as an optomechanical element whose internal degrees of freedom are represented by a two level system the interaction between the field and the atom's two-level internal degree of freedom via photon emission and absorption is much stronger than the effective interaction of the field with the atom's center of mass degree of freedom. The coupling between the optical field and atomic motion arises as the CoM motion alters the field configuration, thereby affecting the atom's internal level activities. Thus when dealing with the case of atoms as an optomechanical element [45]– [52], one needs to regard its internal level dynamics with careful consideration, including the effects of the polarization and spatial structure of the field. Similarly, it has also been shown that the atom's motional degree of freedom can affect the activities of its internal degrees of freedom such as spontaneous emission or motional decoherence as in [76, 77]. While this might be an unarguable example of the relevance of the internal degrees of freedom, one needs to clearly identify in what parameter regimes and for what systems would the internal degrees play a role, and if they do what new physics can be gleaned from their participation in the coupled optical and mechanical dynamics of the optomechanical element. For this reason, we point out the inadequacy in the studies of mirror-field interactions which generically rely upon the effective interaction between the mirror's CoM and the field that obscures the full spectrum of physical effects one can potentially realize with optomechanical systems. For example, when considering the optomechanics of atoms one typically assumes that the field is far off-resonant with respect to the internal atomic resonance, and one can therefore adiabatically eliminate the internal electronic degrees

of freedom from the dynamics to arrive at an effective intensity-position coupling between the field and the atomic CoM motion. We remark that the studies on atom-optomechanics based on this assumption are restrictive in terms of accessing the physical effects in the regime where one probes closer to the atomic resonance, or in other words, one misses out on the scattering component of the total radiation forces while only accounting for the dispersive part [53].

*Quantum-Classical interface* – Moreover, with a microscopic model one can have a general theoretical framework within which one can study the optomechanics of atomic scale systems and larger mechanical oscillators on the same footing. This has also been emphasized in some previous works [70–72] that develop a scattering theory approach towards optomechanics including the backreaction of the optomechanical element on the field self-consistently, an effect typically neglected for the case of atoms. It was shown that such a self-consistent backreaction can lead to a variety of interesting physical effects such as modifications to the optical forces and cooling limit [70,71], access to strong single photon-mirror optomechanical coupling and collective long-ranged interactions in an array of atomic mirrors [72]. Generally for the case of atoms the theories rely on the assumption that atoms are weak scatterers of the field while larger optomechanical systems, on the other hand, affect the field strongly by providing a moving boundary condition. A general theory which can deal with both the cases as two extremes both in terms of including the backreaction effects and the participation of the internal degrees of freedom is still needed, as it would not only provide a more complete theoretical understanding but can potentially also guide one to new physical effects yet to be accessed. Specially given

the vast expanse of the existing optomechanics experiments in terms of parameter regimes from the scale of LIGO down to single atoms and the burgeoning efforts towards realizing and developing an understanding of hybrid quantum systems, a theoretical treatment that can deal with a wide range of setups becomes all the more necessary. A related benefit of using a microscopic model could be to use a "bottom up" approach towards understanding macroscopic quantum phenomena.

*Multimode effects* – Furthermore, one of the ubiquitous assumptions of cavity optomechanics is that of a single mode field, which assumes that the photons would stay in the same cavity mode throughout the system evolution, or equivalently that the mirror never moves fast enough to cause a transition between the different modes of the cavity. However, for non-adiabatic motion of the mirror, one can indeed cause the different modes of the cavity to couple with each other, which demands that one takes into account the multimode nature of the field. One can estimate that this would happen when the cavity mirror oscillates close to the frequency spacing between two adjacent cavity modes, surely enough such a resonant oscillation of the cavity mirror can be used for experimentally relevant purposes such as making a high sensitivity optomechanical displacement transducer [73]. Additionally, for relativistically moving mirrors wherein one might want to study effects such as dynamical Casimir effect, including the multimode vacuum field is inevitable. Not only that, one can also surmise that for fast motion of the mirror's CoM the retardation effects in the response of the internal degrees would become significant, an effect that has not yet been studied in the literature.

Thus, given the incompleteness of the existing theoretical treatments, a micro-

scopic model for optomechanical interactions that can desirably provide a general framework for optomechanical systems over a wide parameter range is much needed, both in terms of furthering the existing theoretical understanding and to better guide the ongoing experimental efforts. We discuss these models in the following section.

## 1.2   Microscopic Models for Optomechanics

In [1], Galley, Behunin and Hu proposed a microscopic model for mirror-field interactions, called the mirror-oscillator-field (MOF) model that takes into account the internal dynamics of the mirror, providing a physically more complete theory for quantum optomechanics (QOM). The mirror as an *optomechanical* element is described as a composite of two separate degrees of freedom corresponding to its center of mass motion (mechanics) and the surface charge that couples with the field (optics). We henceforth refer to these two degrees of freedom as the mechanical degree of freedom (*mdf*) and the internal degree of freedom (*idf*) respectively. The *idf* and the *mdf* are each depicted by a quantum oscillator, with the *idf* coupled to an optical field that is modeled in [1] by a massless scalar field. The *idf* is what provides the indirect interaction between the field and the mirror's CoM motion, with its amplitude taking on field values at the position of the CoM. Compared to the traditional approach where the effect of the mirror on the field is represented by imposing boundary conditions on the field at the position of the mirror, the MOF model captures the mirror-field interaction in a more physically consistent way as both the internal and mechanical degrees of freedom of the mirror enter in determin-

ing the dynamics self-consistently. In [1], it was shown that the different parameters of the *idf* can describe a range of optical activities, from broadband to narrow band reflectivity. With specific parameter choices the authors in [1] made connections to well-known optomechanical models including those of Barton & Calogeracos [67], Law [68] and Golestanian & Kardar [69]. Specifically, drawing a correspondence to the "jellium-type" model for a moving mirror in [67], it can be shown that the model in [1] in appropriate physically motivated parameter regimes mimics the Drude-Lorentz response of bulk metals well. We discuss this correspondence in the optical response in detail in section 1.4.2.

Recently, another mirror-model that invokes the internal degrees of the mirror was also proposed by Wang and Unruh [80], wherein they model the internal degrees of the mirror by a harmonic oscillator that interacts with a massless scalar field. As emphasized in their work, including the coupling of the internal degrees to the field explicitly allows one to describe the optical properties of the mirror self-consistently without having to introduce high-frequency cut-offs artificially, as is often done in perfect-reflector models [83, 91] or other approaches using boundary conditions [81, 82]. Though in their description, the CoM motion is described by a prescribed trajectory rather than being determined self-consistently, unlike the MOF model where the mirror CoM motion is treated as a dynamical variable.

In a similar vein, the advantages of a microscopic model over the usual practice of imposing boundary conditions and the role of the *idf* in capturing additional physical phenomena is further expounded in this work. The model that we study is a modification of the original MOF model in terms of the form of *idf*-field coupling.

12

We use a coupling motivated by the electrodynamic form of interaction considering that we can potentially use our model to study the optomechanics of atomic systems. We then use our rendition of the MOF model to study the quantum entanglement between the mechanical motion of the mirror and the field (2) and that between two mirrors (4).

The motivation for looking at the mirror-field entanglement from a microscopic perspective comes from the fact that the internal degrees of freedom are the vital connection between the field and the CoM motion and including their quantum fluctuations as a separate degree of freedom can be quite relevant in certain parameter regimes. Given that the conventional mechanism of mirror-field entanglement is by means of the effective radiation pressure coupling and there is virtually no consideration of how the mirror's internal structure that gives rise to its optical properties affects the entanglement of its external or mechanical degree of freedom with the field, such an analysis becomes crucial. Even though the full description of this interaction at the microscopic level is quite complex, to gain a qualitative understanding of the coupled interplay of the optical and mechanical degrees of freedom the present relatively simple MOF model can serve the purpose aptly and economically. As we shall see in this work, in some parameter regimes the dynamics of a mirror's *idf* play a nontrivial and even a decisive role in determining the transfer of correlations and hence the entanglement between the *mdf* and the quantum field. As for considering the entanglement between two mechanical oscillators from a microscopic perspective one can think of this as a simplistic toy model to probe into macroscopic quantum phenomena. Since while the presence of entanglement in

13

the quantum world is well-established, its existence in the macroscopic domain still remains to be observed, or its absence concretely understood.

In section 2.3.1, we generalize our model to 3+1 D and apply it to the case of a single atom interacting with a field to study the entanglement between the motion of the atom and the field, using the specifics from the setup of Maunz *et al* [95]. In section 4.1.3, we use the MOF model to look at the motional entanglement between two atoms. While we note that the internal electronic degrees of the atom are not well-described by a harmonic oscillator, in the regime where the atom is very weakly excited, our model should work well for the purposes of a rough estimate.

In the following section we present the MOF model, followed by a description of the classical mechanical and optical properties of the MOF model in 1.4. 1.5 treats the quantum dynamics of the three interlinked subsystems – the *idf*, the *mdf* and the field – which leads to all the interesting physical phenomena in QOM. In particular we show that the usual radiation pressure coupling is recovered as an approximation of the MOF model but one can go beyond these approximations to see new physical effects. The role played by the internal degree of freedom of the mirror is highlighted throughout our analysis.

## 1.3   The Mirror-Oscillator-Field (MOF) Model

Let us consider a point mirror interacting with a massless scalar field in (1+1)-dimensional space-time, the mirror is described by the two independent degrees of freedom - the *mdf* that has a mass $M$ and is suspended in a harmonic potential of

frequency $\mho$ in addition to the *idf* described by another harmonic oscillator of mass $m$ and frequency $\Omega$, as shown in Fig.1.1.
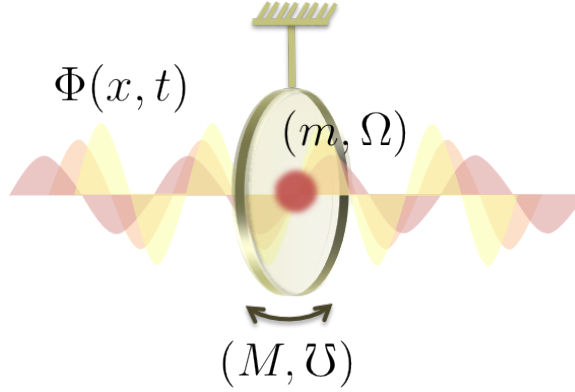


Figure 1.1: Schematic representation of the interaction of a mirror with a field via its internal degree of freedom

While the *mdf* does not interact with the field itself, the *idf* is bilinearly coupled to the quantum field and constrained to be at the center of mass position leading to an effective interaction between the field and the *mdf*, what we observe as the radiation pressure. The *idf*-field interaction determines all the optical properties of the mirror as has also been studied in [1]. We assume that the *idf*-field dynamics that represent the electronic excitations for the case of an atom happen at much faster time scales compared to those of the mechanical motion of the atomic center of mass, such that $\Omega \gg \mho$.

For a non-relativistically moving mirror[1] in the MOF model, the action is

---

[1] For relativistic motion which is required for the treatment of acceleration radiation such as the Unruh effect, one needs to use the proper time, modify the kinetic terms, and take care of the time-slicing scheme. Then the model will become a generalization of the Unruh-DeWitt detector theory [78, 79].

given by

$$S = \int \mathrm{d}t \left[ \left( \frac{1}{2} M \dot{Z}^2 - \frac{1}{2} M \mho^2 Z^2 \right) + \left( \frac{1}{2} m \dot{q}^2 - \frac{1}{2} m \Omega^2 q^2 \right) \right.$$
$$\left. + \int \mathrm{d}x \frac{\epsilon_0}{2} \left\{ (\partial_t \Phi)^2 - c^2 (\partial_x \Phi)^2 + \lambda \dot{q} \Phi \delta(x - Z) \right\} \right] \qquad (1.1)$$

where we denote the center of mass position of the *mdf* by $Z(t)$, the amplitude of

the *idf* by $q(t)$ and the scalar field by $\Phi(x, t)$. We note that $\lambda$ represents the coupling

strength between the field and the *idf*, $\epsilon_0$ stands for the vacuum permittivity and $c$

for the speed of light. In drawing a correspondence between the scalar field and an

electromagnetic field, we observe that the free field Lagrangian would correspond

to that of an EM field if we choose $\Phi(x, t)$ to represent the vector potential $A$. We

have chosen a form of the bilinear coupling motivated by the electrodynamic form

of interaction $\left( \sim \frac{e}{m} p \cdot A \right)$, bearing in mind that the mirror's *idf* can potentially rep-

resent the electronic level structure inside an atom. We note that this is different

from the form of coupling in the original MOF model [1] $(\sim \lambda q \Phi)$. In 1+1 D, a

derivative coupling $(\dot{q} \Phi)$ leads to a radiation reaction force that goes as $\sim \dot{q}$ instead

of $\sim \dddot{q}$, also the derivative coupling ensures that the energy of the system remains

a positive-definite quantity [66]. A similar model for describing mirror-field interac-

tions has also been studied recently in [80]. Noticing that the free space permittivity

in (1+1)-dimensions scales as $\epsilon_0 \sim (\mathrm{Charge})^2 (\mathrm{Time})^2 (\mathrm{Mass})^{-1} (\mathrm{Length})^{-1}$, the free

field Lagrangian in [1] has been rescaled here by a factor of $\epsilon_0$ for dimensional con-

sistency. The $\delta(x - Z)$ factor in the coupling restricts the *idf*-field interaction to

the center of mass position and the position dependence of the scalar field in turn

leads to an effective force on the *mdf*. We choose the coupling $\lambda$ to have the dimen-

16

sions of the electronic charge $e$ and $\Phi(x,t)$ to have the dimensions of $A$. This is in agreement with the correspondence of the MOF model with the Barton-Calogeracos (BC) model [67], where in the limit of adiabatic *idf* evolution the coupling $\lambda$ can be physically identified as the surface charge density.

## 1.4   Classical Optomechanical properties

In this section we will illustrate how the MOF model can describe the classical optical and mechanical properties exhibited by a mirror, leading to the known intensity-position radiation pressure coupling. We begin with deriving the coupled equations of motion for the classical amplitudes of the *mdf*, *idf* and field ($\{\bar{Z}, \dot{\bar{Z}}, \bar{q}, \dot{\bar{q}}, \bar{\Phi}, \dot{\bar{\Phi}}\}$ respectively) from the action in (1.1) ($\delta S = 0$)

$$\ddot{\bar{Z}} + \mho^2 \bar{Z} = \frac{\lambda \dot{\bar{q}}}{M} \partial_x \bar{\Phi}\left(\bar{Z}, t\right) \tag{1.2}$$

$$\ddot{\bar{q}} + \Omega^2 \bar{q} = -\frac{\lambda}{m} \dot{\bar{\Phi}}\left(\bar{Z}, t\right) \tag{1.3}$$

$$\epsilon_0 \left(\ddot{\bar{\Phi}}\left(x, t\right) - c^2 \partial_x^2 \bar{\Phi}\left(x, t\right)\right) = \lambda \dot{\bar{q}} \delta(x - \bar{Z}) \tag{1.4}$$

It can be seen that the moving *idf* acts as a point source for the field and the *idf* is in turn driven by $\dot{\Phi}$ at the center of mass position $\bar{Z}$, which in the electromagnetic correspondence represents the electric field at the CoM position $\left(\dot{\Phi} \sim E\right)$. Also, with $\lambda$ representing the charge density, it can be seen from (1.3) that the force on the surface charge degree of freedom goes as $\sim \lambda \dot{\bar{\Phi}}$. We have assumed here that the mirror center of mass velocity is in the non-relativistic limit, such that $\left|\frac{\mathrm{d}\bar{Z}}{\mathrm{d}t}\right| \ll c$. For a relativistically moving mirror, the *idf* would more generally observe a Doppler

shift of the field with respect to the moving center of mass as (1.3) becomes

$$\ddot{\bar{q}} + \Omega^2 \bar{q} = -\frac{\lambda}{mc} \left( \dot{\bar{Z}}^0 \partial_t + \dot{\bar{Z}}^1 \partial_x \right) \bar{\Phi}(\bar{Z}^\mu) \tag{1.5}$$

where $\bar{Z}^\mu = (\bar{Z}^0(\tau), \bar{Z}^1(\tau))$ is the worldline of the mirror parametrized by its proper time $\tau$, and $\dot{O} \equiv dO/d\tau$. As the motion of the mirror center of mass leads to the motion of the charges sitting on the surface that interact with the field, the surface charges experience a Doppler shifted field which in turn changes their optical response leading to dynamically changing boundary conditions observed by the field.

If one prefers to think in terms of applying boundary conditions on the field, in the MOF model it would correspond to the steady state response of the internal degree of freedom. Thus our model captures the full coupled dynamical interplay as opposed to the fixed boundary conditions in the conventional approach. In fact, a simple generalization of the set up here can deal with a relativistically moving mirror as in the dynamical Casimir effect (DCE), whereas the conventional method of imposing a boundary condition on the field would fail to address dynamical situations wherein the time scales of the mechanical motion are comparable those of *idf*-field interaction dynamics. In such situations one would expect that accounting for the coupled dynamics of the internal and external degrees of freedom would lead to an appreciable correction. [2]

For now, we restrict our attention to a non-relativistically moving mirror. For the case where the system dynamics is driven by an incident field (and not by any

---

[2]This is an important point long explored and resolved in cosmological particle creation which results from the same mechanism but with the expanding universe playing the role of an external agent as in DCE.

external agent which accelerates the mirror as is in the setup of the Unruh effect), this is ensured from the separation of the timescales for the internal and center of mass degrees of freedom ($\Omega \gg \mho$). We will demonstrate this further in Section 1.4.2 for the case of a single mode field.

Knowing the coupled system dynamics, below we first look at how the radiation pressure force arises from our model in the non-relativistic limit.

### 1.4.1 Classical Radiation Pressure Force

As seen from (1.2), the *mdf* is driven non-linearly by both the *idf* and the field. We now eliminate the *idf* from the picture to obtain the mechanical force on the center of mass.

From spatially integrating the field equation of motion (1.4) around the mirror center of mass position $\bar{Z}$, we see that there is a discontinuity in the field spatial derivative. This can be understood as the discontinuity in the magnetic field across the mirror surface in the electromagnetic correspondence ($\partial_x \Phi \sim B$) coming from the surface charge current $\dot{\bar{q}}$. In the non-relativistic limit we find the surface charge current as

$$\lambda \dot{\bar{q}} = -\epsilon_0 c^2 \left[ \partial_x \bar{\Phi} \left( \bar{Z}^+, t \right) - \partial_x \bar{\Phi} \left( \bar{Z}^-, t \right) \right] \tag{1.6}$$

The surface charge current being induced by the discontinuous magnetic field across the center of mass position can be interpreted as the Ampere's law in 1+1 dimensions. We eliminate the *idf* from the center of mass dynamics, defining the spatial

derivative of the field at the center of mass position as

$$\partial_x \bar{\Phi}\left(\bar{Z}, t\right) \equiv \frac{1}{2}\left(\partial_x \bar{\Phi}\left(\bar{Z}^+, t\right) + \partial_x \bar{\Phi}\left(\bar{Z}^-, t\right)\right) \qquad (1.7)$$

Using this, we rewrite CoM dynamics as

$$\ddot{\bar{Z}} + \mho^2 \bar{Z} = -\frac{1}{2M}\epsilon_0 c^2 (\partial_x \bar{\Phi})^2 |_{\bar{Z}^-}^{\bar{Z}^+} \qquad (1.8)$$

Thus, in the MOF model the radiation pressure force can be interpreted as the Lorentz force arising from the interaction of the induced surface charge current (1.6) with the magnetic field $(\partial_x \Phi)$. Such an interpretation of the radiation pressure force as the Lorentz force on induced surface charge currents has been discussed in detail in [75] and agrees with the simple description of radiation pressure on an electric dipole. We notice that the right hand side corresponds to the well-known radiation pressure force $\left(\sim \frac{B^2}{2\mu_0}\right)$ seen by a mirror in the non-relativistic limit [68]. This is justified based on the fact that the electric field vanishes at the mirror position in the co-moving reference frame and the force being proportional to the EM field energy density then goes as $\sim \frac{B^2}{2\mu_0}$. To compare with the expression in [68], we notice that for a perfect mirror there is no field energy density on one side of the mirror $\left(\partial_x \Phi\left(\bar{Z}^+, t\right) = 0\right)$ and we reduce to the known result. For an imperfect mirror there is a finite energy density of the EM field on either side of the surface, hence the net radiation pressure force is given by the difference in the field energy density on either side of the surface as in (1.8).

To compare with the boundary condition approach in more detail, let us consider the mirror-field interaction in terms of the radiation pressure force exerted by

the field on the mirror. We assume that the mirror is generally imperfect and interacts with a scalar field in a region of length $L$. Now similar to the approach of [84], one can consider a co-moving frame of reference with respect to the mirror center of mass to write the Lagrangian density of the field as $\sim \left( \frac{1}{2}\epsilon E'^2 - \frac{1}{2\mu_0}B'^2 \right)$, with $E'$ and $B'$ being the electric and magnetic fields in the co-moving frame and the dielectric permittivity is defined as, say, $\epsilon(x) = \epsilon_0(1 + \chi\delta(x - Z))$ for an infinitely thin dielectric slab. Then in the laboratory frame, the Lagrangian for the oscillating mirror+field system can be written as

$$\mathcal{L}_{BC} = \frac{1}{2}M\dot{Z}^2 - \frac{1}{2}M\mho^2 Z^2 + \int_0^L dx \left[ \frac{1}{2}\epsilon \left( (\partial_t\Phi)^2 - c^2(\partial_x\Phi)^2 \right) + \dot{Z}(\epsilon - 1)(\partial_t\Phi)(\partial_x\Phi) \right]$$

(1.9)

where we have kept terms upto first order in $\dot{Z}$ from the inverse Lorentz transformation. Now in the non-relativistic limit, we drop the velocity dependent term and obtain the Euler-Lagrange equation of motion for the mirror center of mass as

$$\ddot{Z} + \mho^2 Z = -\frac{1}{2M}\epsilon_0 c^2(\partial_x\Phi)^2 \,|_{\bar{Z}_-}^{\bar{Z}_+}$$

(1.10)

which agrees with what we found in (1.8) and also matches up with equation (8) of [84] in the limit of an infinitely thin dielectric membrane where $d \to 0$ and $\chi \to \infty$. While [84] talks of a dielectric slab in a cavity, a more specific situation than what we consider here in the simplistic MOF setup, at the level of the formal expression for the radiation pressure force where we have left the boundary conditions arising from the *idf*-field interaction unspecified we find an agreement between the two approaches. This further reaffirms our intuition that the difference between the boundary condition approach and a microscopic model arises when considering the

dynamical participation of the *idf* explicitly, which in the above expression would show up as the difference in the field configurations on the RHS.

Thus we have arrived at the classical radiation pressure force on the mirror in the non-relativistic CoM motion limit as one would find from imposing fixed boundary conditions on the field. Rather, in this case the boundary conditions resulting from the mirror-field coupling arise self consistently from the dynamical interaction between the moving *idf* and the field, as does the radiation pressure. We note that the formal expression for radiation pressure would remain the same also for a coupling of the form $\sim \lambda q \Phi$. Though the important point to note is that while the form of the radiation pressure force we obtain from including the *idf* is identical to what we get from imposing the fixed boundary conditions, the boundary conditions themselves rather than being fixed are determined by the dynamics of the *idf*-field interaction which depends on the exact form of coupling. This more generally includes retarded influence of the moving surface charges on the field in a dynamical way. To see this more concretely, consider the *idf* amplitude solution from (1.3)

$$\bar{q}(t) = \bar{q}_h(t) + \int_0^t dt' G_i(t - t') \left( -\frac{\lambda}{m} \dot{\bar{\Phi}} \left( \bar{Z}(t'), t' \right) \right) \tag{1.11}$$

where we define $\bar{q}_h$ as the homogeneous solution for the free *idf* evolution and $G_i(t - t') \equiv \frac{\sin(\Omega(t-t'))}{\Omega}$ as the Green's function for the *idf*. We use this to eliminate the *idf*

from the field's equation of motion to get

$$\epsilon_0 \left( \partial_t^2 - c^2 \partial_x^2 \right) \bar{\Phi}\left(x, t\right) + \frac{\lambda^2}{m} \delta\left(x - \bar{Z}(t)\right) \int_0^t dt' \partial_t G_i\left(t - t'\right) \dot{\bar{\Phi}}(\bar{Z}(t'), t')$$

$$= \lambda \dot{\bar{q}}_h \delta\left(x - \bar{Z}(t)\right) \qquad (1.12)$$

We see that the *idf* is driven by the field and influences the field in return, as captured in the second term on the left hand side that represents the retarded influence of the *idf* on the field, meaning that the radiation pressure force depends on the coupled non-Markovian dynamics of the field, center of mass and the *idf*. Thus, we can identify the term $\partial_t G_i\left(t - t'\right) \equiv \chi\left(t - t'\right)$ as the susceptibility function for the mirror. To compare with the case where one applies boundary conditions as opposed to including the *idf* dynamics self-consistently one needs to include the coupling of the *idf* with a bath so as to reach the steady state response of the damped *idf*. We will further illustrate this point and the role of the internal degree of freedom in determining the optical properties of the mirror in the following subsection.

## 1.4.2 Optical properties

To study the optical properties arising from the MOF model let us consider a single mode field $\Phi_\omega(x, t)$ at frequency $\omega$ driving the mirror's *idf*. We can write the self consistent solution for the field dynamics from (1.4) as

$$\Phi(x, t) = \Phi_\omega(x, t) + \lambda \int dt' G_f(x, t; Z(t'), t') \dot{q}(t') \qquad (1.13)$$

where $G_f(x, t; x', t')$ refers to the Green's function of the free field in 1+1 D. Using this solution to determine the response of the *idf* from (1.3), we have

$$\ddot{q} + \Omega^2 q = -\frac{\lambda}{m}\left(\dot{\Phi}_\omega(Z(t), t) + \lambda \int dt' \partial_t G_f(Z(t), t; Z(t'), t')\dot{q}(t')\right) \qquad (1.14)$$

$$\Longrightarrow \ddot{q} + \gamma_f \dot{q} + \Omega^2 q = -\frac{\lambda}{m}\dot{\Phi}_\omega(Z(t), t) \qquad (1.15)$$

where we identified the second term in the RHS of (1.14) as the damping kernel and we find that for non-relativistic mirror motion the damping is always ohmic. The damping of the *idf* coming from its coupling to the continuum of field modes is given by the coefficient $\gamma_f \equiv \frac{\lambda^2}{2m\epsilon_0 c}$. One can then write the solution for the *idf* dynamics as

$$q = -\frac{\lambda}{m}\int dt' \partial_t G_i(t - t')\dot{\Phi}_\omega\left(Z(t'), t'\right) \qquad (1.16)$$

where the Green's function for the *idf* is given as $G_i(t-t') = \frac{\sin(\Omega t)}{\Omega}e^{-\gamma_f(t-t')/2}$. Thus, knowing the response of the *idf*, we can rewrite the field solution from (1.13) with the backreaction of the *idf* included as follows

$$\Phi(x, t) = \Phi_\omega(x, t) - \frac{\lambda^2}{m}\int dt' G_f(x, t; Z(t'), t')\int dt'' \partial_t' G_i(t' - t'')\dot{\Phi}_\omega\left(Z(t''), t''\right)$$

$$(1.17)$$

In the steady state limit, where the response of the *idf* is only at the drive frequency and assuming that the mirror's CoM is at the origin in equilibrium, we make the following plane-wave ansatz for the field

$$\bar{\Phi}(x, t) = \frac{\Omega}{\omega}\Phi_0 e^{-i\omega t}\left(\Theta(-x)\left(e^{ikx} + R(\omega)e^{-ikx}\right) + \Theta(x)T(\omega)e^{ikx}\right) + H.C. \qquad (1.18)$$

where $\Phi_0$ is the amplitude of the field and we have introduced the frequency normalization factor $(\Omega/\omega)$ to take care of the fact that in the EM correspondence the

electric field amplitude ($E \sim \partial_t A$) is independent of the frequency of the field. $R(\omega)$ and $T(\omega)$ refer to the amplitude reflection and transmission coefficients of the point mirror, such that $T(\omega) = 1 + R(\omega)$. This can be readily seen from the continuity of $\partial_t \bar{\Phi}$ across the center of mass position $\bar{Z}$ from (1.4) in the limit of non-relativistic center of mass motion. In considering the interaction of the *idf* with only a single field mode, we include a damping ($\gamma_f$) that arises from its coupling with the remaining field modes. For current purposes, we assume that the damping is small ($\gamma_f \ll \Omega$) so that one can ignore the dissipation of the incident plane wave. As in [1], we assume that in the steady state regime the *idf* oscillates at the frequency of the incident field. In which case, we find

$$q(t) = \frac{-i\omega\lambda}{m(\omega^2 - \Omega^2)}\frac{\Omega}{\omega}\Phi_0 T(\omega)e^{-i\omega t} + H.C. \tag{1.19}$$

From the mirror center of mass dynamics (1.8), we can see that in the presence of the incident drive the center of mass consists of a time-independent and a high frequency ($2\omega$) radiation pressure term, coming from the non-linear interaction of the incident B field and the induced surface charge current. In the limit $\mho \ll \Omega$, the high frequency component of the mirror amplitude denoted by $\bar{Z}_{2\omega}$ scales as $|\bar{Z}_{2\omega}| \sim \frac{\epsilon_0 \Phi_0^2 \Omega^2}{M\omega^2}$, which, in the near field-*idf* resonance regime ($\omega \approx \Omega$), is much smaller compared with the mirror amplitude coming from the constant radiation pressure part $\bar{Z}_0 \sim \frac{\epsilon_0 \Phi_0^2 \Omega^2}{M\mho^2}$, noting that $\frac{\bar{Z}_0}{\bar{Z}_{2\omega}} \sim \frac{\Omega^2}{\mho^2} \gg 1$. Thus we find that the mirror position evolves essentially at its natural frequency $\mho$ under the constant force.

We assume that at the classical level the center of mass motion does not affect

the *idf*-field coupling and the resulting optical properties from the interaction. More explicitly, the phase of the field mode that is resonant with the *idf* changes by a very small amount over the length scales of one amplitude of the *mdf*, that is $\Delta\phi \equiv (\Omega/c)\,\bar{Z}_0 \ll 1$. This restricts the field amplitude to

$$|\Phi_0|^2 \ll \frac{M\mho^2 c}{\Omega^3 \epsilon_0} \tag{1.20}$$

This is a self-consistent validity constraint which ensures that the optical properties of the mirror are unaffected by the center of mass motion to first order, to reaffirm our plane wave ansatz (1.18). Physically speaking we assert that the mirror CoM motion is much smaller than the wavelengths of the field that it interacts with. The sub-wavelength motion approximation is valid for the case of trapped atoms spatially confined in a harmonic trap (trap frequency being $\mho$ in this case), interacting with an optical field of frequency $\omega$.

In the plane wave ansatz, we find the surface charge current for the *idf* (1.6) as

$$\lambda\dot{\bar{q}} = -\epsilon_0 c^2 \partial_x \bar{\Phi}\left(x,t\right)|_{\bar{Z}^-}^{\bar{Z}^+} \approx -2ik\epsilon_0 c^2 \Phi_0 \frac{\Omega}{\omega}e^{-i\omega t}R\left(\omega\right) + H.C.$$

$$= -2i\epsilon_0 \Omega c \Phi_0 e^{-i\omega t}R\left(\omega\right) + H.C. \tag{1.21}$$

We can notice here that the induced surface charge current is proportional to the mirror reflectivity. Thus, as expected, a higher reflectivity leads to a larger radiation pressure force.

Now within the non-relativistic and sub-wavelength CoM motion approximations, we consider the MOF model with the two different forms for the coupling term

- (1) $q\Phi$ (as previously analyzed in [1]) and (2) $\dot{q}\Phi$ - and study the optical properties that arise from these two couplings in different parameter regimes. Through the rest of this work we only consider the $\dot{q}\Phi$ form of coupling.

### 1.4.2.1  $q\Phi$ coupling

Let us first consider the $q\Phi$ coupling as in [1] and start with drawing the correspondence between the interaction term for the scalar field vis-a-vis an EM field. As motivated in the section II.B.1 in [1] when comparing the MOF model with the Barton-Calogeracos (BC) model, we choose the coupling $\lambda$ to have dimensions of the charge density such that dimensionally $\lambda \sim$ (Charge) (Length)$^{-1}$. Going back to the interaction term in the original action we use this to find the dimensions of the scalar field as $\Phi \sim$ (Mass)(Length)$^2$(Time)$^{-2}$/(Charge) and rescale the free field term accordingly, we get for the free field action

$$S_F = \frac{\epsilon_0}{2c^2} \int \mathrm{d}t \int \mathrm{d}x \left( (\partial_t \Phi)^2 - c^2 \left( \partial_x \Phi \right)^2 \right) \tag{1.22}$$

This leads to the coupled *idf*-field equations of motion for a fixed center of mass as

$$\epsilon_0 / c^2 \left( \partial_t^2 \Phi - c^2 \partial_x^2 \Phi \right) = \lambda q \delta(x) \tag{1.23}$$

$$m\ddot{q} + m\Omega^2 q = \lambda \Phi(0, t) \tag{1.24}$$

For a plane wave incident on the mirror, using the ansatz (1.18) to solve for the surface charge current as in (1.21) in the steady state limit we get the reflectivity

for the case of $q\Phi$ coupling as

$$R(\omega) = \frac{-i\lambda^2 c}{i\lambda^2 c + 2m\omega\epsilon_0(\omega^2 - \Omega^2)} \tag{1.25}$$

$$\implies |R(\omega)|^2 = \frac{1}{1 + r_p^2\eta^2(1 - \eta^2)^2} \tag{1.26}$$

where we have defined the ratio of the field to the *idf* frequency as $\eta \equiv \omega/\Omega$ and $r_p \equiv \left(\frac{2m\Omega^3\epsilon_0}{\lambda^2 c}\right) \equiv \Omega/\Omega_P$. We identify the quantity $\Omega_P \equiv \frac{\lambda^2 c}{2m\Omega^2\epsilon_0}$ as the plasma frequency, again motivated by the comparison with the BC model. As found in [1], the mirror becomes perfectly reflecting for 1) infinitely strong *idf*-field coupling, $\lambda \to \infty$, 2) perfect resonance between the *idf* and the incident field, $\omega = \Omega$ or 3) massless *idf*, $m \to 0$. Now observing that the reflection spectrum is completely characterized by the two frequency ratios $r_p$ (ratio of the *idf* to plasma frequency) and $\eta$ (ratio of the field to *idf* frequency), we consider different values for the parameter $r_p$ and look at the reflectance as a function of the field frequency for a fixed plasma frequency, as shown in Fig. 1.1.

To invoke the correspondence with the BC model [67] we need to assume that the *idf* evolves adiabatically in the limit $\{m \to 0, \Omega \to \infty\}$ such that the quantity $m\Omega^2 \equiv \kappa$ that physically corresponds to the mass density of the surface charges stays finite. In this limit since $r_p \gg 1$ ($\Omega \to \infty$), we see a resonant behavior in the reflection spectrum around the *idf* frequency $\Omega$. In the regime where $r_p \ll 1$, the reflection spectrum shows a high frequency cutoff behavior similar to the case of bulk metals with Drude-Lorentz response. As shown in Fig.1.1, given the plasma frequency for silver ($\Omega_P = 1.37 \times 10^{16}$ Hz) [85], we compare the known optical response with our model and find that a *idf* to plasma frequency ratio $r_p \approx 0.3$

28

mimics the cut-off behavior reasonably well. Knowing that the charge carrier density

for silver is $n_s = 5.8 \times 10^{28} m^{-3}$ [85] and using the BC correspondence to find $\lambda = n_s e$,

we can deduce all three *idf* parameter values.
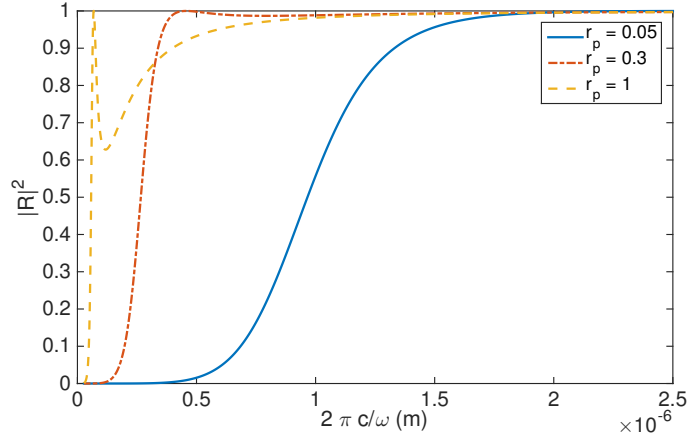


(a)
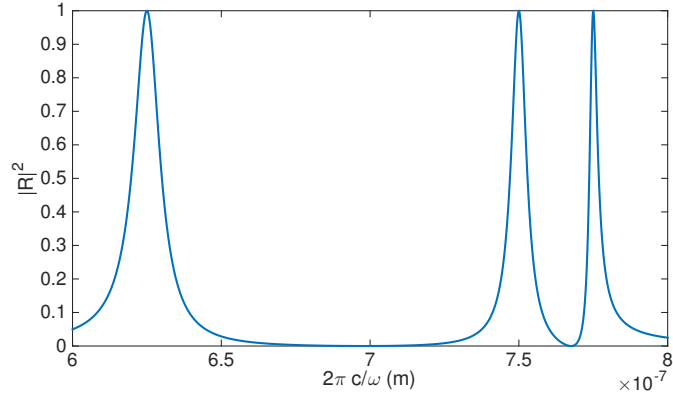
(b)

Figure 1.1: Reflection properties from the two different forms of coupling ($q\Phi$ and $\dot{q}\Phi$) (a) Reflectance as a function the incident field wavelength (in meters) for different *idf* to plasma frequency ratios ($r_p = \Omega/\Omega_P$), the plasma frequency is fixed at $\Omega_P = 1.37 \times 10^{16}$ Hz (for silver) from $q\Phi$ coupling, choosing $r_p \approx 0.3$ mimics the cutoff behavior for silver (b) Reflectance and transmittance spectrum from $\dot{q}\Phi$ coupling to simulate the optical response for a photonic crystal as from the experimental results in [86]. Each resonance corresponds to a separate effective *idf* with resonance frequencies $\Omega = \{3.01 \times 10^{15}\text{Hz}, 2.51 \times 10^{15}\text{Hz}, 2.43 \times 10^{15}\text{Hz}\}$ and corresponding plasma frequencies $\Omega_P = \{0.5 \times 10^{14}\text{Hz}, 0.2 \times 10^{14}\text{Hz}, 0.1 \times 10^{14}\text{Hz}\}$.

## 1.4.2.2 $\dot{q}\Phi$ coupling

As in the previous subsection we find the reflection coefficient for the $\dot{q}\Phi$ coupling as

$$R(\omega) = \frac{-i\lambda^2\omega}{i\lambda^2\omega + 2m\epsilon_0 c(\omega^2 - \Omega^2)}$$

$$\implies |R(\omega)|^2 = \frac{\omega^2/\Omega^2}{\omega^2/\Omega^2 + \left(\frac{2m\epsilon_0 c\Omega}{\lambda^2}\right)^2 (\omega^2/\Omega^2 - 1)^2} = \frac{\eta^2}{\eta^2 + r_p^2(\eta^2 - 1)^2} \tag{1.27}$$

where again we have defined the ratio of the field to *idf* frequency as $\eta \equiv \omega/\Omega$ and the ratio of *idf* to plasma frequency as $r_p \equiv \Omega/\Omega_P = \Omega/(\frac{\lambda^2}{2m\epsilon_0 c})$, redefining the plasma frequency as $\Omega_P = \frac{\lambda^2}{2m\epsilon_0 c}$. We see that mirror becomes perfectly reflecting for the same conditions as in the case of $q\Phi$ coupling $\{\lambda \to \infty, \omega = \Omega, m \to 0\}$. Unlike the $q\Phi$ coupling, we do not see a perfect reflection at $\omega = 0$ which was an artifact of the monopole coupling between the *idf* and the field.

The optical response exhibits a resonant behavior around the *idf* frequency $\Omega$, since the reflectivity is maximum for $\eta = 1$. For this reason it is natural to consider optomechanical elements with built in resonances such as photonic crystals or atoms as an application. We find that one can mimic the optical response of a photonic crystal structure (see Fig.1.1) by choosing the resonant frequency of the *idf* as the resonant mode of the photonic crystal, for multiple resonances we choose multiple internal degrees of freedom such that $\Omega_i = \omega_i^{res}$ at each resonance peak. The sharpness of the resonance is determined by the quantity $r_p^i$, since the parameter $r_p^i$ determines the coupling strength of the field to a particular resonance mode of the structure. Thus one can determine the two parameters that characterize

the optical response in our model, namely $r_p$ and $\Omega$. To completely determine all the parameters of the internal degree of freedom $\{m, \Omega, \lambda\}$ we need to draw an additional physical correspondence between the internal degree of freedom and the physical setup as we did for the previous case of $q\Phi$ coupling by identifying the coupling constant $\lambda$ as the charge density. For the case of a photonic crystals, it has also been shown that the large gradients of reflectivity near the photonic bandgaps can modify the optomechanical damping by irreversibly converting the energy from the thermal fluctuations of the motion to that of the optical field or vice versa via Doppler effect [55].

As we had noticed previously, the mirror reflectivity characterized by the *idf* parameters determines the strength of the induced surface charge current (1.21) which in turn factors into determining the radiation pressure coupling. In the following section we will show that the same applies to the case of coupling between the quantum fluctuations of the mirror and the field. We now turn to look at the coupled quantum dynamics of the three subsystems in the MOF model.

## 1.5 Quantum Dynamics of the Coupled Mirror-Oscillator-Field (MOF) System

Let us perturb the original action (1.1) about the classical solutions as $\{\bar{Z} + \tilde{Z}, \bar{q} + \tilde{q}, \bar{\Phi} + \tilde{\Phi}\}$, with $\tilde{O}$ being the deviations about the classical solutions $\bar{O}$. Assuming that the center of mass motion about $\bar{Z}$ is small and restricted to the sub-wavelength regimes $\left(k\tilde{Z} \ll 1\right)$ for the field modes below a certain high frequency

cutoff, we expand the action up to third order in the fluctuations about the classical solutions ignoring terms that are second order or higher in $k\tilde{Z}$. We go up to third order to specifically include the term that couples the perturbations of all three subsystems (labeled as MOF below) to arrive at the non-linear intensity-position coupling. In the subsequent dynamics we shall only consider bilinear interaction terms to preserve Gaussianity of the individual subsystems. As we will see, truncating the action up to second order corresponds to the linearized approximation in the limit of strong mean-field amplitude, also called a background field expansion in field theory.

We write the perturbed action as

$$S_3 = \int \mathrm{d}t \underbrace{\left(\frac{1}{2}M\dot{\tilde{Z}}^2 - \frac{1}{2}M\mho^2\tilde{Z}^2\right)}_{\text{mdf (M)}} + \underbrace{\left(\frac{1}{2}m\dot{\tilde{q}}^2 - \frac{1}{2}m\Omega^2\tilde{q}^2\right)}_{\text{idf (O)}}$$

$$+ \int \mathrm{d}x \left[ \underbrace{\frac{\epsilon_0}{2}\left(\left(\partial_t\tilde{\Phi}\right)^2 - c^2\left(\partial_x\tilde{\Phi}\right)^2\right)}_{\text{Field (F)}} \right.$$

$$\left. + \lambda\delta\left(x - \bar{Z}\right)\left(\underbrace{\dot{\tilde{q}}\tilde{\Phi}}_{\text{OF}} + \underbrace{\dot{\bar{q}}\left(\partial_x\tilde{\Phi}\right)\tilde{Z}}_{\text{MF}} + \underbrace{\dot{\tilde{q}}\left(\partial_x\bar{\Phi}\right)\tilde{Z}}_{\text{OM}} + \underbrace{\dot{\tilde{q}}\left(\partial_x\tilde{\Phi}\right)\tilde{Z}}_{\text{MOF}}\right) \right] \qquad (1.28)$$

One can observe several points from the above expression, firstly, we find that there is an effective coupling between the fluctuations of the mirror center of mass and the field via the internal degree of freedom as denoted by the terms MF and MOF. To the lowest order, the mirror-field coupling strength is proportional to the classical surface current $\dot{\bar{q}}$, implying that the fluctuations of the field are the most sensitive

to the fluctuations of the mirror center of mass if the surface current is at its largest. In the single field mode case this is proportional to the reflection coefficient of the mirror as seen in (1.21), meaning that a highly reflecting mirror leads to large effective MF coupling strength. Secondly, there is also an effective coupling between the *idf* and the *mdf* fluctuations denoted by the terms OM and MOF, which to the lowest order is proportional to the spatial derivative of the field (or the "magnetic field" B) at the center of mass position. The coupling strengths of the interaction terms between the *idf* and the mirror (OM), and the field and the mirror (MF) are determined by the classical solutions of the field and *idf* amplitudes as found in the previous sections.

We get the following equations of motion for the coupled mirror and field dynamics

$$\ddot{\tilde{Z}} + \mho^2 \tilde{Z} = \frac{\lambda}{M} \left[ \dot{\bar{q}} \partial_x \tilde{\Phi} \left( \bar{Z}, t \right) + \dot{\tilde{q}} \left\{ \partial_x \bar{\Phi} \left( \bar{Z}, t \right) + \partial_x \tilde{\Phi} \left( \bar{Z}, t \right) \right\} \right] \tag{1.29}$$

$$\epsilon_0 \left( \partial_t^2 \tilde{\Phi} - c^2 \partial_x^2 \tilde{\Phi} \right) = \lambda \dot{\tilde{q}} \delta \left( x - \bar{Z} \right) - \lambda \left( \dot{\bar{q}} + \dot{\tilde{q}} \right) \partial_x \left( \delta \left( x - \bar{Z} \right) \right) \tilde{Z} \tag{1.30}$$

It can be seen here that unlike the classical equations of motion, the field fluctuations are not only driven by the *idf* but also by the fluctuations of the center of mass position. From integrating (1.30) around the classical center of mass position $\bar{Z}$, we get the surface current fluctuation as

$$\lambda \dot{\tilde{q}} = -\epsilon_0 c^2 \partial_x \tilde{\Phi} |_{\bar{Z}_-}^{\bar{Z}_+} \tag{1.31}$$

just as the classical version interpreted as the Ampere's Law in 1+1 D in (1.6). Using this and the classical surface current to eliminate the *idf* from the center of

mass dynamics (1.29), we get

$$\ddot{\tilde{Z}} + \mho^2 \tilde{Z} = \frac{-\epsilon_0 c^2}{M} \left[ \left( \partial_x \bar{\Phi} \right) \left( \partial_x \tilde{\Phi} \right) \Big|_{\bar{Z}_-}^{\bar{Z}_+} + \frac{1}{2} \left( \partial_x \tilde{\Phi} \right)^2 \Big|_{\bar{Z}_-}^{\bar{Z}_+} \right] \qquad (1.32)$$

We can see that the first term on the right side corresponds to the radiation pressure coupling in the linearized approximation which is valid for large photon numbers in the presence of a classically driven field. The second term goes beyond this approximation, which corresponds to the intensity-position coupling, required for treating situations with small photon numbers. Considering $\tilde{\Phi}$ represents the quantum fluctuations of the field, we can understand the radiation pressure force at the quantum level as arising from the asymmetry in the field fluctuations on either side of the mirror. Say, if there were a cavity present on one side and free space on the other, the radiation force from the cavity side would be stronger in comparison because of the small quantization volume leading to asymmetry in the density of field modes as in the case of Casimir force [87]. Such an interpretation of Casimir force as a radiation pressure force from the vacuum field has been discussed by Milonni *et al* in [88] for the case of two perfectly conducting plates.

We now restrict ourselves to second order perturbations in the original action, to keep all the interaction terms bilinear such that starting out with Gaussian initial states for the three subsystems, Gaussianity of the individual subsystems is

preserved. We derive the conjugate momenta from the second order action as

$$\tilde{p} = m\dot{\tilde{q}} + \lambda\tilde{\Phi}\left(\bar{Z},t\right) + \lambda\partial_x\bar{\Phi}(\bar{Z},t)\tilde{Z} \tag{1.33}$$

$$\tilde{P} = M\dot{\tilde{Z}} \tag{1.34}$$

$$\tilde{\Pi}(x,t) = \epsilon_0\dot{\tilde{\Phi}}(x,t) \tag{1.35}$$

It can be seen that the fluctuations in the *idf* are influenced by both the *mdf* and the field and hence mediate the effective interactions between the two. Identifying the dynamical variables $\{\tilde{Z}, \tilde{q}, \tilde{\Phi}\}$ as the quantum fluctuations of the *mdf, idf* and the field respectively about their mean-field amplitudes, we arrive at the second order Hamiltonian

$$\tilde{H}_2 \equiv \underbrace{\frac{\tilde{P}^2}{2M} + \frac{1}{2}M\left(\mho^2 + \frac{\lambda^2}{mM}\left(\partial_x\bar{\Phi}(\bar{Z},t)\right)^2\right)\tilde{Z}^2}_{mdf\,(M)} + \underbrace{\frac{\tilde{p}^2}{2m} + \frac{1}{2}m\Omega^2\tilde{q}^2}_{\text{idf}\,(O)}$$

$$+ \underbrace{\int \mathrm{d}x\left(\frac{\tilde{\Pi}^2}{2\epsilon_0} + \frac{1}{2}\epsilon_0 c^2\left(\partial_x\tilde{\Phi}\right)^2\right) + \frac{\lambda^2}{2m}\tilde{\Phi}(\bar{Z},t)^2}_{\text{Field (F)}} - \underbrace{\frac{\lambda}{m}\tilde{p}\tilde{\Phi}(\bar{Z},t)}_{\text{OF}} - \underbrace{\frac{\lambda}{m}\partial_x\bar{\Phi}(\bar{Z},t)\tilde{p}\tilde{Z}}_{\text{OM}}$$

$$+ \underbrace{\frac{\lambda^2}{m}\partial_x\bar{\Phi}(\bar{Z},t)\tilde{\Phi}(\bar{Z},t)\tilde{Z} - \lambda\dot{\tilde{q}}\partial_x\tilde{\Phi}(\bar{Z},t)\tilde{Z}}_{\text{MF}} \tag{1.36}$$

We notice that the *mdf* now observes a renormalized oscillation frequency and the scalar field sees a frequency shift coming from the term quadratic in $\Phi$ which is analogous to the diamagnetic term $\sim \frac{e^2}{2m}A^2$ of the minimal coupling Hamiltonian. The bilinear interaction terms represent the coupling between the *idf* and the field (OF), mirror and the *idf* (OM) and mirror and the field (MF) respectively. Physically, the terms that are second order in $\lambda$ arise from the field-field, mirror-mirror and field-mirror couplings mediated via the quantum fluctuations of the *idf*. The

terms that are first order in $\lambda$ in the couplings between the *idf-mdf* (OM) and *mdf-field* (MF) fluctuations come from the classically driven solutions for the field and the *idf* respectively. Specifically, we note that the MF interaction contains two terms, the first one of which represents the effective mirror-field interaction mediated via the quantum fluctuations of the *idf*, while the second one represents that from the classical surface charge currents. Since the conventional approach does not include the fluctuations of this extra quantum degree of freedom, it misses out on the fluctuation-mediated part of the effective mirror-field coupling. As we shall see later, this term becomes dominant in the strong coupling regime where $(\Omega_P \gg \Omega)$.

It can also be seen that in the absence of a classical drive, the only interaction is between the *idf* and the field (OF) up to second order. To be able to see an effective mirror-field interaction one needs to include third order terms in the fluctuations as illustrated before. These terms would be relevant when one wants to find the forces coming from vacuum fluctuations, which, for example in the case of two mirrors would correspond to the Casimir/ Casimir-Polder forces. Moreover, as our model includes the fluctuations of the mechanical degree of freedom in addition to those of the field, these would give some corrections to the Casimir/Casimir-Polder forces. We note that such phonon loop corrections can possibly be significant if the mass and the oscillation frequency of the mechanical degree of freedom are small, an effect that has not yet been studied in the literature.

Thus far we have arrived at the general form for the quantized Hamiltonian for the coupled subsystems and shall turn to a simpler specific case of a single field mode, a typical assumption in cavity optomechanics, to study the entanglement

dynamics of the system in the following chapter.

## Chapter 2:   Entanglement in the Mirror-Oscillator-Field (MOF) Model

Entanglement between a field and a mechanical oscillator has been widely studied in cavity optomechanical setups in several contexts [17]– [64], with the essential mirror-field coupling mechanism being radiation pressure coupling wherein the field exerts a force on the mirror center of mass by means of photon-momentum transfer and observes a phase shift proportional to the mirror displacement in turn. We now look at the entanglement generation from a microscopic perspective as described by the MOF model, considering only a single mode of the scalar field in our model as in the usual cavity optomechanical setups to deduce some key physical features of the mirror-field entanglement that arise from the inclusion of the *idf*.

The setup that we consider here consists of a mirror described by the MOF model, interacting with a single mode of a cavity. For the sake of simplicity, we choose a ring resonator so that the position of the mirror relative to the cavity end mirrors does not enter as a separate parameter for the traveling wave mode of the cavity. We note that in our model one can treat the quantum fluctuations of the field within the cavity as those of a single field without having to consider separate quantization volumes and boundary conditions on either side of the mirror of interest, since the boundary conditions on the field fluctuations would emerge

self-consistently as the *idf* -field interaction reaches a steady state.
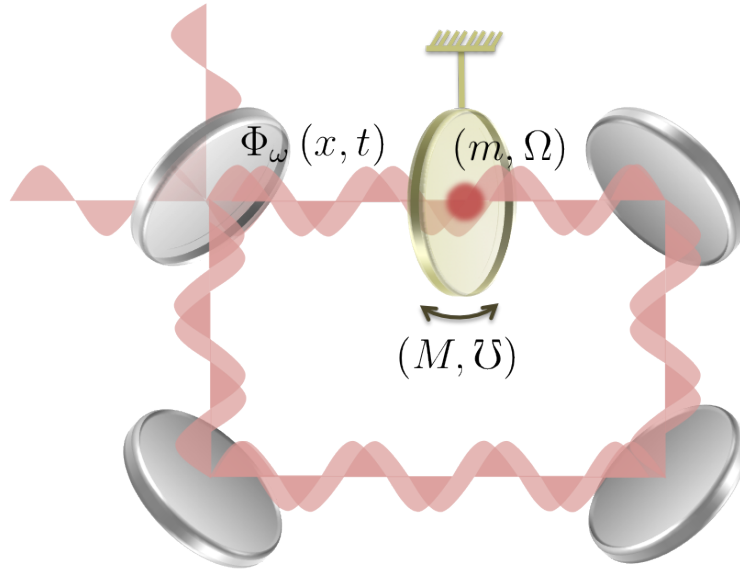


Figure 2.1: Schematic of the setup in consideration – the mirror of interest described by the MOF model, interacts with a single mode field $\Phi_\omega(x,t)$ at frequency $\omega$ in a ring cavity of length $L$.

In the following, we first solve for the quantum dynamics of the coupled mirror-oscillator-field system for a single mode of the scalar field in section 2.1 and discuss the effective couplings between the three pertinent subsystems, then we show how and in what limit one can recover the boundary condition approach for the case of an imperfect mirror inside a cavity in section 2.2 and contrast it with the more general case, in section 2.3 we outline our calculation of the mirror-field entanglement and discuss how it depends on the various parameters involved, finally applying our approach to the case of a single atom interacting with a field mode in 2.3.1 to study the optomechanical entanglement between the atomic center of mass and a field.

## 2.1 Single Field Mode interacting with the Mirror

We first simplify the Hamiltonian (1.36) for the case of a single field mode that is being externally driven to look at the dynamics of the coupled MOF system and then coarse-grain the *idf* to find the sought after mirror-field entanglement. Consider the scalar field in a region of length $L$, the field fluctuations can be written as the sum of all discrete modes of the cavity of length $L$ as $\tilde{\Phi}(x,t) = \sum_n \sqrt{\frac{\hbar}{2\omega_n \epsilon_0 L}}\left(\tilde{a}_n e^{ik_n x} + \tilde{a}_n^\dagger e^{-ik_n x}\right)$, with $\tilde{a}_n^\dagger$ and $\tilde{a}_n$ representing the dimensionless creation and annihilation operators for the nth field mode. We pick a single field mode at frequency $\omega$ interacting with the point mirror at the origin $\left(\bar{Z} = 0\right)$ assuming that the center of mass motion is in the sub-wavelength regime as before.

$$\tilde{\Phi}_\omega(x,t) = \sqrt{\frac{\hbar}{2\omega\epsilon_0 L}}\left(\tilde{a}_\omega e^{ikx} + \tilde{a}_\omega^\dagger e^{-ikx}\right) \tag{2.1}$$

The above expression represents the fluctuations of the free field without any imposed boundary conditions unlike the standard treatment where the quantum fluctuations follow the mode functions of the classical field (see [97] for example). In the steady state, the strength of the field fluctuations would be determined by the boundary conditions as they emerge from the *idf*-field interaction self-consistently.

For a single field mode, we rewrite the free Hamiltonian part in (1.36) as

$$\tilde{H}_{free} \equiv \underbrace{\frac{\tilde{P}^2}{2M} + \frac{1}{2}M\mho'^2\tilde{Z}^2}_{\tilde{H}_M} + \underbrace{\hbar\Omega\left(\tilde{b}^\dagger\tilde{b} + \frac{1}{2}\right)}_{\tilde{H}_O}$$

$$+ \underbrace{\hbar\left(\omega + \frac{\lambda^2}{2m\omega\epsilon_0 L}\right)\left(\tilde{a}_\omega^\dagger\tilde{a}_\omega + \frac{1}{2}\right) + \frac{\lambda^2}{4m\omega\epsilon_0 L}\left((\tilde{a}_\omega)^2 + (\tilde{a}_\omega^\dagger)^2\right)}_{\tilde{H}_F} \qquad (2.2)$$

where we have redefined the dynamical variables associated with the *idf* in terms of the creation annihilation operators $\{\tilde{b}^\dagger, \tilde{b}\}$ as $\tilde{q} = \sqrt{\frac{\hbar}{2m\Omega}}\left(\tilde{b} + \tilde{b}^\dagger\right)$ and $\tilde{p} = -i\sqrt{\frac{\hbar m\Omega}{2}}\left(\tilde{b} - \tilde{b}^\dagger\right)$. The renormalized mechanical frequency is defined as $\mho'^2 \equiv \mho^2 + \frac{\lambda^2}{mM}\left(\partial_x\bar{\Phi}(\bar{Z}, t)\right)^2$. As mentioned in the previous chapter, the correction term $\left(\frac{\lambda^2}{mM}\left(\partial_x\bar{\Phi}(\bar{Z}, t)\right)^2\right)$ contains two contributions - a time dependent part oscillating at a frequency $\sim 2\omega$ and a time-independent part. In the rotating wave approximation (RWA) the time dependent term can be neglected. However, if the field mode was resonant with the *mdf*, one would see parametric amplification of the mirror center of mass motion due to this time dependent part [89]. We estimate the correction from the time independent term to the mechanical oscillation frequency for the case of a single atom interacting with a field mode as $\Delta\mho/\mho \sim 10^{-3}$, for some typical experimental numbers taken from [95, 96].

For the free field part we notice that the interaction leads to an energy correction $\omega \to \omega + \lambda^2/(2m\omega\epsilon_0 L)$ that is second order in $\lambda$, this corresponds to the shift coming from the diamagnetic contribution for the EM case $\left(\sim \frac{e^2}{2m}A^2\right)$ as indicated in the previous chapter. This diamagnetic term also leads to the fast oscillating terms for the free field ($\sim 2\omega$), which correspond to the photon-pair production and annihilation as in the case of dynamical Casimir effect [89–92].

42

Moving to the interaction picture with respect to $\tilde{H}_0 = \tilde{H}_O + \tilde{H}_F$ to eliminate the fast dynamics of the system and invoking RWA, we write the interaction Hamiltonian in a simplified form as

$$\tilde{H}_{int} \equiv \hbar \left( \alpha_{OF} \boldsymbol{b}^\dagger \boldsymbol{a} e^{-i\Delta t} + \alpha_{OF}^* \boldsymbol{b} \boldsymbol{a}^\dagger e^{i\Delta t} \right) + \hbar \left( \alpha_{OM} \boldsymbol{b} e^{i\Delta t} + \alpha_{OM}^* \boldsymbol{b}^\dagger e^{-i\Delta t} \right) \left( \tilde{c} + \tilde{c}^\dagger \right)$$

$$+ \hbar \left( \alpha_{MF} \boldsymbol{a} + \alpha_{MF}^* \boldsymbol{a}^\dagger \right) \left( \tilde{c} + \tilde{c}^\dagger \right) \tag{2.3}$$

Here the operators in the interaction picture are defined as $\{\boldsymbol{a}, \boldsymbol{a}^\dagger\} \equiv \{\tilde{a}_\omega e^{i\omega t}, \tilde{a}_\omega^\dagger e^{-i\omega t}\}$ and $\{\boldsymbol{b}, \boldsymbol{b}^\dagger\} \equiv \{\tilde{b} e^{i\Omega t}, \tilde{b}^\dagger e^{-i\Omega t}\}$ and the detuning $\Delta \equiv \omega - \Omega$ represents the detuning between the field and the *idf*. The operators $\{\tilde{c}, \tilde{c}^\dagger\}$ correspond to the creation and annihilation operators for the phononic excitations of the *mdf*, with $\tilde{Z} = \sqrt{\frac{\hbar}{2M\mho'}} \left( \tilde{c} + \tilde{c}^\dagger \right) \equiv \sqrt{\frac{\hbar}{M\mho'}} \boldsymbol{Z}$ and $\tilde{P} = -i\sqrt{\frac{\hbar M\mho'}{2}} \left( \tilde{c} - \tilde{c}^\dagger \right) \equiv \sqrt{\hbar M\mho'} \boldsymbol{P}$. The operators $\boldsymbol{Z}$ and $\boldsymbol{P}$ are the dimensionless position and momentum fluctuations for the mirror center of mass. In moving to the interaction picture we have ignored the second order correction terms $(\sim \lambda^2/m)$ in the free field Hamiltonian $\tilde{H}_F$.

The coefficients $\alpha_{ij}$s represent the effective bilinear coupling strengths between the single excitations of the three subsystems with

$$\alpha_{OF} \equiv -\frac{i\lambda}{2} \sqrt{\frac{\Omega}{m\omega\epsilon_0 L}} = -i\sqrt{\frac{\Omega_P \Omega c}{2\omega L}} \tag{2.4}$$

$$\alpha_{OM} \equiv \frac{\Omega\Phi_0 \lambda}{2c} \sqrt{\frac{\Omega}{mM\mho'}} = \Omega\Phi_0 \sqrt{\frac{\Omega_P \Omega \epsilon_0}{2M\mho' c}} \tag{2.5}$$

$$\alpha_{MF} \equiv \frac{\Omega\Phi_0}{2c} \sqrt{\frac{1}{M\mho'\omega\epsilon_0 L}} \left( -\frac{i\lambda^2}{m} + 2\epsilon_0 c\omega R^*(\omega) \right)$$

$$= \frac{\Omega A_0}{L} \sqrt{\frac{\hbar}{2M\mho'}} \left( -\frac{i\Omega_P}{\omega} + R^*(\omega) \right) \tag{2.6}$$

where we have defined the dimensionless field amplitude $A_0 \equiv \Phi_0 / \sqrt{\frac{\hbar}{2\omega\epsilon_0 L}}$.

It can be seen from (2.6) that for a perfectly reflecting mirror $(R^*(\omega) \to -1)$

the second term in the effective coupling strength $\alpha_{MF}$ between the *mdf* and the field is the same as what one finds from standard boundary condition approach [63]. We explain the correspondence with an imperfect mirror in section 2.2.

As we had pointed in (1.36) as well, the two terms in the effective mirror-field coupling $\alpha_{MF}$ denote the interaction mediated via the quantum fluctuations of the *idf* and its classical amplitude respectively. It can then be seen that since the usual boundary condition approach ignores the presence of the quantum fluctuations of the internal degree of freedom, one misses out on the contribution from the first term. Therefore, in the limit where $|R(\omega)| \ll |\Omega_P/\omega|$, the boundary condition approach can no longer be a good description for the system dynamics.

We note that all the effective coupling strengths contain the *idf* mass and charge parameters in the combination $\sim \lambda^2/m$ which corresponds to the plasma frequency $\Omega_P (\equiv \lambda^2/(2m\epsilon_0 c))$, meaning that one can deduce all the effective single excitation couplings ($\alpha_{ij}$s) from the two parameters that also completely characterize the reflection spectrum, $\Omega$ and $\Omega_P$ as defined in section 1.4.2. Thus given the reflection spectrum of a mirror, one can find the parameters $\Omega_P$ and $\Omega$, knowing which at the various effective coupling strengths can be found. Fig.2.1 shows the dependence of the reflection coefficient and these effective couplings on the dimensionless plasma frequency ($\Omega_P/\Omega$) and detuning ($\Delta/\Omega$). This is expected since in our treatment when considering the mean field solutions we assume that the center of mass motion does not determine the *idf*-field interaction, particularly because we assume non-relativistic center of mass motion and that the center of mass motion amplitude is restricted to the Lamb-Dicke limit such that it does not affect the

classical optical properties. Therefore within the current approximations the mean field amplitudes that determine the coupling between the quantum fluctuations of the different subsystems can be deduced from the boundary condition approach.

It can also be observed from (2.4)–(2.6) that the coupling strengths increase as the original *idf*-field coupling $\lambda$ increases and decrease as the *idf* mass $m$ increases, meaning that a "lighter" *idf* leads to stronger effective coupling strengths. Also, a heavier mirror CoM couples more weakly to the *idf* and the field. The effective *idf*-field coupling $\alpha_{OF}$ is independent of the driving field amplitude $\Phi_0$ as expected, since as one sets the drive amplitude to zero it can be seen that there is no mirror-field and *idf*-mirror interaction in second order except the *idf*-field coupling from the direct interaction. To be able to see any coupling and hence entanglement between the mirror and the field in that case one needs to include the higher order terms as was discussed before.

We also note here that in the weak coupling regime where $\Omega_P \ll 1$, the mirror reflectivity and the effective mirror-field coupling strength $\alpha_{MF}$ as a function of the *idf*-field detuning peaks sharply at resonance ($\Delta = 0$) as seen from Fig.2.1(a) and Fig.2.1(d). The field amplitude and detuning with respect to the *idf* change the coupling strengths appreciably. While in the standard treatment of mirror-field interactions via boundary conditions it is common to study the effect of the field intensity on the mirror-field coupling, we highlight that including the presence of *idf* lets us see the effect of the field-*idf* detuning on the mirror-field interaction, allowing us to probe the effective coupling strength as a function of the reflection properties of the mirror.

(a)



(b)



(c)

46
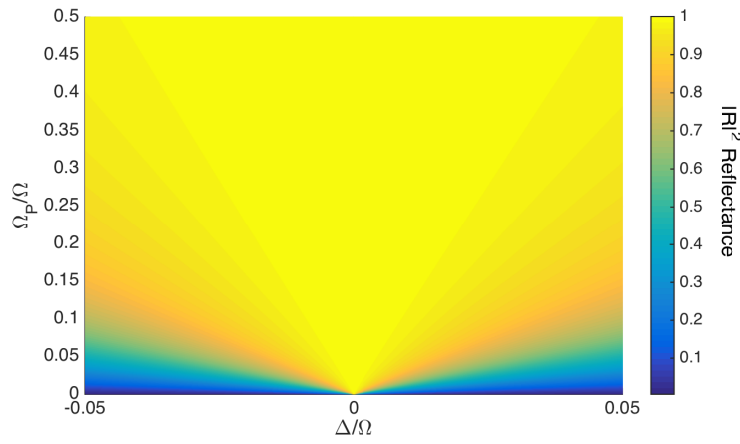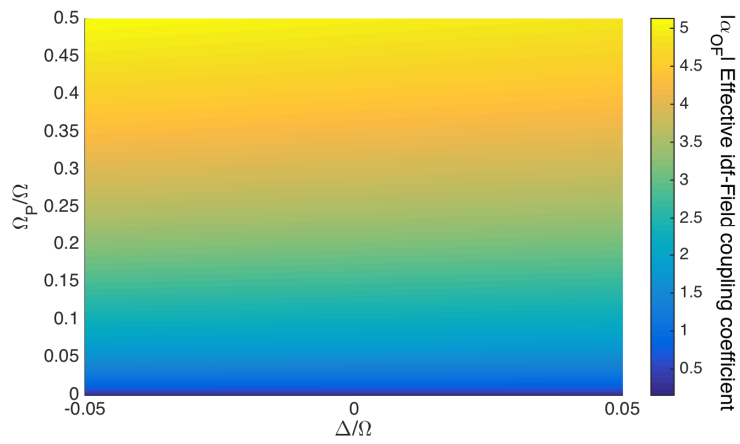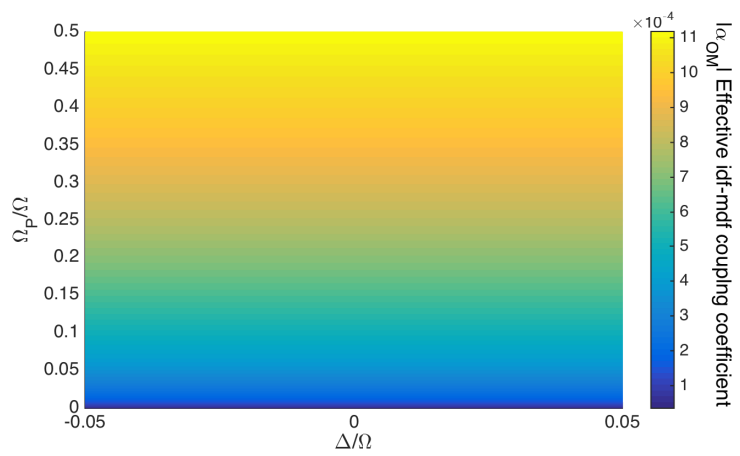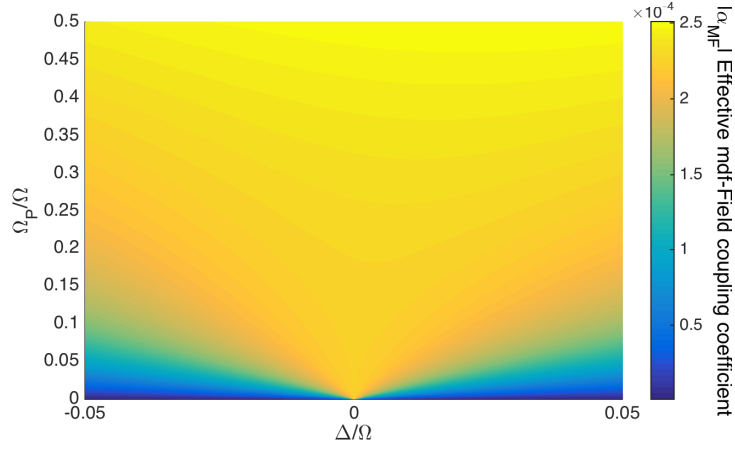
(d)

Figure 2.1: (a) Reflectance as a function of the dimensionless parameter $\Omega_P/\Omega$ (ratio of the plasma frequency to the *idf*'s natural frequency) and the *idf*-field detuning $\Delta/\Omega$. It can be seen that for weaker coupling corresponding to $\Omega_P/\Omega \ll 1$, the reflection spectrum has a sharper resonance. The effective bilinear coupling strengths for both (b)*idf*-field ($\alpha_{OF}$) and (c)*idf*-*mdf* ($\alpha_{OM}$) increase with increasing plasma frequency as $\sim \sqrt{\Omega_P}$. (d)The effective *mdf*-field coupling coefficient ($\alpha_{MF}$) in the weak coupling limit is largely determined by the reflection coefficient, while for strong coupling the fluctuation mediated part becomes relevant, as can be seen from (2.6).

Now we use the interaction Hamiltonian (2.3) to write the equations of motion

in terms of the coupling constants $\alpha_{ij}$s as

$$\frac{\mathrm{d}\boldsymbol{Z}}{\mathrm{d}t} = \mho'\boldsymbol{P} \tag{2.7}$$

$$\frac{\mathrm{d}\boldsymbol{P}}{\mathrm{d}t} = -\mho'\boldsymbol{Z} - 2\left(\mathrm{Re}\alpha_{OM}\mathbf{q} - \mathrm{Im}\alpha_{OM}\boldsymbol{p}\right) - 2\left(\mathrm{Re}\alpha_{MF}\boldsymbol{\Phi} - \mathrm{Im}\alpha_{MF}\boldsymbol{\Pi}\right) - \Gamma\boldsymbol{P} + \boldsymbol{\Xi} \tag{2.8}$$

$$\frac{\mathrm{d}\boldsymbol{q}}{\mathrm{d}t} = \Delta\boldsymbol{p} - |\alpha_{OF}|\boldsymbol{\Phi} - 2\mathrm{Im}\alpha_{OM}\boldsymbol{Z} \tag{2.9}$$

$$\frac{\mathrm{d}\boldsymbol{p}}{\mathrm{d}t} = -\Delta\boldsymbol{q} - |\alpha_{OF}|\boldsymbol{\Pi} - 2\mathrm{Re}\alpha_{OM}\boldsymbol{Z} \tag{2.10}$$

$$\frac{\mathrm{d}\boldsymbol{\Phi}}{\mathrm{d}t} = |\alpha_{OF}|\boldsymbol{q} - 2\mathrm{Im}\alpha_{MF}\boldsymbol{Z} \tag{2.11}$$

$$\frac{\mathrm{d}\boldsymbol{\Pi}}{\mathrm{d}t} = |\alpha_{OF}|\boldsymbol{p} - 2\mathrm{Re}\alpha_{MF}\boldsymbol{Z} \tag{2.12}$$

wherein we have redefined the slow moving dimensionless *idf* and the field quadratures as $\boldsymbol{q} \equiv \frac{\boldsymbol{b}e^{i\Delta t} + \boldsymbol{b}^\dagger e^{-i\Delta t}}{\sqrt{2}}$, $\mathbf{p} \equiv -i\frac{\boldsymbol{b}e^{i\Delta t} - \boldsymbol{b}^\dagger e^{-i\Delta t}}{\sqrt{2}}$, $\boldsymbol{\Phi} \equiv \frac{\boldsymbol{a} + \boldsymbol{a}^\dagger}{\sqrt{2}}$ and $\boldsymbol{\Pi} \equiv -i\frac{\boldsymbol{a} - \boldsymbol{a}^\dagger}{\sqrt{2}}$. Also, to account for the fluctuation-dissipation mechanism for the mirror center of mass resulting from its coupling to the thermal bath, we have introduced the mechanical damping $\Gamma$ and noise $\boldsymbol{\Xi}$ for the mirror. Invoking the Born-Markov approximation, the correlation function of the noise is given as $\langle\boldsymbol{\Xi}\left(t\right)\boldsymbol{\Xi}\left(t'\right)\rangle = \frac{4\Gamma k_B T_m}{\hbar\mho}\delta(t-t')$, with $T_m$ as the temperature of the thermal bath.

Now let us consider that the *idf* is coupled to the continuum of field modes with a coupling of the form $\dot{q}\Phi_i$, where $\Phi_i$ represents the i$^{th}$ field mode, leading to a damping coefficient $\gamma_f$. Also, to mimic the scattering of surface charges by lattice ions of the mirror, we introduce a dissipative bath of internal degrees of freedom such that each bath oscillator is coupled to the *idf* with a coupling of the form $q \cdot q_i$, where $q_i$ represents the position variable for the i$^{th}$ bath oscillator, giving an effective damping coefficient of $\gamma_i$ for the *idf*. We write the dynamics of the *idf* including the

phenomenological damping and noise as

$$\frac{\mathrm{d}\boldsymbol{q}}{\mathrm{d}t} = \Delta\boldsymbol{p} - |\alpha_{OF}|\boldsymbol{\Phi} - 2\mathrm{Im}\alpha_{OM}\boldsymbol{Z} - \gamma_f\boldsymbol{q} + \xi_f \tag{2.13}$$

$$\frac{\mathrm{d}\boldsymbol{p}}{\mathrm{d}t} = -\Delta\boldsymbol{q} - |\alpha_{OF}|\boldsymbol{\Pi} - 2\mathrm{Re}\alpha_{OM}\boldsymbol{Z} - \gamma_i\boldsymbol{p} + \xi_i \tag{2.14}$$

where the correlators of the noise operators $\xi_f$ and $\xi_i$ in the Born-Markov approximation are given as $\langle \xi_f(t)\xi_f(t')\rangle = \frac{4\gamma_f k_B T_f}{\hbar\Omega}\delta(t-t')$ and $\langle \xi_i(t)\xi_i(t')\rangle = \frac{4\gamma_i k_B T_i}{\hbar\Omega}\delta(t-t')$ with $T_f$ and $T_i$ corresponding to the temperatures of the field and the *idf* bath.

Now using separation of time scales, we find the steady state *idf* amplitudes as

$$\boldsymbol{q}_{st} = -\frac{\gamma_i\hat{C}_1 + \Delta\hat{C}_2}{\Delta^2 + \gamma_i\gamma_f} \tag{2.15}$$

$$\boldsymbol{p}_{st} = \frac{\Delta\hat{C}_1 - \gamma_f\hat{C}_2}{\Delta^2 + \gamma_i\gamma_f} \tag{2.16}$$

where the operators $\hat{C}_i$s stand for $\hat{C}_1 \equiv |\alpha_{OF}|\boldsymbol{\Phi} + 2\mathrm{Im}\alpha_{OM}\boldsymbol{Z} - \xi_f$ and $\hat{C}_2 \equiv |\alpha_{OF}|\boldsymbol{\Pi} + 2\mathrm{Re}\alpha_{OM}\boldsymbol{Z} - \xi_i$, considering that the dynamics of the *idf* happens at a much faster timescale than all the other variables involved. We note that the steady state amplitudes are small since $\{\gamma_{i,f}, \Delta\}$ exceed all the other time scales for the separation of timescales to be self-consistent. For the case of near perfect reflection since the detuning $\Delta$ is small, for the steady state amplitudes to vanish, we must have $\gamma_{i,f} \gg \Delta$.

For the case of fast *idf* dynamics, we eliminate the *idf* from the equations of

motion for the *mdf* to obtain the effective CoM motion as follows

$$\frac{d^2 \boldsymbol{Z}}{dt^2} = -\mho' \boldsymbol{Z} + \frac{2}{\Delta^2 + \gamma_i \gamma_f} \left( \left( \text{Re}\alpha_{OM}\gamma_i + \text{Im}\alpha_{OM}\Delta \right) \hat{C}_1 + \left( \text{Re}\alpha_{OM}\Delta - \text{Im}\alpha_{OM}\gamma_f \right) \hat{C}_2 \right)$$

$$- 2 \left( \text{Re}\alpha_{MF}\boldsymbol{\Phi} - \text{Im}\alpha_{MF}\boldsymbol{\Pi} \right) - \Gamma \boldsymbol{P} + \boldsymbol{\Xi} \tag{2.17}$$

$$= -\mho'' \boldsymbol{Z} + g_\Phi \boldsymbol{\Phi} + g_\Pi \boldsymbol{\Pi} + \boldsymbol{\Xi}' \tag{2.18}$$

where we have defined the new effective mechanical oscillation frequency and noise

as

$$\mho'' \equiv \mho' + \frac{1}{\gamma_i \gamma_f + \Delta^2} \left( \left( \text{Re}\alpha_{OM}^2 + \text{Im}\alpha_{OM}^2 \right) \Delta + \text{Re}\alpha_{OM}\text{Im}\alpha_{OM} \left( \gamma_i - \gamma_f \right) \right) \tag{2.19}$$

$$\boldsymbol{\Xi}' \equiv \boldsymbol{\Xi} - \frac{2}{\gamma_i \gamma_f + \Delta^2} \left[ \left( \text{Re}\alpha_{OM}\gamma_i + \text{Im}\alpha_{OM}\Delta \right) \xi_f + \left( \text{Re}\alpha_{OM}\Delta - \text{Im}\alpha_{OM}\gamma_f \right) \xi_i \right]$$

$$\tag{2.20}$$

and the effective mirror-field coupling coefficients are given by

$$g_\Phi \equiv -2\text{Re}\alpha_{MF} + \frac{2\left| \alpha_{OF} \right|}{\gamma_i \gamma_f + \Delta^2} \left( \text{Re}\alpha_{OM}\gamma_i + \text{Im}\alpha_{OM}\Delta \right) \tag{2.21}$$

$$g_\Pi \equiv 2\text{Im}\alpha_{MF} + \frac{2\left| \alpha_{OF} \right|}{\gamma_i \gamma_f + \Delta^2} \left( \text{Re}\alpha_{OM}\Delta - \text{Im}\alpha_{OM}\gamma_f \right) \tag{2.22}$$

Here we note that the correction terms from that come from eliminating the *idf* are small since we assume that for the validity of separation of timescales we have $\{\gamma_i, \gamma_f, \Delta\}$ greater than all the other rates involved. Thus having eliminated the *idf* from the equation of motion for the mirror CoM, we can rewrite the effective radiation pressure force from (2.17) as

$$F_{RP}^{st} \equiv g_\Phi \boldsymbol{\Phi} + g_\Pi \boldsymbol{\Pi} \tag{2.23}$$

We note that while the dynamical variables corresponding to the *idf* have been eliminated, the coefficients $g_{\Phi,\Pi}$ are generally dependent on the *idf* parameters.

To compare this with the case of an isolated *idf*, without any coupling to the environment, we can identify the radiation pressure force from (2.8) as

$$\tilde{F}_{rad} \equiv -2\left(\mathrm{Re}\alpha_{OM}\mathbf{q} - \mathrm{Im}\alpha_{OM}\mathbf{p}\right) - 2\left(\mathrm{Re}\alpha_{MF}\boldsymbol{\Phi} - \mathrm{Im}\alpha_{MF}\boldsymbol{\Pi}\right) \qquad (2.24)$$

Here we see that the linearized radiation pressure force depends on both the fluctuations of the *idf* and the field variables. Hence as long as the *idf* fluctuations are non-vanishing, the radiation pressure shot noise is determined by the shot noise of both the field and the *idf*, meaning that in order to go below the standard quantum limit for the radiation pressure force one needs to take into consideration the squeezing of the *idf* quadratures in addition to those of the field [93, 94].

Further, from (2.7)–(2.12) we write the solutions to the equations of motion for the *idf* and the field variables as

$$\mathbf{q}(t) = \mathbf{q}_h(t) + \int_0^t \mathrm{d}t' G_o(t - t')\left(-\Delta|\alpha_{OF}|\boldsymbol{\Pi}(t') - \Delta\alpha_{OM}\mathbf{Z}(t') + 2|\alpha_{OF}|\mathrm{Im}\alpha_{MF}\mathbf{Z}(t')\right)$$

$$(2.25)$$

$$\mathbf{p}(t) = \mathbf{p}_h(t) + \int_0^t \mathrm{d}t' G_o(t - t')\left(\Delta|\alpha_{OF}|\boldsymbol{\Phi}(t') + 2|\alpha_{OF}|\mathrm{Re}\alpha_{MF}\mathbf{Z}(t') - \alpha_{OM}\mathbf{P}(t')\right)$$

$$(2.26)$$

$$\boldsymbol{\Phi}(t) = \boldsymbol{\Phi}_h(t) + \int_0^t \mathrm{d}t' G_f(t - t')\left(\Delta|\alpha_{OF}|\mathbf{p}(t') - 2\mathrm{Im}\alpha_{MF}\mathbf{P}(t')\right) \qquad (2.27)$$

$$\boldsymbol{\Pi}(t) = \boldsymbol{\Pi}_h(t) + \int_0^t \mathrm{d}t' G_f(t - t')\left(-\Delta|\alpha_{OF}|\mathbf{q}(t') - |\alpha_{OF}|\alpha_{OM}\mathbf{Z}(t') - 2\mathrm{Re}\alpha_{MF}\mathbf{P}(t')\right)$$

$$(2.28)$$

Here we have defined the *idf* and the field Green's functions as $G_O(t) \equiv \frac{\sin(\sqrt{|\alpha_{OF}|^2 + \Delta^2}t)}{\sqrt{|\alpha_{OF}|^2 + \Delta^2}}$ and $G_f(t) \equiv \frac{\sin(|\alpha_{OF}|t)}{|\alpha_{OF}|}$ and the homogeneous solutions as $\{\mathbf{q}_h, \mathbf{p}_h, \boldsymbol{\Phi}_h, \boldsymbol{\Pi}_h\}$. It

can be seen that the frequency of oscillations for the slow moving *idf* variables is $\Omega_{idf} \equiv \sqrt{|\alpha_{OF}^2| + \Delta^2}$ and that for the slow moving field variables is $\Omega_f \equiv |\alpha_{OF}|$. In the steady state limit, we can use these solutions to rewrite the equation of motion for the late time mirror CoM dynamics as

$$M \left( \partial_t^2 + \mho'^2 \right) \mathbf{Z}(t) + \Gamma \frac{d\mathbf{Z(t)}}{dt} + \int_0^t dt' G_o(t - t') \left( -\Delta \alpha_{OM}^2 + 2\alpha_{OF} \mathrm{Im}\alpha_{MF}\alpha_{OM} \right) \mathbf{Z}(t') =$$

$$\int_0^t dt' G_o(t - t') \left( 2\alpha_{OM}\Delta|\alpha_{OF}|\mathbf{\Pi}(t') \right) + \int_0^t dt' G_f(t - t') \left( 2\mathrm{Re}\alpha_{MF}\Delta|\alpha_{OF}|\mathbf{p}(t') \right.$$

$$\left. + 2\mathrm{Im}\alpha_{MF}\Delta|\alpha_{OF}|\mathbf{q}(t') \right) + \mathbf{\Xi} \qquad (2.29)$$

On the left side one can identify the two terms in the integral as the retarded influence of mirror-idf-idf-mirror interaction and the mirror-idf-field-mirror interaction respectively. The first term on the right side denotes the mirror being driven by the *idf*-influenced field and the second term stands for the mirror being driven by the field-influenced *idf*. We can see that in the absence of any detuning the CoM motion is only driven by the thermal noise term.

At this point one can also make a crucial observation that for a strongly damped *idf* coupled to two separate baths, if we compare the dynamics for the mirror center of mass and the field with what one obtains from the usual boundary condition considerations we obtain an agreement between the two if the steady state *idf* amplitudes are vanishingly small. We illustrate this comparison in detail in the following section.

## 2.2 Comparison with the boundary condition approach

Let us consider the mirror-field interaction in terms of the radiation pressure force exerted by the field on the mirror using the boundary condition approach, as is prevalent in the literature. We assume that the mirror is generally imperfect and interacts with a scalar field in a region of length $L$. Now similar to the approach of [84], one can consider a co-moving frame of reference with respect to the mirror center of mass to write the Lagrangian density of the field as $\sim \left(\frac{1}{2}\epsilon E'^2 - \frac{1}{2\mu_0}B'^2\right)$, with $E'$ and $B'$ being the electric and magnetic fields in the co-moving frame. Then in the lab frame, the Lagrangian for the oscillating mirror+field system can be written as

$$\mathcal{L}_{BC} = \frac{1}{2}M\dot{Z}^2 - \frac{1}{2}M\mho^2 Z^2 + \int_0^L \mathrm{d}x \left[\frac{1}{2}\epsilon\left((\partial_t\Phi)^2 - c^2(\partial_x\Phi)^2\right) + \dot{Z}(\epsilon - 1)(\partial_t\Phi)(\partial_x\Phi)\right]$$

(2.30)

where we have kept terms upto first order in $\dot{Z}$ from the inverse Lorentz transformation, and the dielectric permittivity is defined as, say, $\epsilon(x) = \epsilon_0(1 + \chi\delta(x - Z))$ for an infinitely thin dielectric slab. Now in the non-relativistic limit, we drop the velocity dependent term and obtain the Euler-Lagrange equation of motion for the mirror center of mass as

$$\ddot{Z} + \mho^2 Z = -\frac{1}{2M}\epsilon_0 c^2 (\partial_x\Phi)^2 |_{\bar{Z}_-}^{\bar{Z}_+}$$

(2.31)

which agrees with what we found in (1.8) in section 1.4.1 and also matches up with equation (8) of [84] in the limit of an infinitely thin dielectric membrane where $d \to 0$ and $\chi \to \infty$. While [84] talks of a dielectric slab in a cavity, a more specific

situation than what we had considered in the simplistic MOF setup, at the level of the formal expression for the radiation pressure force where we have left the boundary conditions arising from the *idf*-field interaction unspecified we find an agreement between the two approaches. This further reaffirms our intuition that the difference between the a boundary condition approach and a microscopic model arises when considering the dynamical participation of the *idf* explicitly, which in the above expression would show up as the difference in the field configurations on the RHS.

Now, we use the radiation pressure force $\left( F_{RP} \equiv -\frac{1}{2M}\epsilon_0 c^2 \left(\partial_x \Phi\right)^2 \big|_{\bar{Z}_-}^{\bar{Z}_+} \right)$ from the above expression to write the linearized Hamiltonian for the mirror+field system as

$$\tilde{H}_{BC} = \frac{\hbar \mho}{2}\left(\boldsymbol{P}^2 + \boldsymbol{Z}^2\right) + \int_0^L \mathrm{d}x \left(\frac{\tilde{\Pi}^2}{2\epsilon_0} + \frac{\epsilon_0}{2}c^2 \left(\partial_x \tilde{\Phi}\right)^2\right) - \epsilon_0 c^2 \left(\partial_x \bar{\Phi}\partial_x \tilde{\Phi}\right)\big|_{\bar{Z}_-}^{\bar{Z}_+} Z_{ZPM}\boldsymbol{Z}$$

(2.32)

where we use the dimensionless position and momentum fluctuations $\boldsymbol{Z}$ and $\boldsymbol{P}$ for the mirror center of mass as in (2.7)–(2.12).

Now assuming that the field has only one mode, we use the plane wave ansatz in (1.18) for the classical part of the field and (2.1) for the quantum fluctuations to rewrite the Hamiltonian as

$$\tilde{H}_{BC} = \frac{\hbar \mho}{2}\left(\boldsymbol{P}^2 + \boldsymbol{Z}^2\right) + \hbar\omega \boldsymbol{a}^\dagger \boldsymbol{a} - \hbar\left(\frac{\Omega}{L}Z_{ZPM}A_0\right)\left(R^*\left(\omega\right)\boldsymbol{a} + R\left(\omega\right)\boldsymbol{a}^\dagger\right)\boldsymbol{Z} \quad (2.33)$$

Here the pre-factor $\left(\frac{\Omega}{L}Z_{ZPM}A_0\right)$ in the interaction term is the standard optomechanical coupling as in [63] with $Z_{ZPM} \equiv \sqrt{\frac{\hbar}{M\mho}}$ as the zero point motion length for the center of mass motion and $A_0$ as the dimensionless field amplitude. We note

54

that here we have implicitly assumed a weak mirror-field interaction so that the quantum fluctuations of the field on the either side of the mirror remain uniform in the space without any discontinuity across the mirror center of mass position.

Now moving to a rotating frame with respect to the free field Hamiltonian $\left(\boldsymbol{H}_F \equiv \hbar\omega\boldsymbol{a}^\dagger\boldsymbol{a}\right)$ leads us to the following equations of motion for the dimensionless field and mirror variables

$$\frac{\mathrm{d}\boldsymbol{Z}}{\mathrm{d}t} = \mho\boldsymbol{P} \tag{2.34}$$

$$\frac{\mathrm{d}\boldsymbol{P}}{\mathrm{d}t} = -\mho\boldsymbol{Z} + \sqrt{2}\mathrm{Re}\beta_{MF}\boldsymbol{\Phi} - \sqrt{2}\mathrm{Im}\beta_{MF}\boldsymbol{\Pi} - \Gamma P + \Xi \tag{2.35}$$

$$\frac{\mathrm{d}\boldsymbol{\Phi}}{\mathrm{d}t} = \sqrt{2}\mathrm{Im}\beta_{MF}\boldsymbol{Z} \tag{2.36}$$

$$\frac{\mathrm{d}\boldsymbol{\Pi}}{\mathrm{d}t} = \sqrt{2}\mathrm{Re}\beta_{MF}\boldsymbol{Z} \tag{2.37}$$

where we have defined the effective mirror field coupling strength from the boundary condition approach as

$$\beta_{MF} \equiv \frac{\Omega}{L}Z_{ZPM}A_0R^*\left(\omega\right) \tag{2.38}$$

It can be seen that in the weak coupling limit $(\Omega_P/\Omega \ll 1)$, the effective mirror-field coupling coefficient in (2.6) reduces to $\alpha_{MF} \approx -\beta_{MF}/\sqrt{2}$ and in the limit of vanishingly small *idf* fluctuations the coupled mirror-field equations of motion in (2.7), (2.8), (2.11) and (2.12) are the same as (2.34)–(2.37). From (2.15) and (2.16), it can be seen that the steady state *idf* amplitudes are negligibly small in the strong *idf* damping and/or large *idf*-field detuning regime.

To further demonstrate an agreement between the two approaches, in Fig. 2.2 we look at the mirror-field entanglement found from the boundary condition approach and the MOF model. We find that, as expected for a strongly damped

internal degree of freedom one sees a perfect overlap of the log negativity from either approach. More importantly, we also note that that when the *idf* is undamped one can possibly get a larger steady-state optomechanical entanglement.
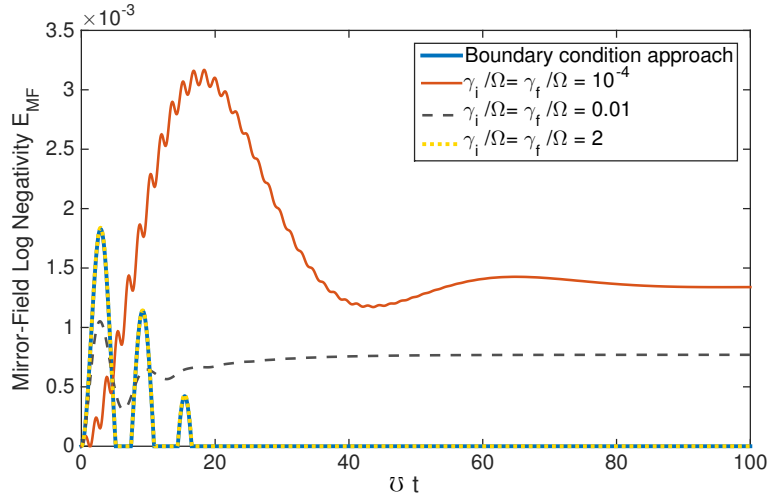


Figure 2.2: Evolution of mirror-field entanglement as measured by the logarithmic negativity $E_{MF}$ (see Appendix A for definition) as obtained from the boundary condition approach and the coupled MOF dynamics. We find that for an isolated *idf* the time scale for entanglement is largely determined by the effective *idf*-field coupling ($\alpha_{OF}$). The two approaches concur in the weak coupling limit for a strongly damped *idf* as seen from the overlap of the solid blue and dashed yellow curves (the differences between the two are too small for the resolution of the plot). The parameters values, in natural units where c=1, $\hbar = 1$ and $e = \sqrt{4\pi\alpha}$ used here are $m = 0.001$, $\Omega = 100$, $M = 10$, $\mho = 0.1$, $\Omega_P = 0.05$, $A_0 = 10^{-4}$ and $T_m = T_i = 0.1$. The effective *idf*-field coupling strength, $|\alpha_{OF}|/\mho \approx 16$, determines the time scale for entanglement dynamics for the case of an undamped *idf*.

## 2.3 Entanglement dynamics in the coupled MOF system

In this section we briefly outline a method for calculating the covariance matrix for the coupled MOF system numerically and use it to obtain the entanglement between the mirror CoM and the field as a function of various parameters involved. To evaluate the covariance matrix of the three coupled subsystems one can find the normal modes of the system from (2.7)–(2.12) and their time evolution to obtain the expectation values of the operator correlations numerically. Defining the MOF covariance matrix $\mathcal{V}_{MOF}$ as

$$
\mathcal{V}_{MOF} = \begin{pmatrix} \mathbf{V_{MM}} & \mathbf{V_{MF}} & \mathbf{V_{OM}} \\ \mathbf{V_{MF}^T} & \mathbf{V_{FF}} & \mathbf{V_{OF}} \\ \mathbf{V_{OM}^T} & \mathbf{V_{OF}^T} & \mathbf{V_{OO}} \end{pmatrix} \tag{2.39}
$$

where the on-diagonal sub-matrix $\mathbf{V_{kk}}$ stands for the covariance matrix of the $k^{th}$ reduced subsystem, defined as $(\mathbf{V_{kk}})_{ij} \equiv \frac{1}{2}\left\langle \{X_i^{(k)}, X_j^{(k)}\}\right\rangle$, with $X_i^{(k)}$ and $X_j^{(k)}$ representing the i and j quadratures corresponding to the position and momentum variables of the $k^{th}$ reduced subsystem, more explicitly $\boldsymbol{X}^{(k)} \equiv \{\tilde{x}^{(k)}, \tilde{p}^{(k)}\}$. Here, $\{\mathcal{O}_1, \mathcal{O}_2\}$ denotes the anti-commutator between the operators $\mathcal{O}_1$ and $\mathcal{O}_2$. The off-diagonal sub-matrix $\mathbf{V_{kl}}$ consists of the correlations between the $k^{th}$ and the $l^{th}$ subsystems, such that $(\mathbf{V_{kl}})_{ij} \equiv \frac{1}{2}\left\langle \{X_i^{(k)}, X_j^{(l)}\}\right\rangle$, where the i and j quadrature components belong to different subsystems. The average is taken over the initial density operator of the three subsystems at $t = 0$ which we assume to be in a thermal state with a temperature determined by that of the corresponding bath.

More explicitly, the initial density matrix of the overall system can be written as

$$\rho(0) = \rho_M^{T_m} \otimes \rho_i^{T_i} \otimes \rho_f^{T_f} \tag{2.40}$$

where the density matrix $\rho_k^{T_k}$ for subsystem $k$ corresponds to a thermal distribution with temperature $T_k$.

To specifically find the CoM-field entanglement, we then choose to look at the part of the covariance matrix that represents the mirror CoM and field reduced covariance matrices and correlations, that is,

$$\mathcal{V}_{MF} = \begin{pmatrix} \mathbf{V_M} & \mathbf{V_{MF}} \\ \mathbf{V_{MF}^T} & \mathbf{V_F} \end{pmatrix} \tag{2.41}$$

and find the logarithmic negativity $E_N^{MF}$ as obtained based on the positive partial transpose (PPT) criteria for determining separability (see Appendix A for details). It can be shown that calculating the MF entanglement from the sub covariance matrix $\mathcal{V}_{MF}$ is equivalent to coarse-graining over the internal degree of freedom and then finding the MF entanglement, we illustrate this point in detail in Appendix B.

Having found the reduced covariance matrix for the coupled mirror CoM and field mode, we now consider the entanglement dynamics between the two as a function of the various parameters involved. The parameters pertaining to the three subsystems and the assumptions made are summarized in table 2.1.

For example, in the previous section in Fig. 2.2, we looked at the entanglement between the mirror center of mass and the field as a function of the *idf* damping rates $\gamma_i$ and $\gamma_f$. As pointed earlier the boundary condition limit is approached when the internal degree of freedom is strongly damped, which makes physical sense since

| Mirror center of mass | Mirror's internal degree of freedom | Field |
|---|---|---|
| $\mho$ (Frequency of the mechanical oscillator) | $\Omega$ (*idf* resonance frequency) | $\omega$ (Frequency of the field mode) |
| $M$ (Mirror mass ) | $\Omega_P$ (*idf*-field coupling) | $\Phi_0$ (Field amplitude) |
| $\Gamma$ (Mechanical damping) | $\gamma_f$, $\gamma_i$ (*idf* damping rates from interaction with the two baths) | $\Gamma_F$ (Field mode damping) |
| $T_m$ (Mechanical bath temperature) | $T_f$, $T_i$ (Field and *idf* bath temperatures) | $T_f$ (Field bath temperature) |

Table 2.1: Parameters pertaining to the three subsystems – the mirror's *mdf* , *idf* and the single mode field $\Phi_\omega$. The assumptions restricting these parameters in our analysis are 1.) $\mho \ll \Omega$, for a slow-moving mirror, 2.) weak-coupling between the *idf* and the field such that $\Omega_P \ll \Omega$, 3.) $\Delta \ll \Omega$ for the rotating-wave approximation, 4.) $|\Phi_0|^2 \ll \frac{M\mho^2 c}{\Omega^3 \epsilon_0}$ for weak-driving to ensure small amplitude of the mirror motion and 5.) Markovian noise and Ohmic dissipation for the three subsystems, such that $\hbar\Gamma \ll k_B T_m$ and $\hbar\gamma_{i,f} \ll k_B T_{i,f}$.

one would expect that an instantaneous response from the *idf* should correspond to the limit $\gamma_{i,f}/\Omega \gg 1$. We note that in our simplistic model of the internal structure of the mirror one requires two baths to see this correspondence, so that the steady state amplitudes for the *idf* go to zero. For realistic mirrors, the effect of coupling

to one of the baths would correspond to the presence of many internal degrees of freedom as we suggested earlier. It can also be observed from Fig. 2.2 that for an isolated *idf* there are faster oscillations at a frequency determined by the effective *idf*-field coupling coefficient $|\alpha_{OF}|$. This can be understood from considering the solutions to the equations of motion for an isolated *idf* (2.25)–(2.28). We also note that on increasing the *idf* damping there is a smaller steady state entanglement between the mirror CoM and the field for the chosen set of parameter values as detailed in the caption of Fig. 2.2. Similarly, it can also be seen from (2.15) and (2.16) that if the field mode is far detuned from the resonance of the *idf*, then the *idf* amplitudes vanish as well. For a far detuned field, the boundary condition limit can be observed with only one of the damping rates ($\gamma_i$ or $\gamma_f$) being large. On the other hand, if the detuning of the field mode is small with respect to the internal resonance and the *idf* is underdamped, we expect to see a deviation from the boundary condition approach. For this parameter regime one can observe some interesting features in the entanglement dynamics as shown in Fig. 2.3. As was discussed before, at the *idf*-field resonance ($\Delta \to 0$) the reflection coefficient and hence the effective mirror-field coupling strength goes to its maximum value (See Fig.2.1(a) and Fig. 2.1(d)). As a result, we observe in Fig.2.3 that there is a peak in the mirror-field entanglement near *idf*-field resonance. This effect is not considered in the standard treatment of optomechanical interactions since the internal degree is coarse-grained over a priori to arrive at the boundary conditions for the field. The peak in the entanglement is more pronounced in the weak-coupling regime where the reflection coefficient has a sharper peak at resonance as seen from Fig.2.1(a) and
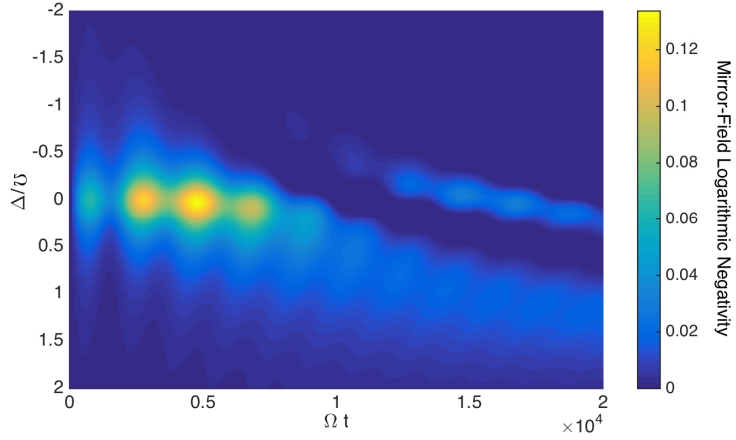
Figure 2.3: Mirror-Field entanglement given by the logarithmic negativity for an undamped *idf* as a function of the dimensionless *idf*-field detuning ($\Delta/\mho$) and dimensionless time ($\Omega t$). We observe that the entanglement peaks for a resonant *idf*-field interaction at ($\Delta/\mho = 0$) and for $\Delta/\mho = -1$ ($\Omega = \omega + \mho$), the entanglement is sustained for longer times. The oscillation time scales are determined by the effective *idf*-field coupling ($|\alpha_{OF}|$). The parameters values, in units where c=1, $\hbar = 1$ and $e = \sqrt{4\pi\alpha}$, used here are $m = 0.001$, $\Omega = 100$, $M = 10$, $\mho = 0.1$, $\Omega_P = 0.05$, $A_0 = 10^{-4}$ and $T = 1000$.

Fig.2.1(d). It can also be observed that for $\Delta/\mho = -1$ or equivalently $\Omega = \omega + \mho$, the entanglement is sustained for longer times. Physically, this pertains to the process wherein a field photon and a mirror phonon combine to give a single *idf* excitation (or vice versa), corresponding to the two-mode squeezing Hamiltonian which then entangles the field and the mirror modes as a result of the interaction. Such an observation had also been made in [63] for the case of a cavity driven with a red detuned drive in the sideband resolved regime where it was shown that the steady

state entanglement goes to a maximum when the cavity-drive detuning was equal to the mechanical oscillation frequency. Drawing an analogy between the two cases, we find that cavity resonance for the usual cavity optomechanical setups is similar to the *idf* in the MOF model in that they both mediate the interaction between the mechanical motion of the mirror and the external field.

In the following subsection, we consider the case of an atom interacting with a field as an example to make some numerical estimates for a realistic setup .

## 2.3.1   Atom-Field Optomechanical Entanglement from the MOF model

Let us consider an atom interacting with at single mode cavity field as an optomechanical element described by the MOF model. As we have pointed earlier for the case of an isolated atom the role of its internal electronic degrees of freedom is indispensable. Here we use the MOF model to describe the atom-field interaction within a cavity, using some typical numbers from the experiment by Maunz *et al.* [95, 96] to find the entanglement between the atomic CoM motion and the field.

First we show that our analysis is readily generalizable to 3+1 dimensions by changing the normalization factors for the field appropriately. Rewriting the original action as

$$
S = \int \mathrm{d}t \left[ \left( \frac{1}{2} M \dot{\boldsymbol{R}}^2 - \frac{1}{2} M \mho^2 \boldsymbol{R}^2 \right) + \left( \frac{1}{2} m \dot{\boldsymbol{q}}^2 - \frac{1}{2} m \Omega^2 \boldsymbol{q}^2 \right) \right.
$$
$$
\left. + \int \mathrm{d}^3 \boldsymbol{r} \frac{\epsilon_0}{2} \left\{ (\partial_t \boldsymbol{\Phi})^2 - c^2 \left( \boldsymbol{\nabla_r} \times \boldsymbol{\Phi} \right)^2 + \lambda \dot{\boldsymbol{q}} \cdot \boldsymbol{\Phi} \delta^3 (\boldsymbol{r} - \boldsymbol{R}) \right\} \right] \qquad (2.42)
$$

where $\boldsymbol{R}$ now refers to the mirror's CoM coordinates, $\boldsymbol{q}$ is the 3 dimensional *idf* amplitude, say, representing the motion of an electron within the atom and $\boldsymbol{\Phi}$ is the

vector potential of the EM field. We note here that the dimensions of the vacuum permittivity change from $\epsilon_0^{(1D)} \sim \frac{(\text{Charge})^2(\text{Time})^2}{(\text{Mass})(\text{Length})}$ to $\epsilon_0^{(3D)} \sim \frac{(\text{Charge})^2(\text{Time})^2}{(\text{Mass})(\text{Length})^3}$ by a factor of $(\text{Length})^{-2}$. In the following we shall argue that this factor roughly corresponds to the cross sectional area of the driving field. Similarly, for the quantized field the normalization factor becomes $\sqrt{\frac{\hbar}{2\epsilon_0 \omega L}} \rightarrow \sqrt{\frac{\hbar}{2\epsilon_0 \omega \mathcal{A} L}}$. Also, for relating the power $\mathcal{P}$ of the incident drive to the vector potential, one would use $\Phi_0 = \frac{1}{\omega}\sqrt{\frac{\mathcal{P}}{\mathcal{A}\epsilon_0 c}}$ instead of $\Phi_0 = \frac{1}{\omega}\sqrt{\frac{\mathcal{P}}{\epsilon_0 c}}$ in 1+1 dimensions.

From (2.42) it can be seen that the equations of motion for the classical solutions of the coupled field and *idf* degrees of freedom as in (1.3) and (1.4) for 3+1 D become

$$\ddot{\bar{q}} + \Omega^2 \bar{q} = -\frac{\lambda}{m}\dot{\bar{\Phi}}\left(\bar{R}, t\right) \tag{2.43}$$

$$\epsilon_0 \left(\ddot{\bar{\Phi}}\left(r, t\right) - c^2 \nabla_r^2 \bar{\Phi}\left(r, t\right)\right) = \lambda \dot{\bar{q}}\delta^3(r - \bar{R}) \tag{2.44}$$

Now considering that we have a driving field of the form $\mathbf{\Phi} = \mathbf{\Phi}_0 \frac{\Omega}{\omega} f(x, y)g(z, t)$, where $f(x, y)$ represents the gaussian transverse mode function of the field and the longitudinal part $g(z, t)$ similar to the 1+1 D plane wave ansatz can be written as

$$g(z, t) = e^{-i\omega t}\left[\left(e^{ik_z z} + e^{-ik_z z}R(\omega)\right)\Theta(\bar{Z} - z) + e^{ik_z z}T(\omega)\Theta(z - \bar{Z})\right] + H.C. \tag{2.45}$$

For the purposes of rough estimation we assume that the atom does not scatter in the transverse directions such that the transverse mode function $f(x, y)$ is continuous across the position of the atom. Integrating the field equation of motion (2.44) around the position of the atom $\bar{Z}$ in z and over the $x$-$y$ plane, we obtain the

63

"electron current"

$$\lambda\dot{\bar{q}} = -\epsilon_0 c^2 \boldsymbol{\Phi}_0 \frac{\Omega}{\omega} \left( \int_{-\infty}^{\infty} \mathrm{d}x \int_{-\infty}^{\infty} \mathrm{d}y f(x,y) \right) \partial_z \left( g(z) \right) |_{\bar{Z}^-}^{\bar{Z}^+} \tag{2.46}$$

$$= -2i\epsilon_0 k_z c \boldsymbol{\Phi}_0 \frac{\Omega}{\omega} \mathcal{A} R(\omega) e^{-i\omega t} + H.C. \tag{2.47}$$

where in the last step we have replaced the integral over the transverse mode function $\mathcal{A} \equiv \left( \int_{-\infty}^{\infty} \mathrm{d}x \int_{-\infty}^{\infty} \mathrm{d}y f(x,y) \right)$ by defining the cross-sectional area of the incident beam as $\mathcal{A}$.

Also, solving for steady-state *idf* dynamics from (2.43) we find

$$\lambda\dot{\bar{q}} = \frac{-\omega^2 \lambda^2}{m\left(\omega^2 - \Omega^2\right)} \frac{\Omega}{\omega} \boldsymbol{\Phi}_0 f(\bar{X},\bar{Y}) T(\omega) e^{-i\omega t} + H.C. \tag{2.48}$$

Further assuming that the normalized mode function $f(\bar{X},\bar{Y}) = 1$ at the atomic CoM position, from (2.47) and (2.48) one can obtain the reflection coefficient as

$$R(\omega) = \frac{-i\lambda^2\omega}{i\lambda^2\omega + 2m\mathcal{A}\epsilon_0 c(\omega^2 - \Omega^2)} = \frac{-i\Omega_P^{(3D)}\omega}{i\Omega_P^{(3D)}\omega + (\omega^2 - \Omega^2)} \tag{2.49}$$

where we have defined the 3D plasma frequency as

$$\Omega_P^{(3D)} \equiv \frac{\lambda^2}{2m\epsilon_0 c\mathcal{A}} \tag{2.50}$$

Thus, from the above expression and general dimensional considerations it can be seen that in going from 1+1 D to 3+1 D, one can replace the vacuum permittivity by $\epsilon_0 \to \epsilon_0 \mathcal{A}$, where $\mathcal{A}$ is some characteristic cross-sectional area, which in this case corresponds to the cross section of the beam.

Now to identify the various degrees of freedom from our model in the given setup, we note that the atomic CoM motion corresponds to the mechanical degree of freedom, assuming that the atom sits in a harmonic trapping potential, such that

we have for the *mdf* parameters – $M = 1.4 \times 10^{-25}$ kg as the atomic mass of Rb$^{85}$, $\mho \approx 100$ kHz as the trap frequency from [96], $\Gamma \approx 10 s^{-1}$ from typical trap lifetimes as in [95, 96] and temperatures for the mechanical bath as $T_m \sim 1$ mK.

For the field, we choose $\omega = \Omega + \Delta_a$, where $\Delta_a \approx 100$ MHz is the detuning of the cavity field with respect to the atomic resonance. The cavity damping rate for a typical $Q \approx 5 \times 10^5$ is $\Gamma_F \sim \frac{c}{QL} \approx 2.5$ MHz, given the cavity length of $L = 120\mu$m. We assume the input power to be $\mathcal{P} \approx 0.01$ pW, such that $\Phi_0 = \frac{1}{\omega}\sqrt{\frac{\mathcal{P}Q}{\mathcal{A}\epsilon_0 c}} \approx 2 \times 10^{-14}$ Vs/m, where the beam cross sectional area $\mathcal{A} \approx 7 \times 10^{-10}$ m$^2$. The vector potential associated with a single photon is $\Phi_{00} \approx 1.7 \times 10^{-13}$ Vs/m. We note that the power inside the cavity is enhanced by the quality factor and one would like to ensure that it remains small enough so that the higher lying levels in the harmonic oscillator model of the *idf* do not get populated.

The internal degree of freedom can be identified as the electronic transitions between the different levels of the atom, which we assume to be harmonic as well with a frequency given by the transition frequency for the $5^2 S_{1/2} F = 3 \leftrightarrow 5^2 P_{3/2} F = 4$ transition, such that $\Omega/(2\pi c) \approx \frac{1}{780 \times 10^{-9}}$ m$^{-1}$. While the linear model is not a very good approximation generally, in the weak-excitation limit one can map it to the two-level approximation, where it should work as well.

From (2.50), the "plasma frequency" is given as $\Omega_P = \frac{e^2}{2m_e \epsilon_0 c \mathcal{A}} \approx 7.5 \times 10^3$ Hz. Considering that the atom-electric field dipole coupling for a single photon (vacuum Rabi frequency) in our model can be expressed as $\hbar g = \frac{e}{m_e} p_{zpf} \Phi_{zpf}$, where $p_{zpf} = \sqrt{\frac{\hbar m_e \Omega}{2}}$ and $\Phi_{zpf} = \sqrt{\frac{\hbar}{2\omega\epsilon_0 \mathcal{A}L}}$ are the zero point fluctuations of the electron

momentum and the field vector potential, such that

$$g^{(MOF)} = \frac{e}{\sqrt{2m_e\epsilon_0 c\mathcal{A}}}\sqrt{\frac{\Omega c}{2\omega L}} = \sqrt{\Omega_P}\sqrt{\frac{\Omega c}{2\omega L}} \tag{2.51}$$

Evaluating this for the given parameter values we find $g^{(MOF)} \approx 97$ MHz, which agrees extremely well with the value of the vacuum Rabi frequency $g \approx 100$ MHz from [95].

The damping rate for the *idf* is given by the cavity modified damping $\gamma_f \approx$ 10 MHz from the coupling of the electron to the field mode continuum. We note that there is only one bath for the *idf* in this case unlike what we had considered earlier when comparing our model with the boundary condition approach. Thus setting $\gamma_i = 0$, we observe that for small enough detunings the coupled motion-spin-field dynamics for an atom interacting with the field will differ from those obtained from boundary condition considerations, this can be seen from comparing (2.7), (2.8), (2.11) and (2.12) to (2.34)–(2.37) respectively.

Using these parameter values we find the effective coupling strength between the *idf* and the field as $\alpha_{OF} \sim 0.1$ GHz, the effective *idf-mdf* coupling as $\alpha_{OM} \sim 60$ MHz and the effective *mdf*- field coupling to be $\alpha_{MF} \sim 60$ MHz. We note that the reflection coefficient being small $R(\omega) \sim 10^{-4}$, the imaginary part of the effective *mdf*-field coupling coefficient from the fluctuation mediated coupling is much larger than that mediated by the classical *idf* amplitude, such that $\text{Im}\alpha_{MF}/\text{Re}\alpha_{MF} \sim 10^{13}$, which also alludes to the fact that one can not use boundary conditions to describe the dynamics for the coupled atom-spin-field system.

(a) Entanglement between the atomic CoM motion and the field mode as a function of the detuning of the field with respect to the atomic resonance frequency $\Omega$ and time. We fix all the other parameters as $Q = 5 \times 10^5$ for the quality factor of the cavity, $L = 120\mu$m for the cavity length, $\mathcal{A} \approx \pi(15\mu \text{ m})^2$ for the field cross sectional area, $\mathcal{P} = 0.01$ pW for the driving field power, $2\pi c/\Omega = 780$ nm for the $idf$ resonance, $m = m_e$ for the $idf$ mass, $\lambda = e$ for the $idf$-field coupling strength, $\gamma_f \approx 18$ MHz for the $idf$ damping, $M = 1.4 \times 10^{-25}$ kg for the atomic mass, $\mho = 100 kHz$ for the trap frequency, $T_m = 1$ mK for the temperature of the mechanical and $T_i = T_f = 100$ K for the field and the $idf$ bath temperatures.
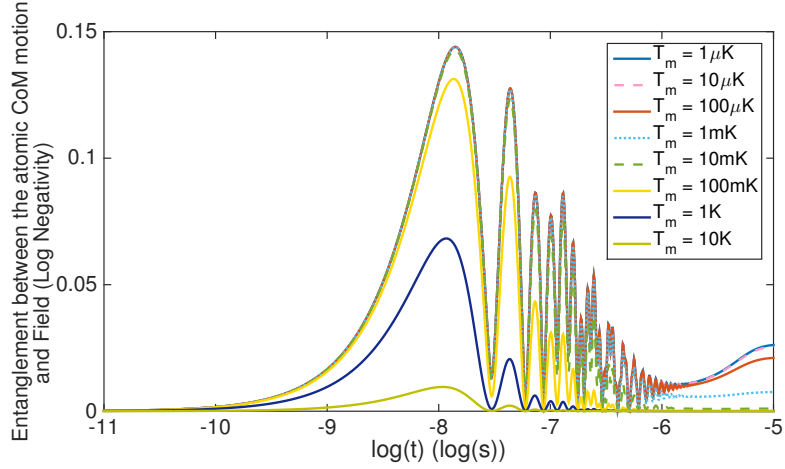
(b) Entanglement between the atomic CoM motion and the field mode as a function of the temperature of the mechanical bath, all the other values being fixed as detailed in (a) and the field detuning set at 100 MHz.
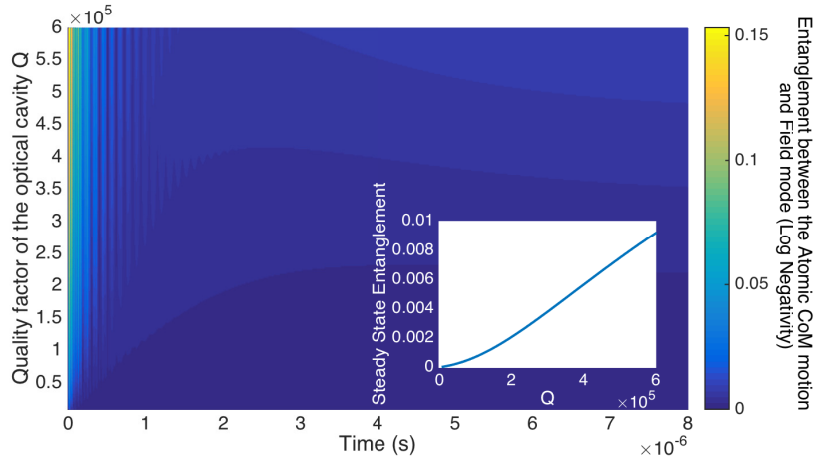


(c) Atom-field optomechanical entanglement as a function of the cavity Q factor, which changes the field damping rate and the field amplitude in turn, all the other values being fixed as detailed in (a) and the field detuning set at 100 MHz.

Figure 2.3: Optomechanical entanglement between the motion of a trapped atom in a cavity and the cavity field, with parameter values taken from the experiment by Maunz *et al.* [95]. We choose different values of the field detuning, temperature for the mechanical bath and cavity Q factors.

# Chapter 3:    Two Mirror Interaction in the Mirror-Oscillator-Field (MOF) model

While quantum mechanics has been exceedingly successful in describing a range of physical phenomena in the quantum realm, the emergence of classical behavior from quantum theory still remains to be understood at a concrete level. For example, there is no detailed explanation as to why the quintessential features of quantum theory such as superposition and entanglement disappear as one goes to macroscopic scales. Several existing justifications for such observations range from the lack of experimental sophistication, in that one can not isolate the system well enough from its environment to prevent decoherence, to more fundamental constraints coming from models that allude to a more complete theory including gravitational effects [106]. As both experimental and theoretical efforts to gain more insight into macroscopic quantum mechanics and quantum-to-classical transitions grow, given its extensive range of experiments in terms of length and mass scales, optomechanics provides an ideal testbed for studying these issues.

The issue that we address in this chapter is that of entanglement between two mechanical degrees of freedom, which, given the susceptibility of quantum correlations to environmental influences, is a challenging phenomenon to observe for

macroscopic objects. Entanglement between two mechanical oscillators was first experimentally demonstrated by Jost *et al* [107], with the vibrational modes of two individual ion pairs representing the two mechanical degrees of freedom. The essential idea of the experiment was to entangle the spins of two ion pairs which can be accomplished with high fidelity, followed by transferring the spin-spin entanglement on to the motional degrees of freedom of the ion pairs. While this experiment explicitly leveraged the internal degrees of the mechanical oscillators to create two entangled mechanical oscillators, other proposed experimental schemes that talk about entanglement of larger mechanical systems such as that between two dielectric membranes suspended in a Fabry-Perot cavity [108] and $\mu$g scale mirrors in a ring cavity setup [109], are based on the conventional boundary condition approach without any reference to the mirrors' internal structures.

In this chapter we look at the entanglement between the mechanical degrees of freedom of two mirrors in the MOF model. Introducing an additional mirror that possesses an internal and a mechanical degree of freedom of its own to our previous setup, we consider the classical and quantum dynamics of the coupled mirror+field+mirror system and study the entanglement between the two mechanical degrees of freedom pertaining to the two mirrors. As we have highlighted earlier, one of the advantages of using the MOF model is that one can bridge the disparity in the theoretical treatments of setups at different scales such as between atomic scale mechanical oscillators and nanoscale mirrors. It can even allow for coupling two different "kinds" of mirrors as in the state-of-the-art hybrid setups where, for example, one can couple a dielectric membrane to an atomic ensemble [49, 50]. In

the following, we first introduce the setup in consideration in section 3.1, study its classical dynamics and optomechanical properties in section 3.2, then moving to a quantum mechanical description of the system dynamics in section 3.3 we study the specific case of a single mode field interacting with the two mirrors in section 4.1 to arrive at the entanglement between the mirrors' centers of mass in 4.1.2. We also demonstrate the correspondence between the boundary condition approach and MOF model as applied to the two mirror setup in 4.1.1. Lastly, in 4.1.3 we apply our theory to the case of two atoms interacting with a common field and study the entanglement between the motion of two individual atoms.

## 3.1   The Mirror-Oscillator-Field-Oscillator-Mirror (MOFOM) setup

Let us consider two mirrors $\mathcal{M}_1$ and $\mathcal{M}_2$ interacting with a massless scalar field in (1+1)-dimensional space-time. As before, each mirror is described by two independent degrees of freedom – an internal degree of freedom ($idf_j$) modeled by a harmonic oscillator of mass $m_j$ and frequency $\Omega_j$, and a mechanical degree of freedom ($mdf_j$) with a mass $M_j$ in a harmonic potential of frequency $\mho_j$, with $j = \{1, 2\}$, as shown in Fig.3.1. We assume that the mirror $\mathcal{M}_1$ is located at $x = 0$ and $\mathcal{M}_2$ at $x = d$, separated by a distance $d$.

As before, the two internal degrees of freedom of the mirrors $idf_1$ and $idf_2$ are bilinearly coupled to the field and constrained to be at the center of mass positions $Z_1$ and $Z_2$ respectively, leading to an effective interaction between the field and the two mechanical degrees of freedom and, as a consequence, an effective interaction
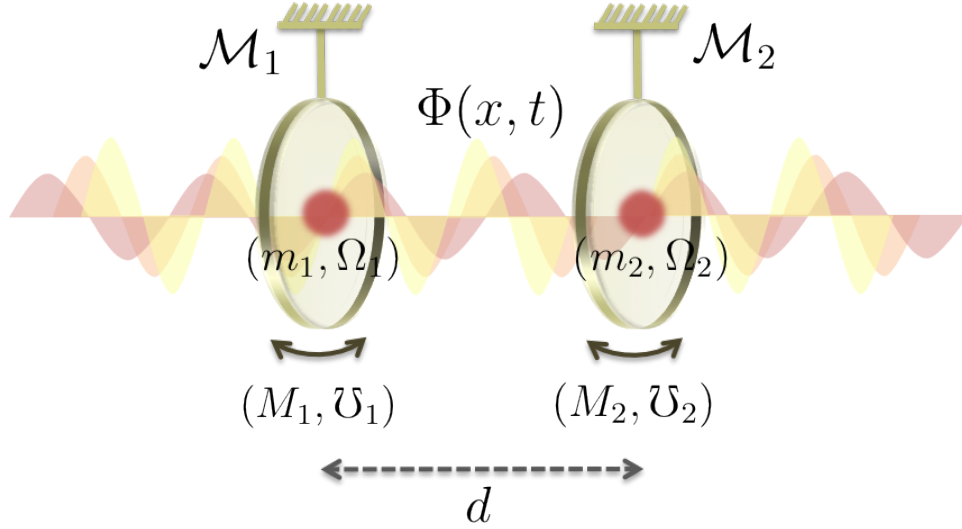
Figure 3.1: Schematic representation of the interaction of two mirrors $\mathcal{M}_1$ and $\mathcal{M}_2$ with a field via their internal degrees of freedom. A classical field incident from the left on $\mathcal{M}_1$ gets reflected and transmitted at the two center of mass positions, $x = 0$ and $x = d$. Each mirror is a composite of an internal and a mechanical degree of freedom, described by four separate harmonic oscillators of masses and frequencies given by $\{m_j, \Omega_j\}$ and $\{M_j, \mho_j\}$ respectively.

between the two mechanical degrees of freedom as well. The optical properties of the system arise from the coupling of the two internal degrees of freedom to the field as in the case of a single mirror.

We allow the two mirrors to possess different mechanical properties and internal structures such that, in general, $M_1 \neq M_2, \mho_1 \neq \mho_2, m_1 \neq m_2, \Omega_1 \neq \Omega_2$ and $\lambda_1 \neq \lambda_2$, so that one can potentially study the entanglement between two different kinds of mirrors. As before we assume that the *idf*-field dynamics happen at much faster time scales compared to those of the mechanical motion, such that $\Omega_j \gg \mho_j$

for both the mirrors.

Assuming non-relativistic center of mass motion for the mirrors, we write the action for the coupled mirrors+field system as

$$S = \int \mathrm{d}t \left[ \int \mathrm{d}x \frac{\epsilon_0}{2} \left( (\partial_t \Phi)^2 - c^2 (\partial_x \Phi)^2 \right) + \sum_{j=1,2} \left\{ \left( \frac{1}{2} M_j \dot{Z}_j^{\,2} - \frac{1}{2} M_j \mho_j^2 Z_j^2 \right) \right. \right.$$
$$\left. \left. + \left( \frac{1}{2} m_j \dot{q}_j^2 - \frac{1}{2} m_j \Omega_j^2 q_j^2 \right) + \int \mathrm{d}x \lambda_j \dot{q}_j \Phi \delta(x - Z_j) \right\} \right] \tag{3.1}$$

where we denote the center of mass positions of the two $mdf$s by $Z_{1,2}(t)$, the amplitude of the $idf$s by $q_{1,2}(t)$ and the scalar field by $\Phi(x,t)$. There are two interaction terms that couple both the $idf$s to the field depending on the respective center of mass positions $Z_j$, thereby giving a radiation force on the mirrors. We note that there is no direct coupling between the degrees of freedom pertaining to separate mirrors, internal or external, and all the interactions between the two mirrors are mediated via the field. Thus, the separation of the two mirrors plays an important role in determining the effective interaction between the mirrors as the relative coupling of the field to each $idf$ depends on the distance $d$ between the two center of mass positions.

Again, in the electromagnetic correspondence we identify $\lambda$ as the surface charge density, choosing the coupling $\lambda$ to have the dimensions of the electronic charge $e$ and $\Phi(x,t)$ to have the dimensions of the vector potential $A$. In a more generalized version of our present work, depending on the optical behavior of the two mirrors, one could also allow for the individual mirrors to have different forms of the $idf$-field coupling. For example, one might want to use a $\sim q\Phi$ coupling term for one of the two mirrors as in [1] and $\sim \dot{q}\Phi$ coupling for the other, choosing the

appropriate form depending on the optical properties of the mirror as discussed in section 1.4.2.

In the following section we study the classical dynamics of the coupled mirror+field+mirror system, to obtain the optomechanical properties as in section 1.4.

## 3.2 Classical Optomechanical properties

In this section we consider the classical optical and mechanical properties of the two mirror system in the MOF model, starting with deriving the coupled equations of motion for the classical amplitudes of the two $mdf$s, the $idf$s and the field $\{\bar{Z}_j, \dot{\bar{Z}}_j, \bar{q}_j, \dot{\bar{q}}_j, \bar{\Phi}, \dot{\bar{\Phi}}\}$, where $j = \{1, 2\}$ stands for the variables pertaining to the mirror $\mathcal{M}_j$. Expanding the action (3.1) up to first order in the deviations $\{\delta Z_j, \delta \dot{Z}_j, \delta q_j, \delta \dot{q}_j, \delta \Phi, \delta \dot{\Phi}\}$ from the mean field values

$$S_1 = \int \mathrm{d}t \int \mathrm{d}x \left[ \epsilon_0 \left( \dot{\bar{\Phi}} \delta \dot{\Phi} - c^2 \partial_x \bar{\Phi} \delta (\partial_x \Phi) \right) \right] + \sum_{j=1,2} \left[ M_j \dot{\bar{Z}}_j \delta \dot{Z}_j - M_j \mho_j^2 \bar{Z}_j \delta Z_j \right.$$

$$\left. + \left( m_j \dot{\bar{q}}_j \delta \dot{q}_j - m_j \Omega_j^2 \bar{q}_j \delta q_j + \lambda_j \dot{\bar{q}}_j \delta \Phi \left( \bar{Z}_j, t \right) + \lambda_j \bar{\Phi} \left( \bar{Z}_j, t \right) \delta \dot{q}_j + \lambda_j \dot{\bar{q}}_j \partial_x \bar{\Phi} \left( \bar{Z}_j, t \right) \delta Z_j \right) \right]$$

$$(3.2)$$

$$= \int \mathrm{d}t \left[ \sum_{j=1,2} \left\{ \left( -\frac{\mathrm{d}}{\mathrm{d}t} \left( M_j \dot{\bar{Z}}_j \right) - M_j \mho_j^2 \bar{Z}_j + \lambda \dot{\bar{q}}_j \partial_x \bar{\Phi} \left( \bar{Z}_j, t \right) \right) \delta Z_j \right. \right.$$

$$\left. + \left( -\frac{\mathrm{d}}{\mathrm{d}t} \left( m_j \dot{\bar{q}}_j + \lambda_j \bar{\Phi} \left( \bar{Z}_j, t \right) \right) - m_j \Omega_j^2 \bar{q}_j \right) \delta q_j \right\}$$

$$\left. + \int \mathrm{d}x \left( -\epsilon_0 \frac{\mathrm{d}\dot{\bar{\Phi}}}{\mathrm{d}t} + \epsilon_0 c^2 \partial_x^2 \bar{\Phi} + \sum_{j=1,2} \lambda_j \dot{\bar{q}}_j \delta (x - \bar{Z}_j) \right) \delta \Phi \right] \qquad (3.3)$$

one arrives at the following equations of motion for the two mirrors' mechanical and internal degrees of freedom ($j = 1, 2$) respectively

$$\ddot{\bar{Z}}_j + \mho_j^2 \bar{Z}_j = \frac{\lambda_j \dot{\bar{q}}_j}{M_j} \partial_x \bar{\Phi} \left( \bar{Z}_j, t \right) \tag{3.4}$$

$$\ddot{\bar{q}}_j + \Omega_j^2 \bar{q}_j = -\frac{\lambda_j}{m_j} \dot{\bar{\Phi}} \left( \bar{Z}_j, t \right) \tag{3.5}$$

and for the field we obtain

$$\epsilon_0 \left( \ddot{\bar{\Phi}} \left( x, t \right) - c^2 \partial_x^2 \bar{\Phi} \left( x, t \right) \right) = \sum_{j=1,2} \lambda_j \dot{\bar{q}}_j \delta(x - \bar{Z}_j) \tag{3.6}$$

One can make several observations at this point as for the case of a single mirror. Firstly, as seen from (3.6), the two moving *idf*s act as point sources for the field, each located at $\bar{Z}_{1,2}(t)$. The *idf*s are in turn driven by the "electric field" evaluated at the center of mass positions $\left( \dot{\bar{\Phi}} \left( \bar{Z}_j(t), t \right) \right)$ for the respective mirrors, as can be seen from (3.5). From (3.5) it can be seen that the two CoMs for the mirrors are driven non-linearly by the respective Lorentz forces acting on their "surface charge currents" ($\lambda_j \dot{\bar{q}}_j$) in the presence of a "magnetic field" $\left( \partial_x \bar{\Phi} \left( \bar{Z}_j(t), t \right) \right)$ at their center of mass position. We also note from (3.6) that it is the field that carries the influence of the dynamics of each mirror, hence mediating an effective interaction between the two.

As before, we shall assume that the mirrors' center of mass motion is non-relativistic $\left( \left| \frac{d\bar{Z}_j}{dt} \right| \ll c \right)$, meaning that we ignore the corrections coming from the Doppler shift seen by the surface charges and their consequent response. Further, we assume that the center of mass motion for both the mirrors is small in amplitude compared to the wavelength of the field modes that are nearly resonant with the

75

internal degrees of freedom for the two mirrors, so that one can ignore the backreaction of the center of mass motion on the interaction between the respective *idf*s and the field. In the following two subsections we solve the coupled equations of motion within these assumptions to obtain the classical amplitudes of the mirror and field degrees of freedom for the case where an incident field drives the system.

### 3.2.1  Classical Radiation Pressure Force

Let us consider the dynamics of the center of mass motion for the mirror $\mathcal{M}_j$. From integrating the field equation of motion (3.6) around the center of mass position $\bar{Z}_j$, we see that there is a discontinuity in the field spatial derivative. As in section 1.4.1, this can be understood as the equivalent of Ampere's law such that a discontinuity in the magnetic field $(\partial_x \bar{\Phi} \sim B)$ across the mirror center of mass positions $\bar{Z}_j$, leads to an induced surface charge current $\dot{\bar{q}}_j$.

We find the surface charge current for $\mathcal{M}_j$ as

$$\lambda \dot{\bar{q}}_j = -\epsilon_0 c^2 \partial_x \bar{\Phi}\big|_{\bar{Z}_j^-}^{\bar{Z}_j^+} \tag{3.7}$$

Eliminating the *idf*s from the center of mass dynamics in (3.4), defining the spatial derivative of the field at each center of mass position as

$$\partial_x \bar{\Phi}\left(\bar{Z}_j, t\right) \equiv \frac{\left(\partial_x \bar{\Phi}\left(\bar{Z}_j^+, t\right) + \partial_x \bar{\Phi}\left(\bar{Z}_j^-, t\right)\right)}{2} \tag{3.8}$$

we rewrite equation of motion for the two *mdf*s

$$\ddot{\bar{Z}}_j + \mho_j^2 \bar{Z}_j = -\frac{1}{2M_j} \epsilon_0 c^2 (\partial_x \bar{\Phi})^2 \big|_{\bar{Z}_j^-}^{\bar{Z}_j^+} \tag{3.9}$$

76

It can be seen from above that the radiation pressure force on the mirrors'
CoMs is given by the discontinuity of the energy density across their center of mass
positions, which, considering that the electric field at either mirror CoM position
vanishes in the co-moving reference frame for a perfect mirror, goes as $\sim \frac{B^2}{2\mu_0}\Big|_{\bar{Z}_j^-}$
akin to [68]. The more general case of imperfect mirrors was discussed in section 2.2
where we showed that the radiation pressure force from the RHS of (3.9) does indeed
correspond to the formal expression that one obtains from a boundary condition
approach such as in [84]. However, we note that since the field configuration instead
of being governed by some fixed boundary conditions is determined by the dynamical
interaction between the field and the two moving *idf*s the radiation pressure force
evaluated from the two approaches is in fact different. To see this more explicitly,
we consider the coupled dynamics of the two *idf*s and the field, writing the solution
for the equations of motion for the internal degrees of freedom as

$$\bar{q}_j(t) = \bar{q}_j^{(h)}(t) + \int_0^t dt' G_j^{(i)}(t-t') \left(-\frac{\lambda_j}{m_j}\dot{\bar{\Phi}}\left(\bar{Z}_j(t'), t'\right)\right) \tag{3.10}$$

where we define $\bar{q}_j^{(h)}$ as the homogeneous solution for the free evolution of *idf* $_j$ and
$G_j^{(i)}(t-t') \equiv \frac{\sin(\Omega_j(t-t'))}{\Omega_j}$ as the Green's function for the *idf* $_j$. We use this to eliminate
the two *idf*s from the field's equation of motion to get

$$\epsilon_0 \left(\partial_t^2 - c^2\partial_x^2\right)\bar{\Phi}\left(x,t\right) + \sum_{j=1,2}\frac{\lambda_j^2}{m_j}\delta\left(x-\bar{Z}_j(t)\right)\int_0^t dt'\partial_t G_j^{(i)}\left(t-t'\right)\dot{\bar{\Phi}}(\bar{Z}_j(t'),t')$$

$$= \sum_{j=1,2}\lambda_j\dot{\bar{q}}_j^{(h)}\delta\left(x-\bar{Z}_j(t)\right)$$

$$\tag{3.11}$$

Here one can identify the second term on the left hand side as the backreaction of

the moving *idf*s on the field, thus the field configuration depends on the coupled dynamics of the field, the internal degrees of the mirrors and their center of mass positions. In contrast with the case where one applies boundary conditions on the two mirrors, here one includes the full dynamics of the internal degrees instead of assuming a steady state response. We will study this point further in the next section as we look at the optical properties of the two mirror system for the case of a single field mode.

### 3.2.2 Optical properties

Let us consider a single mode field at frequency $\omega$ and amplitude $\Phi_0$ driving the two mirrors' *idf*s. Assuming that the CoM motion for both the mirrors about their equilibrium positions at $x = 0$ and $x = d$ is small enough such that the interaction of the field with the respective *idf*s remains unaffected by the CoM motion of the mirrors, we make the following plane-wave ansatz for the field

$$
\begin{aligned}
\Phi_\omega\left(x, t\right) = \Phi_0 \frac{\Omega_0}{\omega} e^{-i\omega t} &\left[\Theta(-x)\left\{e^{ikx} + R_1\left(\omega\right)e^{-ikx}\right\}\right. \\
&+ \left(\Theta(x) - \Theta(x-d)\right)\left\{T_1\left(\omega\right)e^{ikx} + R_2\left(\omega\right)e^{-ik(x-d)}\right\} \\
&\left.+ \Theta(x-d)T_2\left(\omega\right)e^{ik(x-d)}\right] + H.C.
\end{aligned}
\tag{3.12}
$$

where we assume that the field is incident from the left on $\mathcal{M}_1$ as in Fig. 3.1, and $R_1\left(\omega\right)$ and $T_2\left(\omega\right)$ are the overall reflection and transmission coefficients for the two mirror system, while $T_1\left(\omega\right)$ and $R_2\left(\omega\right)$ represent the amplitudes of the left and right moving field components in the region between the two mirrors. We note that the absolute value of the coefficients $T_1\left(\omega\right)$ and $R_2\left(\omega\right)$ can exceed 1, meaning that there

is a buildup of the field within the "cavity" formed between the two mirrors. The reflection and transmission coefficients for the overall system ($R_1(\omega)$ and $T_2(\omega)$) are indeed restricted to be less than 1 in magnitude. We have further assumed that the damping coming from the interaction of the two *idf*s with the remaining field modes is negligibly small. From imposing continuity on the field amplitude at $x = 0$ and at $x = d$ we have

$$1 + R_1(\omega) = T_1(\omega) + R_2(\omega) e^{ikd}$$

$$\implies T_1(\omega) = 1 + R_1(\omega) - R_2(\omega) e^{ikd} \tag{3.13}$$

$$T_1(\omega) e^{ikd} + R_2(\omega) = T_2(\omega)$$

$$\implies T_2(\omega) = (1 + R_1(\omega)) e^{ikd} + R_2(\omega) \left(1 - e^{2ikd}\right) \tag{3.14}$$

where we have used (3.13) to arrive at (3.14). Assuming that in the steady state limit the two *idf*s oscillate at the same frequency as that of the incident field, such that $\bar{q}_j = q_j^{(0)} e^{-i\omega t} + H.C.$, then we have from (3.7) for $\mathcal{M}_1$

$$\lambda_1 q_1^{(0)} (-i\omega) e^{-i\omega t} = -\epsilon_0 c^2 \partial_x \left. \Phi_\omega \right|_{\bar{Z}_1^-}^{\bar{Z}_1^+} \tag{3.15}$$

$$\implies \lambda_1 q_1^{(0)} (-i\omega) e^{-i\omega t} = -\epsilon_0 c^2 \Phi_0 \frac{\Omega_0}{\omega} e^{-i\omega t} \left[ (ik) \left( T_1(\omega) - R_2(\omega) e^{ikd} \right) - (ik) (1 - R_1(\omega)) \right] \tag{3.16}$$

$$\implies \lambda_1 q_1^{(0)} = 2\epsilon_0 c \Phi_0 \frac{\Omega_0}{\omega} \left[ R_1(\omega) - R_2(\omega) e^{ikd} \right] \tag{3.17}$$

where we have used (3.13) in the last step. One can interpret this as the induced surface charge current or the momentum kick from the field to the first mirror, which goes as $\left( R_2(\omega) e^{ikd} - R_1(\omega) \right)$ or $(1 - T_1(\omega))$. Similarly, from (3.7) for the second

mirror $\mathcal{M}_2$

$$\lambda_2 q_2^{(0)} (-i\omega) e^{-i\omega t} = -\epsilon_0 c^2 \partial_x \left. \Phi_\omega \right|_{\bar{Z}_2^-}^{\bar{Z}_2^+} \tag{3.18}$$

$$\implies \lambda_2 q_2^{(0)} (-i\omega) e^{-i\omega t} = -\epsilon_0 c^2 \Phi_0 \frac{\Omega_0}{\omega} e^{-i\omega t} \left[ (ik) T_2 (\omega) - (ik) \left( T_1 (\omega) e^{ikd} - R_2 (\omega) \right) \right] \tag{3.19}$$

$$\implies \lambda_2 q_2^{(0)} = 2\epsilon_0 c \Phi_0 \frac{\Omega_0}{\omega} R_2 (\omega) \tag{3.20}$$

where again, we have used (3.13) and (3.14) to eliminate the transmission coefficients in the last step. We note that the induced surface charge current for $\mathcal{M}_2$ goes as $R_2 (\omega)$.

Now using the plane wave ansatz to rewrite the equations of motion for the two internal degrees of freedom, we get

$$q_1^{(0)} \left( \Omega_1^2 - \omega^2 \right) = -\frac{\lambda_1}{m_1} \Phi_0 \frac{\Omega_0}{\omega} (-i\omega) (1 + R_1 (\omega))$$

$$\implies \lambda_1 q_1^{(0)} = \frac{i\omega \lambda_1^2}{m_1 \left( \Omega_1^2 - \omega^2 \right)} \Phi_0 \frac{\Omega_0}{\omega} (1 + R_1 (\omega)) \tag{3.21}$$

$$q_2^{(0)} \left( \Omega_2^2 - \omega^2 \right) = -\frac{\lambda_2}{m_2} \Phi_0 \frac{\Omega_0}{\omega} (-i\omega) \left[ T_1 (\omega) e^{ikd} + R_2 (\omega) \right]$$

$$\implies \lambda_2 q_2^{(0)} = \frac{i\omega \lambda_2}{m_2 \left( \Omega_2^2 - \omega^2 \right)} \Phi_0 \frac{\Omega_0}{\omega} \left[ (1 + R_1 (\omega)) e^{ikd} + R_2 (\omega) \left( 1 - e^{2ikd} \right) \right] \tag{3.22}$$

From comparing (3.17) with (3.21), and (3.20) with (3.22), we have

$$R_1 (\omega) - R_2 (\omega) e^{ikd} = \frac{i\omega \Omega_{P1}}{\Omega_1^2 - \omega^2} (1 + R_1 (\omega)) \tag{3.23}$$

$$R_2 (\omega) = \frac{i\omega \Omega_{P2}}{\Omega_2^2 - \omega^2} \left[ (1 + R_1 (\omega)) e^{ikd} + R_2 (\omega) \left( 1 - e^{2ikd} \right) \right] \tag{3.24}$$

where we have defined the "plasma frequencies" $\Omega_{Pj} = \lambda_j^2 / (2 m_j \epsilon_0 c)$ for each of the mirrors. Further, defining the dimensionless quantities $\eta_j \equiv \frac{i\omega \Omega_{Pj}}{\Omega_j^2 - \omega^2}$, we can obtain

the reflection and transmission coefficients for the two mirrors as

$$R_1(\omega) = \frac{\eta_1 + \eta_2 e^{2ikd} + \eta_1\eta_2 \left(e^{2ikd} - 1\right)}{1 - \eta_1 - \eta_2 + \eta_1\eta_2 \left(1 - e^{2ikd}\right)} \tag{3.25}$$

$$T_1(\omega) = \frac{1 - \eta_2}{1 - \eta_1 - \eta_2 + \eta_1\eta_2 \left(1 - e^{2ikd}\right)} \tag{3.26}$$

$$R_2(\omega) = \frac{\eta_2 e^{ikd}}{1 - \eta_1 - \eta_2 + \eta_1\eta_2 \left(1 - e^{2ikd}\right)} \tag{3.27}$$

$$T_2(\omega) = -\frac{e^{ikd}}{1 - \eta_1 - \eta_2 + \eta_1\eta_2 \left(1 - e^{2ikd}\right)} \tag{3.28}$$

It can be seen from the above expressions that if the coupling of the second mirror's *idf* with the field approaches zero as $\eta_2 \to 0$, then the reflection coefficient $R_1(\omega) \to \frac{\eta_1}{1-\eta_1}$ which is consistent with what we had found for the single mirror case and $R_2(\omega) \to 0$ as expected. Similarly for $\eta_1 \to 0$, we find $R_{1,2}(\omega) \to \frac{\eta_2 e^{2ikd}}{1-\eta_2}$ and $T_2(\omega) \to \frac{-e^{ikd}}{1-\eta_2}$. We look at the overall reflection and transmission coefficients of the coupled system ($R_1(\omega)$ and $T_2(\omega)$) as a function of the field frequency in Fig. 3.2 (a) for different separations between the two mirrors and for different values of the plasma frequencies.
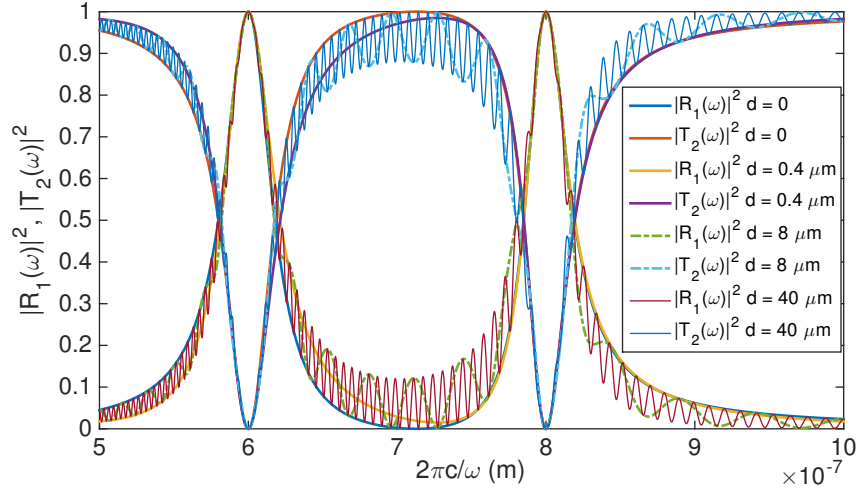
(a) Reflectance and transmittance for the two mirror system as a function of the incident field frequency plotted for different values of the mirror separation for fixed plasma frequencies $\Omega_{P1}/\Omega_1 \approx 0.4$ and $\Omega_{P2}/\Omega_2 \approx 0.3$.
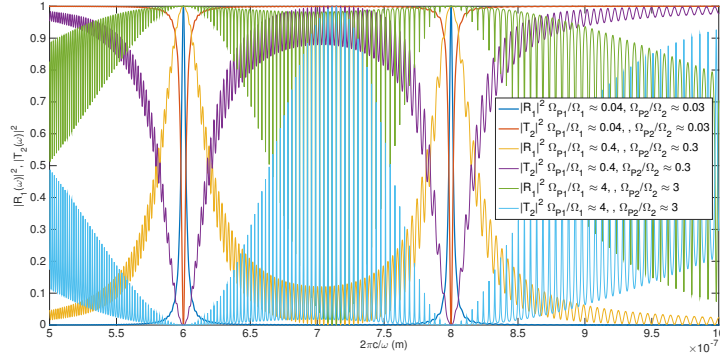


(b) Reflectance and transmittance for the two mirror system as a function of the incident field frequency plotted for different values of the plasma frequencies for a fixed separation of the mirrors $d = 0.8 \mu$m.

Figure 3.2: Optical properties of the two mirror system as for different separation between the two mirrors and *idf* plasma frequencies. We note that the reflection peaks at the internal resonance frequencies of the two mirrors, that is, for $\omega = \Omega_1 = 2\pi c/(600\,nm)$ and $\omega = \Omega_2 = 2\pi c/(800\,\text{nm})$.

As before, we note that the reflection coefficient peaks when the field is resonant with the *idf* of either of the two mirrors. For the distance dependence, we observe high frequency oscillations in the reflection coefficient corresponding to the free spectral range of the cavity formed by the mirrors that scale as $\sim d$. This comes from the resonance condition of the cavity formed by the two mirrors. Also, one can note from Fig. 3.2 (b) that on increasing the *idf*-field coupling strengths, the reflection and transmission coefficients depend strongly on the mirror separation $d$, whereas for weakly coupled *idf*s, the distance dependence does not play much of a role. To illustrate this point better, we plot the reflection as a function of the mirror separation and the field frequency in Fig. 3.3. More specifically, we observe from Fig. 3.3 that for weak-coupling between the *idf*s and the field the distance dependence of the reflection coefficients is prominent closer to the *idf* resonance. In the following section we consider the quantum dynamics of the two mirrors coupled to the field.

## 3.3 Quantum dynamics of the coupled mirror-oscillator-field-oscillator-mirror (MOFOM) system

Let us perturb the original action (3.1) for the MOFOM system about the classical solutions as $\left\{ \bar{Z}_j + \tilde{Z}_j, \bar{q}_j + \tilde{q}_j, \bar{\Phi} + \tilde{\Phi} \right\}$, where $\tilde{O}$ represent the deviations about the classical solutions $\bar{O}$. Assuming that the center of mass motion about $\bar{Z}_j$ is small for both the mirrors and restricted to the Lamb-Dicke limit $\left( k\tilde{Z}_j \ll 1 \right)$ for the field modes below a certain high frequency cutoff, we expand the action up
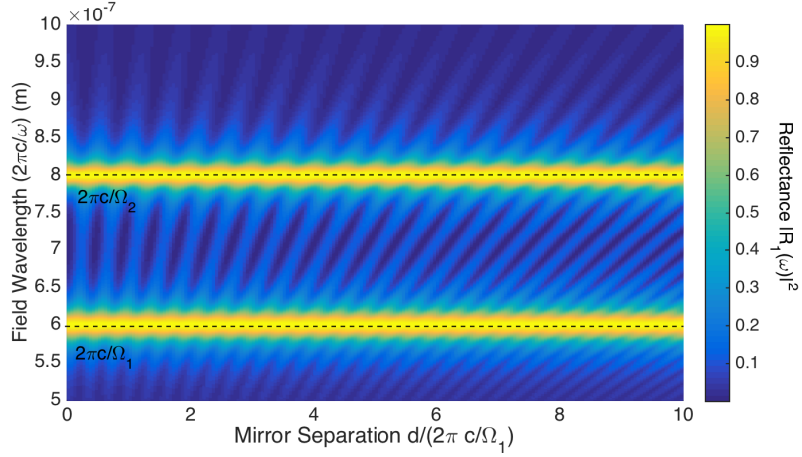
(a) $\Omega_{P1}/\Omega_1 \approx 0.04$ and $\Omega_{P2}/\Omega_2 \approx 0.06$
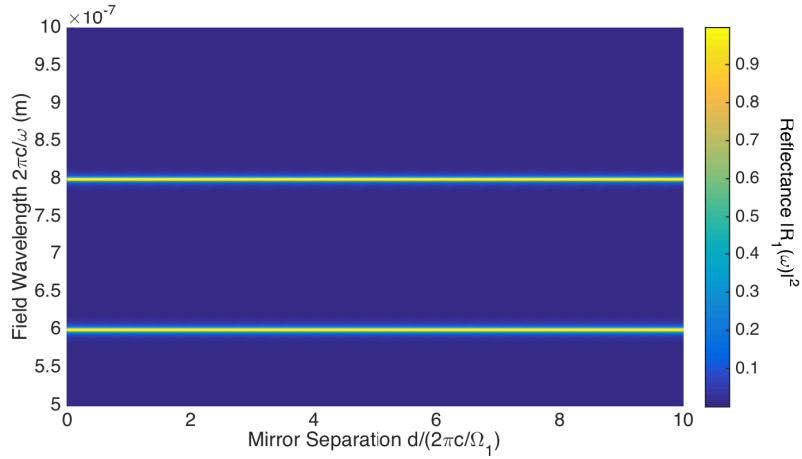


(b) $\Omega_{P1}/\Omega_1 \approx 0.004$ and $\Omega_{P2}/\Omega_2 \approx 0.006$ for the mirrors $\mathcal{M}_1$ and $\mathcal{M}_2$ respectively.

Figure 3.3: Total reflectance of the two mirror system $|R_1(\omega)|^2$ as a function of the dimensionless mirror separation $d/(2\pi c/\Omega_1)$ and field frequency for two different values of the *idf* plasma frequencies. It can be seen that for weak *idf*-field coupling strengths of the two mirrors there is almost no dependence of the reflectance on the mirror separation away from the *idf* resonances $\Omega_{1,2}$, whereas for larger plasma frequencies the distance dependence is more marked for all $\omega$.

to third order in the fluctuations about the classical solutions ignoring terms that are second order or higher in $k\tilde{Z}_j$. Going up to third order allows us to see the intensity-position coupling between the field and the mirrors' CoMs. When looking at the dynamics we restrict ourselves to bilinear interaction terms so that starting with initial Gaussian states for all subsystems the subsequent dynamics preserves Gaussianity.

The perturbed action can be written as

$$
S_3 = \int \mathrm{d}t \left[ \underbrace{\sum_{j=1,2} \left( \frac{1}{2} M_j \dot{\tilde{Z}}_j^2 - \frac{1}{2} M_j \mho_j^2 \tilde{Z}_j^2 \right)}_{mdf_j(\,M_j)} + \underbrace{\sum_{j=1,2} \left( \frac{1}{2} m_j \dot{\tilde{q}}_j^2 - \frac{1}{2} m_j \Omega_j^2 \tilde{q}_j^2 \right)}_{idf_j(\,O_j)} \right. \tag{3.29}
$$

$$
+ \int \mathrm{d}x \left\{ \underbrace{\frac{\epsilon_0}{2} \left( \left( \partial_t \tilde{\Phi} \right)^2 - c^2 \left( \partial_x \tilde{\Phi} \right)^2 \right)}_{\text{Field (F)}} \right.
$$

$$
\left. \left. + \sum_{j=1,2} \lambda_j \delta \left( x - \bar{Z}_j \right) \left( \underbrace{\dot{\tilde{q}}_j \tilde{\Phi}}_{O_j F} + \underbrace{\dot{\bar{q}}_j \left( \partial_x \tilde{\Phi} \right) \tilde{Z}_j}_{M_j F} + \underbrace{\dot{\tilde{q}}_j \left( \partial_x \bar{\Phi} \right) \tilde{Z}_j}_{O_j M_j} + \underbrace{\dot{\tilde{q}}_j \left( \partial_x \tilde{\Phi} \right) \tilde{Z}_j}_{M_j O_j F} \right) \right\} \right]
$$

$$
\tag{3.30}
$$

One can observe several points from the above expression, firstly, as for the case of a single mirror there is an effective coupling between the fluctuations of each mirror's center of mass and the field via its internal degree of freedom as denoted by the terms $M_j F$ and $M_j O j F$. From the mirror-field coupling terms $M_j F$, we note that the strength of coupling for each mirror's center of mass is proportional to the classical surface current $\dot{\bar{q}}_j$, implying that the fluctuations of the field are the most sensitive to the fluctuations of the mirror center of mass if the surface current is at its largest.

It can be seen from (3.17) and (3.20) that the surface current at the mirror $\mathcal{M}_1$ goes as $\sim \left( R_1\left(\omega\right) - R_2\left(\omega\right) e^{ikd} \right)$ and at the second mirror as $\sim R_2\left(\omega\right)$. Also, as for the single mirror, the effective coupling between the *idf* and the *mdf* fluctuations for each mirror denoted by the terms O$j$M$j$ is proportional to the spatial derivative of the field (or the "magnetic field" B) at the mirrors' center of mass position $\bar{Z}_j$. Again, for the mirror $\mathcal{M}_1$ this goes as $\sim \left( 1 - R_2\left(\omega\right) e^{ikd} \right)$ and for mirror $\mathcal{M}_2$ as $\sim T_1(\omega)$.

From (3.30) we obtain the equations of motion for the mirrors' CoMs and the field dynamics as

$$\ddot{\tilde{Z}}_j + \mho_j^2 \tilde{Z}_j = \frac{\lambda_j}{M_j} \left[ \dot{\bar{q}}_j \partial_x \tilde{\Phi} \left( \bar{Z}_j, t \right) + \dot{\tilde{q}}_j \left\{ \partial_x \bar{\Phi} \left( \bar{Z}_j, t \right) + \partial_x \tilde{\Phi} \left( \bar{Z}_j, t \right) \right\} \right] \tag{3.31}$$

$$\epsilon_0 \left( \partial_t^2 \tilde{\Phi} - c^2 \partial_x^2 \tilde{\Phi} \right) = \sum_{j=1,2} \left[ \lambda_j \dot{\tilde{q}}_j \delta \left( x - \bar{Z}_j \right) - \lambda_j \left( \dot{\bar{q}}_j + \dot{\tilde{q}}_j \right) \partial_x \left( \delta \left( x - \bar{Z}_j \right) \right) \tilde{Z}_j \right] \tag{3.32}$$

Integrating (3.32) around the classical center of mass position $\bar{Z}_j$, we get the surface current fluctuation for the mirror $\mathcal{M}_j$ as

$$\lambda_j \dot{\tilde{q}}_j = -\epsilon_0 c^2 \partial_x \tilde{\Phi} |_{\bar{Z}_j^-}^{\bar{Z}_j^+} \tag{3.33}$$

just as the classical version (3.7), this can be interpreted as the Ampere's Law in 1+1 D . Using this and the classical surface current from (3.7) to eliminate the *idf*s from the center of mass dynamics in (3.31), we get

$$\ddot{\tilde{Z}}_j + \mho_j^2 \tilde{Z}_j = \frac{-\epsilon_0 c^2}{M_j} \left[ \left( \partial_x \bar{\Phi} \right) \left( \partial_x \tilde{\Phi} \right) \Big|_{\bar{Z}_j^-}^{\bar{Z}_j^+} + \frac{1}{2} \left( \partial_x \tilde{\Phi} \right)^2 \Big|_{\bar{Z}_j^-}^{\bar{Z}_j^+} \right] \tag{3.34}$$

As in (1.32), we see that the first term on the right side corresponds to the radiation pressure coupling in the linearized approximation and the second term

86

corresponds to the intensity-position coupling. We note that for the case of two mirrors, the quantum fluctuations of the field on one side of the mirrors $\mathcal{M}_j$ would be determined by the quantization volume of the cavity formed between the two mirrors that depends on the separation $d$. The fluctuation force arising from the asymmetry of the density of field modes on either side of the mirrors is the Casimir force between the two [87, 88].

We now restrict ourselves to second order perturbations in the original action, to keep all the interaction terms bilinear such that for Gaussian initial states, the reduced density operators of the individual subsystems remain Gaussian at all times. We derive the conjugate momenta as

$$\tilde{p}_j = m_j \dot{\tilde{q}}_j + \lambda_j \tilde{\Phi}\left(\bar{Z}_j, t\right) + \lambda_j \partial_x \bar{\Phi}(\bar{Z}_j, t)\tilde{Z}_j \tag{3.35}$$

$$\tilde{P}_j = M_j \dot{\tilde{Z}}_j \tag{3.36}$$

$$\tilde{\Pi}(x, t) = \epsilon_0 \dot{\tilde{\Phi}}(x, t) \tag{3.37}$$

It can be seen that the fluctuations in the $idf$s of each mirror are influenced by those of their respective $mdf$s and of the field at the corresponding center of mass position, thus mediating an effective interaction between the mechanical motion of the two mirrors and the field. Identifying the dynamical variables $\{\tilde{Z}_j, \tilde{q}_j, \tilde{\Phi}\}$ as the quantum fluctuations of $mdf_j$, $idf_j$ and the field respectively about their mean-field

amplitudes, we arrive at the second order Hamiltonian

$$
\begin{aligned}
\tilde{H}_2 \equiv \sum_{j=1,2} \Bigg[ &\underbrace{\frac{\tilde{P}_j^2}{2M_j} + \frac{1}{2}M_j\left(\mho_j^2 + \frac{\lambda_j^2}{m_j M_j}\left(\partial_x\bar{\Phi}(\bar{Z}_j,t)\right)^2\right)\tilde{Z}_j^2}_{mdf_j(\mathrm{M}_j)} + \underbrace{\frac{\tilde{p}_j^2}{2m_j} + \frac{1}{2}m_j\Omega_j^2\tilde{q}_j^2}_{idf_j(\mathrm{O}_j)} \\
&+ \underbrace{\int \mathrm{d}x\left(\frac{\tilde{\Pi}^2}{2\epsilon_0} + \frac{1}{2}\epsilon_0 c^2\left(\partial_x\tilde{\Phi}\right)^2\right) + \sum_{j=1,2}\left[\frac{\lambda_j^2}{2m_j}\tilde{\Phi}(\bar{Z}_j,t)^2\right.}_{\text{Field (F)}} \underbrace{\left.- \frac{\lambda_j}{m_j}\tilde{p}_j\tilde{\Phi}(\bar{Z}_j,t)\right.}_{\mathrm{O}_j\mathrm{F}} \\
&\underbrace{- \frac{\lambda_j}{m_j}\partial_x\bar{\Phi}(\bar{Z}_j,t)\tilde{p}_j\tilde{Z}_j}_{\mathrm{O}_j\mathrm{M}j} + \underbrace{\frac{\lambda_j^2}{m_j}\partial_x\bar{\Phi}(\bar{Z}_j,t)\tilde{\Phi}(\bar{Z}_j,t)\tilde{Z}_j - \lambda_j\dot{\tilde{q}}_j\partial_x\tilde{\Phi}(\bar{Z}_j,t)\tilde{Z}_j}_{\mathrm{M}j\mathrm{F}}\Bigg] \quad (3.38)
\end{aligned}
$$

We note from the first term labeled $\mathrm{M}_j$ that two $mdf$s observe a renormalized oscillation frequency that we will denote as $\mho_j'$, such that $\mho_j'^2 \equiv \mho_j^2 + \frac{\lambda_j^2}{m_j M_j}\left(\partial_x\bar{\Phi}(\bar{Z}_j,t)\right)^2$. The scalar field sees a frequency shift coming from the terms quadratic in $\tilde{\Phi}\left(\bar{Z}_j,t\right)$, analogous to the diamagnetic term $\sim \frac{e^2}{2m}A^2$ of the minimal coupling Hamiltonian. The bilinear interaction terms represent the coupling between the $idf$s and the field ($\mathrm{O}j\mathrm{F}$), $mdf$s and the corresponding $idf$s ($\mathrm{O}j\mathrm{M}j$) and the $mdf$s and the field ($\mathrm{M}j\mathrm{F}$) respectively. Again, we note that there are no terms that couple the internal or external degrees of freedom between $\mathcal{M}_1$ and $\mathcal{M}_2$. The terms that are second order in $\lambda_j$ arise from the couplings mediated via the quantum fluctuations of the $idf$s and the terms that are first order in $\lambda_j$ come from the classically driven solutions for the field and the $idf$s respectively. As in the single mirror case, we note that the $\mathrm{M}j\mathrm{F}$ interaction contains two terms, the first one of which represents the effective field interaction mediated via the quantum fluctuations of the $idf_j$, while the second one represents that from the classical surface charge currents. Ignoring the fluctuations of the internal degrees of freedom, one misses out on the fluctuation-mediated part

of the effective mirror-field coupling.

In the absence of a classical drive, the only interaction up to second order is between the $idf$s and the field ($OjF$). To be able to see an effective $mdf$-field interaction and subsequently an interaction between the two mirrors one needs to include third order terms in the fluctuations as illustrated before. To understand the dynamics better, in the following section we study the above Hamiltonian for the case of a driven single field mode and find the entanglement between the two mirrors' CoMs, coarse-graining over their internal degrees of freedom.

# Chapter 4: Two Mirror Entanglement in the Mirror-Oscillator-Field (MOF) model

## 4.1 Single Field Mode interacting with the Two Mirrors

In typical optomechanical setups, when one talks about the entanglement between two mechanical oscillators the essential mechanism for entanglement is via the radiation pressure exerted on the mirrors by a common EM field. One can think of the CoMs of each mirror being correlated with the field by the means of radiation pressure force and as a result of transfer of correlations, the two mechanical degrees of freedom could be entangled as well. In the following, we look at the entanglement between two mechanical oscillators taking into consideration their internal degrees of freedom that couple to a common field. For simplicity we assume that the field has a single mode, as is usual in cavity optomechanical setups. Like the single mirror case, we expect that the inclusion of mirrors' *idf*s would lead to new physical features in the entanglement of the two mechnical degrees of freedom.
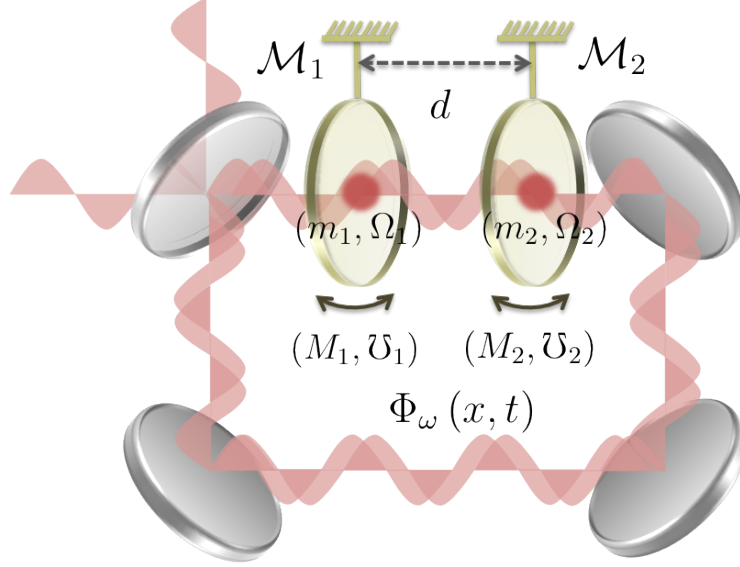
Figure 4.1: Schematic of the setup in consideration – two mirrors described by the MOF model interacting with a single mode field $\Phi_\omega(x, t)$ in a ring cavity.

We first simplify the Hamiltonian (3.38) for the case of a single field mode that is being externally driven to look at the dynamics of the coupled MOFOM system. Consider the scalar field in a region of length $L$, the field fluctuations can then be written as the sum of all discrete modes of the cavity of length $L$ as $\tilde{\Phi}(x, t) = \sum_n \sqrt{\frac{\hbar}{2\omega_n \epsilon_0 L}} \left( \tilde{a}_n e^{ik_n x} + \tilde{a}_n^\dagger e^{-ik_n x} \right)$, with $\tilde{a}_n^\dagger$ and $\tilde{a}_n$ representing the creation and annihilation operators for the $n^{\text{th}}$ field mode. We pick a single field mode at frequency $\omega$ interacting with the two mirrors at $\bar{Z}_{1,2}$. The fluctuations of the free field at the center of mass positions for the two mirrors are given as

$$\tilde{\Phi}_\omega\left(\bar{Z}_{1,2}, t\right) = \sqrt{\frac{\hbar}{2\omega\epsilon_0 L}} \left( \tilde{a}_\omega e^{ik\bar{Z}_{1,2}} + \tilde{a}_\omega^\dagger e^{-ik\bar{Z}_{1,2}} \right) \tag{4.1}$$

We note that unlike usual practice here we have not imposed any boundary

conditions on the field fluctuations, which should arise self-consistently from the interaction of the two *idf*s with the field in the steady state limit.

Redefining the dynamical variables associated with the *idf*s in terms of the creation and annihilation operators $\{\tilde{b}_j^\dagger, \tilde{b}_j\}$ as $\tilde{q}_j = \sqrt{\frac{\hbar}{2m_j\Omega_j}}\left(\tilde{b}_j + \tilde{b}_j^\dagger\right)$ and $\tilde{p}_j = -i\sqrt{\frac{\hbar m_j \Omega_j}{2}}\left(\tilde{b}_j - \tilde{b}_j^\dagger\right)$, we can rewrite the non-interacting part of the Hamiltonian (3.38) for a single field mode as follows

$$
\tilde{H}_{free} \equiv \sum_{j=1,2} \left[ \underbrace{\frac{\tilde{P}_j^2}{2M_j} + \frac{1}{2}M_j \mho_j'^2 \tilde{Z}_j^2}_{\tilde{H}_{M_j}} + \underbrace{\hbar\Omega_j \left(\tilde{b}_j^\dagger \tilde{b}_j + \frac{1}{2}\right)}_{\tilde{H}_{O_j}} \right]
$$

$$
+ \underbrace{\hbar\left(\omega + \sum_{j=1,2}\left(\frac{\lambda_j^2}{2m_j\omega\epsilon_0 L}\right)\right)\left(\tilde{a}_\omega^\dagger \tilde{a}_\omega + \frac{1}{2}\right) + \sum_{j=1,2}\left(\frac{\lambda_j^2}{4m_j\omega\epsilon_0 L}\right)\left(\left(\tilde{a}_\omega\right)^2 e^{2ik\bar{Z}_j} + \left(\tilde{a}_\omega^\dagger\right)^2 e^{-2ik\bar{Z}_j}\right)}_{\tilde{H}_F}
$$

$$(4.2)$$

where we have defined the renormalized mechanical oscillation frequency for the two mirrors as

$$
\mho_1'^2 \equiv \mho_1^2 + \frac{\lambda_1^2}{m_1 M_1}\left[\partial_x \bar{\Phi}\left(\bar{Z}_1, t\right)\right]^2
$$

$$
= \mho_1^2 - \frac{\lambda_1^2}{m_1 M_1 c^2}\Phi_0^2 \Omega_0^2 \left[\left(T_1\left(\omega\right) - R_1\left(\omega\right)\right)^2 e^{-2i\omega t} + \left(T_1^*\left(\omega\right) - R_1^*\left(\omega\right)\right)^2 e^{2i\omega t}\right.
$$

$$
\left. -2\left|\left(T_1\left(\omega\right) - R_1\left(\omega\right)\right)\right|^2\right]
$$

$$(4.3)$$

$$
\mho_2'^2 \equiv \mho_2^2 + \frac{\lambda_2^2}{m_2 M_2}\left[\partial_x \bar{\Phi}\left(\bar{Z}_2, t\right)\right]^2
$$

$$
= \mho_2^2 - \frac{\lambda_2^2}{m_2 M_2 c^2}\Phi_0^2 \Omega_0^2 \left[\left(T_1\left(\omega\right)\right)^2 e^{2ikd}e^{-2i\omega t} + \left(T_1^*\left(\omega\right)\right)^2 e^{-2ikd}e^{2i\omega t} - 2\left|\left(T_1\left(\omega\right)\right)\right|^2\right]
$$

$$(4.4)$$

assuming that the ansatz (3.12) applies for the mean field and the reflection and transmission coefficients $R_{1,2}(\omega)$ and $T_{1,2}(\omega)$ are as found in (3.25)–(3.28). The correction term $\left(\frac{\lambda_j^2}{m_j M_j}\left(\partial_x \bar{\Phi}(\bar{Z}_j, t)\right)^2\right)$ contains two contributions – a time dependent part oscillating at a frequency $\sim 2\omega$ which can be neglected in the rotating-wave approximation (RWA) and a time-independent part that contributes a correction term to the mechanical oscillation frequency which goes roughly as $\sim \sqrt{\frac{\Omega_{P_j}\epsilon_0}{M_j}}\Phi_0\Omega_0$. However, if the field mode was resonant with either of the $mdf$s, one would see parametric amplification of the corresponding mirror's center of mass motion [89]. For the free field part in (4.2) we notice that the interaction leads to an energy correction $\omega \to \omega + \sum_{j=1,2} \lambda_j^2/(2m_j\omega\epsilon_0 L)$ that is second order in $\lambda_j$s, this corresponds to the shift coming from the diamagnetic contribution for the EM case $\left(\sim \frac{e^2}{2m}A^2\right)$ as indicated in chapter 2 as well. This diamagnetic term also leads to the fast oscillating terms for the free field ($\sim 2\omega$), which correspond to the photon-pair production and annihilation as in the case of dynamical Casimir effect [89–92].

Moving to the interaction picture with respect to $\tilde{H}_0 = \tilde{H}_F + \sum_{j=1,2}\tilde{H}_{O_j}$ to eliminate the fast dynamics of the system and invoking RWA, we write the interaction Hamiltonian in a simplified form as

$$
\begin{aligned}
H_{int} = \sum_{j=1,2} \Big[ &\hbar\left(\alpha_{O_j F}\boldsymbol{a}\boldsymbol{b}_j^\dagger e^{-i\Delta_j t} + \alpha_{O_j F}^*\boldsymbol{a}^\dagger \boldsymbol{b}_j e^{i\Delta_j t}\right) \\
&+ \hbar\left(\alpha_{O_j M_j}\boldsymbol{b}_j e^{i\Delta_j t} + \alpha_{O_j M_j}^*\boldsymbol{b}_j^\dagger e^{-i\Delta_j t}\right)\left(\tilde{c}_j + \tilde{c}_j^\dagger\right) \\
&+ \hbar\left(\alpha_{M_j F}\boldsymbol{a} + \alpha_{M_j F}^*\boldsymbol{a}^\dagger\right)\left(\tilde{c}_j + \tilde{c}_j^\dagger\right)\Big]
\end{aligned}
\tag{4.5}
$$

where we have defined the operators in the interaction picture as $\{\boldsymbol{a}, \boldsymbol{a}^\dagger\} \equiv \{\tilde{a}_\omega e^{i\omega t}, \tilde{a}_\omega^\dagger e^{-i\omega t}\}$ and $\{\boldsymbol{b}_j, \boldsymbol{b}_j^\dagger\} \equiv \{\tilde{b}_j e^{i\Omega_j t}, \tilde{b}_j^\dagger e^{-i\Omega_j t}\}$ and the detuning $\Delta_j \equiv \omega - \Omega_j$ represents the de-

tuning between the field and the *idf* for the mirror $\mathcal{M}_j$. The operators $\{\tilde{c}_j, \tilde{c}_j^\dagger\}$ correspond to the creation and annihilation operators for the phononic excitations of the *mdf* corresponding to $\mathcal{M}_j$, with $\tilde{Z}_j = \sqrt{\frac{\hbar}{2M_j \mho'_j}}\left(\tilde{c}_j + \tilde{c}_j^\dagger\right) \equiv \sqrt{\frac{\hbar}{M_j \mho'_j}}\boldsymbol{Z}_j$ and $\tilde{P}_j = -i\sqrt{\frac{\hbar M_j \mho'_j}{2}}\left(\tilde{c}_j - \tilde{c}_j^\dagger\right) \equiv \sqrt{\hbar M_j \mho'_j}\boldsymbol{P}_j$. The operators $\boldsymbol{Z}_j$ and $\boldsymbol{P}_j$ are the dimensionless position and momentum fluctuations for $\mathcal{M}_j$'s center of mass. In moving to the interaction picture we have ignored the second order correction terms $\left(\sim \sum_{j=1,2} \lambda_j^2/m_j\right)$ in the free field Hamiltonian $\tilde{H}_F$.

The effective coupling coefficients are given as

$$\alpha_{O_1 F} = -i\frac{\lambda_1}{2m_1}\sqrt{\frac{m_1 \Omega_1}{\omega \epsilon_0 L}} = -i\sqrt{\frac{\Omega_1 \Omega_{P1} c}{2\omega L}} \tag{4.6}$$

$$\alpha_{O_2 F} = -i\frac{\lambda_2}{2m_2}\sqrt{\frac{m_2 \Omega_2}{\omega \epsilon_0 L}}e^{ikd} = -i\sqrt{\frac{\Omega_2 \Omega_{P2} c}{2\omega L}}e^{ikd} \tag{4.7}$$

$$\alpha_{O_1 M_1} = \frac{\lambda_1}{2m_1 c}\Phi_0 \Omega_0 \sqrt{\frac{m_1 \Omega_1}{M_1 \mho'_1}}\left(1 - R_2^*(\omega)e^{-ikd}\right)$$
$$= \Phi_0 \Omega_0 \sqrt{\frac{\Omega_1 \Omega_{P1} \epsilon_0}{2M_1 \mho'_1 c}}\left(1 - R_2^*(\omega)e^{-ikd}\right) \tag{4.8}$$

$$\alpha_{O_2 M_2} = \frac{\lambda_2}{2m_2 c}\Phi_0 \Omega_0 \sqrt{\frac{m_2 \Omega_2}{M_2 \mho'_2}}T_1^*(\omega)e^{-ikd}$$
$$= \Phi_0 \Omega_0 \sqrt{\frac{\Omega_2 \Omega_{P2} \epsilon_0}{M_2 \mho'_2 c}}T_1^*(\omega)e^{-ikd} \tag{4.9}$$

$$\alpha_{M_1 F} = -\Phi_0 \Omega_0 \sqrt{\frac{\omega \epsilon_0}{M_1 \mho'_1 \omega L}}\left(R_1^*(\omega) - R_2^*(\omega)e^{-ikd}\right)$$
$$- i\Omega_{P1}\Phi_0 \Omega_0 \sqrt{\frac{\epsilon_0}{\omega L M_1 \mho'_1}}\left(1 - R_2^*(\omega)e^{-ikd}\right)$$
$$= -\Phi_0 \Omega_0 \sqrt{\frac{\epsilon_0}{M_1 \mho'_1 L}}\left[\omega\left(R_1^*(\omega) - R_2^*(\omega)e^{-ikd}\right) + i\Omega_{P1}\left(1 - R_2^*(\omega)e^{-ikd}\right)\right]$$
$$\tag{4.10}$$

$$\alpha_{M_2 F} = -\Phi_0 \Omega_0 \sqrt{\frac{\omega \epsilon_0}{M_2 \mho'_2 L}}R_2^*(\omega)e^{ikd} - i\Omega_{P2}\Phi_0 \Omega_0 \sqrt{\frac{\epsilon_0}{\omega L M_2 \mho'_2}}T_1^*(\omega)$$
$$= -\Phi_0 \Omega_0 \sqrt{\frac{\epsilon_0}{M_2 \mho'_2 \omega L}}\left[\omega R_2^*(\omega)e^{ikd} - i\Omega_{P2}T_1^*(\omega)\right] \tag{4.11}$$

From the above expressions we can observe several key points, starting with the effective $mdf$-field coupling in equations (4.10) and (4.11), we see that the first and the second terms correspond to the interaction mediated by the mean field and the field fluctuations respectively. In comparing with the boundary condition approach, as we will show in section 4.1.1, one finds that while there is an agreement between the mean field contribution in the MOF model and the boundary condition approach, the latter ignores the fluctuation mediated term. The fluctuation mediated part becomes relevant in the parameter regimes where $|\Omega_{P1}/\omega| \gg \left| \frac{R_1(\omega) - R_2(\omega)e^{ikd}}{1 - R_2(\omega)e^{ikd}} \right| \equiv |r_1/r_2|$ for $\mathcal{M}_1$, where we have defined $r_1 \equiv R_1(\omega) - R_2(\omega)e^{ikd}$ and $r_2 \equiv 1 - R_2(\omega)e^{ikd}$. This condition is generally dependent on the mirror separation $d$ as opposed to the condition for $\mathcal{M}_2$, which requires $|\Omega_{P2}/\omega| \gg |R_2(\omega)/T_1(\omega)|$. For the mirror $\mathcal{M}_1$ the coupling strength is dependent on the separation $d$ because of the interference with the reflected field from the second mirror, while for the mirror $\mathcal{M}_2$ the distance dependence only contributes up to a phase factor. In Fig. 4.2 and Fig. 4.3 we show how the distance dependence determines which term dominates among the two, by plotting the quantities $\Lambda_1 \equiv |r_1/r_2|/(\Omega_{P1}/\omega)$ for the first mirror and $\Lambda_2 \equiv |R_2/T_1|/(\Omega_{P2}/\omega)$ for the second.

Again, all effective coupling strengths can be expressed as a function of the $idf$ resonance frequencies $\Omega_j$ and plasma frequencies $\Omega_{Pj}$ which can be deduced from the reflection and transmission properties of the system along with the mirror separation.

Also, it can be seen that as one turns the classical field off, the effective couplings between the mirrors' $mdf$s and their respective $idf$s and the field vanish

95
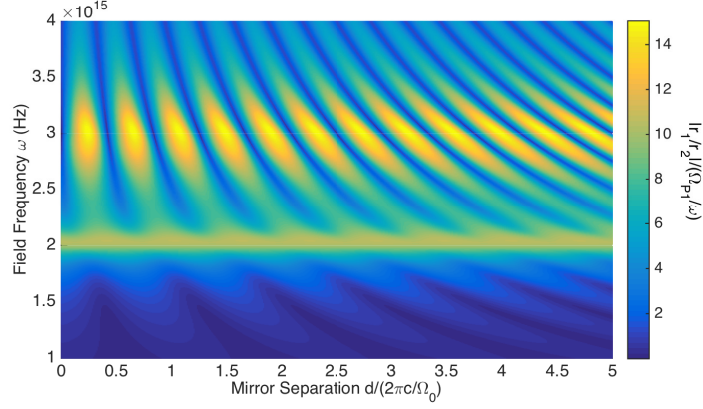
(a)
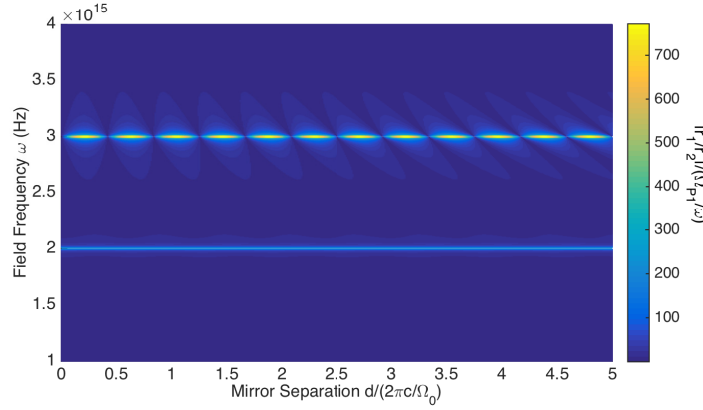


(b)

Figure 4.2: Mean-field vis-á-vis fluctuation mediated $mdf$-field coupling – the ratio $\Lambda_1 \equiv |r_1/r_2|/(\Omega_{P1}/\omega)$ that determines the relative contributions of the mean-field mediated interaction to the fluctuation mediated interaction for the effective $mdf$-field coupling coefficient $\alpha_{M_1F}$ of the first mirror's CoM, for (a) $\Omega_{P1}/\Omega_1 = 0.1$ and (b) $\Omega_{P1}/\Omega_1 = 1 \times 10^{-3}$. For a strong $idf$-field coupling there is an appreciable dependence of the ratios $\Lambda_j$ on the mirror separation $d$. For weak $idf$-field coupling, the distance dependence is restricted to near the internal resonance of the mirrors, which occur at $\Omega_1 = 2 \times 10^{15}$ Hz and $\Omega_2 = 3 \times 10^{15}$ Hz.
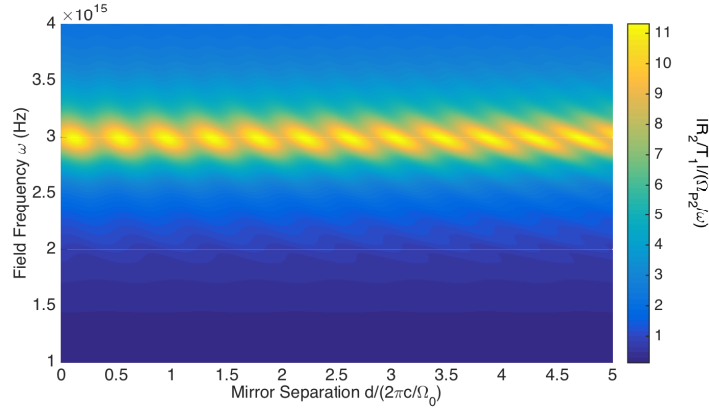
(a)
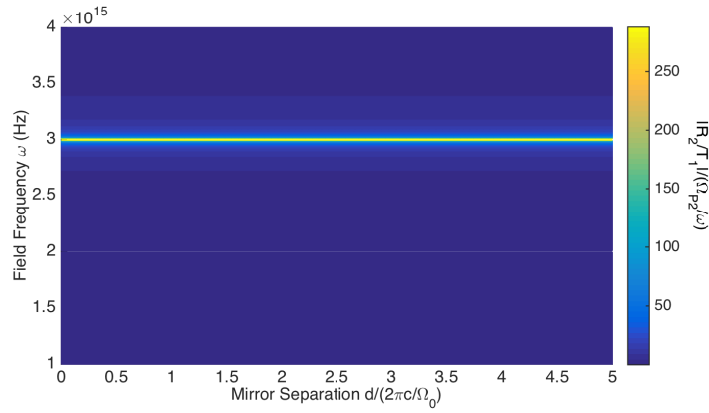


(b)

Figure 4.3: Mean-field vis-á-vis fluctuation mediated *mdf*-field coupling – The quantity $\Lambda_2 \equiv |R_2/T_1|/(\Omega_{P2}/\omega)$ that determines the relative contributions of the mean-field mediated interaction to the fluctuation mediated interaction for the effective *mdf*-field coupling coefficient $\alpha_{M_2 F}$ of the second mirror's CoM, for (a) $\Omega_{P2}/\Omega_2 = 0.1$ and (b) $\Omega_{P2}/\Omega_2 = 10^{-4}$. For a strong *idf*-field coupling there is an appreciable dependence of the ratios $\Lambda_j$ on the mirror separation $d$. For weak *idf*-field coupling, the distance dependence is restricted to near the internal resonance of the mirrors, which occur at $\Omega_1 = 2 \times 10^{15}$ Hz and $\Omega_2 = 3 \times 10^{15}$ Hz.

while the coupling between the two *idf*s and the field remain unchanged. Thus, even for no driving field, the fluctuations of the *idf*s and the field get entangled. Though to see the entanglement of the field with the mechanical degrees of freedom or that between the two *mdf*s, one needs to include higher order intensity-position coupling terms.

Now, to solve for the system dynamics we write the equations of motion from (4.5) as

$$\frac{\mathrm{d}\boldsymbol{Z}_j}{\mathrm{d}t} = \mho'_j \boldsymbol{P}_j \tag{4.12}$$

$$\frac{\mathrm{d}\boldsymbol{P}_j}{\mathrm{d}t} = -\mho'_j \boldsymbol{Z}_j - 2\left(\mathrm{Re}\alpha_{O_j M_j}\mathbf{q}_j - \mathrm{Im}\alpha_{O_j M_j}\boldsymbol{p}_j\right) - 2\left(\mathrm{Re}\alpha_{M_j F}\boldsymbol{\Phi} - \mathrm{Im}\alpha_{M_j F}\boldsymbol{\Pi}\right) - \Gamma_j \boldsymbol{P}_j + \boldsymbol{\Xi}_j \tag{4.13}$$

$$\frac{\mathrm{d}\boldsymbol{q}_j}{\mathrm{d}t} = \Delta_j \boldsymbol{p}_j - |\alpha_{O_j F}|\boldsymbol{\Phi} - 2\mathrm{Im}\alpha_{O_j M_j}\boldsymbol{Z}_j \tag{4.14}$$

$$\frac{\mathrm{d}\boldsymbol{p}_j}{\mathrm{d}t} = -\Delta_j \boldsymbol{q}_j - |\alpha_{O_j F}|\boldsymbol{\Pi} - 2\mathrm{Re}\alpha_{O_j M_j}\boldsymbol{Z}_j \tag{4.15}$$

$$\frac{\mathrm{d}\boldsymbol{\Phi}}{\mathrm{d}t} = |\alpha_{O_j F}|\boldsymbol{q}_j - 2\mathrm{Im}\alpha_{M_j F}\boldsymbol{Z}_j \tag{4.16}$$

$$\frac{\mathrm{d}\boldsymbol{\Pi}}{\mathrm{d}t} = |\alpha_{O_j F}|\boldsymbol{p}_j - 2\mathrm{Re}\alpha_{M_j F}\boldsymbol{Z}_j \tag{4.17}$$

wherein we have redefined the slow moving dimensionless *idf* and the field quadratures as $\boldsymbol{q}_j \equiv \frac{\boldsymbol{b}_j e^{i\Delta_j t} + \boldsymbol{b}_j^\dagger e^{-i\Delta_j t}}{\sqrt{2}}$, $\boldsymbol{p}_j \equiv -i\frac{\boldsymbol{b}_j e^{i\Delta_j t} - \boldsymbol{b}_j^\dagger e^{-i\Delta_j t}}{\sqrt{2}}$, $\boldsymbol{\Phi} \equiv \frac{\boldsymbol{a} + \boldsymbol{a}^\dagger}{\sqrt{2}}$ and $\boldsymbol{\Pi} \equiv -i\frac{\boldsymbol{a} - \boldsymbol{a}^\dagger}{\sqrt{2}}$. Also, to account for the fluctuation-dissipation mechanism for the mirrors' mechanical motion resulting from coupling to their respective environments, we have introduced the mechanical dampings $\Gamma_j$ and noise $\boldsymbol{\Xi}_j$. In the Markovian limit, the correlation function of the noise is given as $\langle \boldsymbol{\Xi}_j(t) \boldsymbol{\Xi}_j(t') \rangle = \frac{4\Gamma_j k_B T_j^{(m)}}{\hbar \mho'_j}\delta(t - t')$, with $T_j^{(m)}$ as the temperature of the thermal bath for the mirror $\mathcal{M}_j$.

Now to account for the fluctuation and dissipation mechanisms for the two in-

ternal degrees of freedom we consider the coupling of the two $idf$s to the continuum of field modes with a coupling of the form $\dot{q}_j \Phi_i$, where $\Phi_i$ represents the $i^{th}$ field mode, leading to a damping coefficient $\gamma_j^{(f)}$ and noise $\xi_j^{(f)}$, such that $\left\langle \xi_j^{(f)}(t)\xi_j^{(f)}(t') \right\rangle = \frac{4\gamma_j^{(f)} k_B T^{(f)}}{\hbar \Omega_j} \delta(t-t')$, with $T^{(f)}$ as the temperature of the field bath. Additionally we introduce baths of internal degrees of freedom for each $idf$ such that each bath oscillator is coupled to the $idf$ with a coupling of the form $q_j \cdot q_j^{(k)}$, where $q_j^{(k)}$ represents the position variable for the $k^{th}$ bath oscillator for $idf_j$, giving an effective damping coefficient of $\gamma_j^{(i)}$ and noise $\xi_j^{(i)}$, such that $\left\langle \xi_j^{(i)}(t)\xi_j^{(i)}(t') \right\rangle = \frac{4\gamma_j^{(i)} k_B T^{(i)}}{\hbar \Omega_j} \delta(t-t')$, where $T^{(i)}$ corresponds to the temperature associated with the bath of the internal oscillators. Rewriting the equations of motion for the two $idf$s (4.14) and (4.15) including the phenomenological damping and noise we get

$$\frac{\mathrm{d}\boldsymbol{q}_j}{\mathrm{d}t} = \Delta_j \boldsymbol{p}_j - |\alpha_{O_j F}|\boldsymbol{\Phi} - 2\mathrm{Im}\alpha_{O_j M_j}\boldsymbol{Z}_j - \gamma_j^{(f)}\boldsymbol{q}_j + \xi_j^{(f)} \tag{4.18}$$

$$\frac{\mathrm{d}\boldsymbol{p}_j}{\mathrm{d}t} = -\Delta_j \boldsymbol{q}_j - |\alpha_{O_j F}|\boldsymbol{\Pi} - 2\mathrm{Re}\alpha_{O_j M_j}\boldsymbol{Z}_j - \gamma_j^{(i)}\boldsymbol{p}_j + \xi_j^{(i)} \tag{4.19}$$

Now assuming that the dynamics of the internal degrees of freedom is much faster than the other variables involved, we use separation of time scales to find the steady state $idf$ amplitudes as

$$\boldsymbol{q}_j^{st} = -\frac{\gamma_j^{(i)}\hat{C}_j^{(1)} + \Delta_j \hat{C}_j^{(2)}}{\Delta_j^2 + \gamma_j^{(i)}\gamma_j^{(f)}} \tag{4.20}$$

$$\boldsymbol{p}_j^{st} = \frac{\gamma_j^{(f)}\hat{C}_j^{(2)} - \Delta_j \hat{C}_j^{(1)}}{\Delta_j^2 + \gamma_j^{(i)}\gamma_j^{(f)}} \tag{4.21}$$

where the operators $\hat{C}_j^{(k)}$s stand for $\hat{C}_j^{(1)} \equiv |\alpha_{O_j F}|\boldsymbol{\Phi} + 2\mathrm{Im}\alpha_{O_j M_j}\boldsymbol{Z}_j - \hat{\xi}_j^{(f)}$ and $\hat{C}_j^{(2)} \equiv |\alpha_{O_j F}|\boldsymbol{\Pi} + 2\mathrm{Re}\alpha_{O_j M_j}\boldsymbol{Z}_j - \hat{\xi}_j^{(i)}$. It can be seen that the steady state $idf$ amplitudes are self-consistently negligibly small given that one requires $\{\gamma_j^{(i,f)}, \Delta_j\}$ to be

greater than all the other frequencies involved to be able to invoke the separation of timescales assumption.

### 4.1.1 Comparison with the boundary condition approach

In this section we consider the coupled dynamics for the mirrors' centers of mass and the field from the boundary condition approach, where we show how one can find an agreement with what we obtain from the MOF model provided that the *idf* amplitudes vanish.

As discussed in the section 2.2, we write the linearized Hamiltonian for the mirror+field+mirror system in the boundary condition approach as

$$
\tilde{H}_{BC} = \left[ \sum_{j=1,2} \frac{\hbar \eth_j}{2} \left( \boldsymbol{P}_j^2 + \boldsymbol{Z}_j^2 \right) + \int_0^L \mathrm{d}x \left( \frac{\tilde{\Pi}^2}{2\epsilon_0} + \frac{\epsilon_0}{2} c^2 \left( \partial_x \tilde{\Phi} \right)^2 \right) \right.
$$
$$
\left. - \sum_{j=1,2} \epsilon_0 c^2 \left( \partial_x \bar{\Phi} \partial_x \tilde{\Phi} \right) \big|_{\bar{Z}_j^-}^{\bar{Z}_j^+} Z_{ZPM,j} \boldsymbol{Z}_j \right] \tag{4.22}
$$

where $\boldsymbol{Z}_j$ and $\boldsymbol{P}_j$ are the dimensionless position and momentum fluctuations for the mirror center of mass as in (4.12)–(4.17).

Assuming that the field has only one mode, we use the plane wave ansatz in (3.12) for the classical part of the field and (2.1) for the quantum fluctuations to rewrite the Hamiltonian as

$$
\tilde{H}_{BC} = \hbar \omega \boldsymbol{a}^\dagger \boldsymbol{a} + \sum_{j=1,2} \left[ \frac{\hbar \eth_j}{2} \left( \boldsymbol{P}_j^2 + \boldsymbol{Z}_j^2 \right) - \hbar \left( \frac{\Omega_0}{L} Z_{ZPM,j} A_0 \right) \left( r_j^*(\omega) \boldsymbol{a} + r_j(\omega) \boldsymbol{a}^\dagger \right) \boldsymbol{Z}_j \right]
$$
$$
\tag{4.23}
$$

where $r_1(\omega) \equiv R_1(\omega) - R_2(\omega) e^{ikd}$ and $r_2(\omega) \equiv R_2(\omega)$. Now moving to a rotating

frame with respect to the free field Hamiltonian $\left(\boldsymbol{H}_F \equiv \hbar\omega\boldsymbol{a}^\dagger\boldsymbol{a}\right)$ leads us to the following equations of motion for the dimensionless field and mirror variables

$$\frac{\mathrm{d}\boldsymbol{Z}_j}{\mathrm{d}t} = \mho\boldsymbol{P}_j \tag{4.24}$$

$$\frac{\mathrm{d}\boldsymbol{P}_j}{\mathrm{d}t} = -\mho\boldsymbol{Z}_j + \sqrt{2}\mathrm{Re}\beta_{M_jF}\boldsymbol{\Phi} - \sqrt{2}\mathrm{Im}\beta_{M_jF}\boldsymbol{\Pi} \tag{4.25}$$

$$\frac{\mathrm{d}\boldsymbol{\Phi}}{\mathrm{d}t} = \sqrt{2}\sum_{j=1,2}\mathrm{Im}\beta_{M_jF}\boldsymbol{Z}_j \tag{4.26}$$

$$\frac{\mathrm{d}\boldsymbol{\Pi}}{\mathrm{d}t} = \sqrt{2}\sum_{j=1,2}\mathrm{Re}\beta_{M_jF}\boldsymbol{Z}_j \tag{4.27}$$

where $\beta_{M_jF} \equiv \frac{\Omega}{L}Z_{ZPM}A_0 r_j^*(\omega)$ are the effective coupling coefficient for the mirror $\mathcal{M}_j$ and the field. It can be seen from Fig. 4.2 and Fig. 4.3 that in the weak coupling limit $(\Omega_{Pj}/\omega \ll 1)$ where one can generally ignore the fluctuation mediated term unless very close to resonance, the effective mirror-field coupling coefficient in (4.10) and (4.11) then reduces to $\alpha_{M_jF} \approx -\beta_{M_jF}/\sqrt{2}$. Also for a negligibly small steady state amplitudes of the two internal degrees of freedom as in (4.20) and (4.21) we can see an agreement between the equations of motion for the mirrors' centers of mass and the field in the microscopic picture (4.12), (4.13), (4.16) and (4.17), and those obtained from the boundary condition considerations above in (4.24)–(4.27). We also illustrate this agreement in terms of the entanglement between the two *mdf*s and that between the field and the CoM for mirror $\mathcal{M}_1$ in Fig. 4.4, wherein we show that for strongly damped internal degrees of freedom the entanglement found from the boundary condition considerations matches with that from the MOF model.
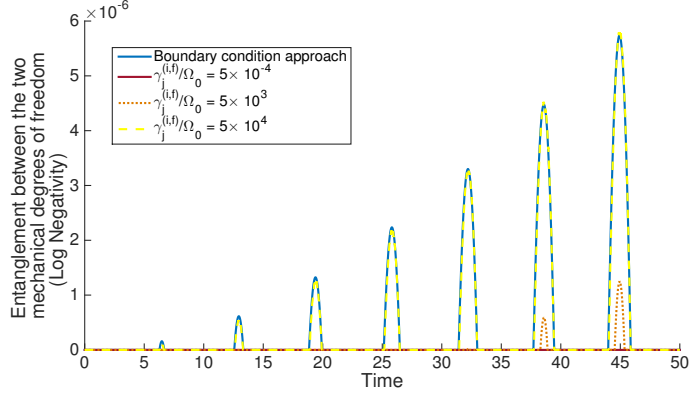
(a) Entanglement between the two *mdf*s as a function of time for different damping rates for the mirrors' internal degrees of freedom. The overlap between the solid blue and dashed yellow curves indicates that the boundary condition approach agrees with the MOF model for strong enough damping of the two internal degrees of freedom (any differences between the two curves are smaller than the resolution of the plot).
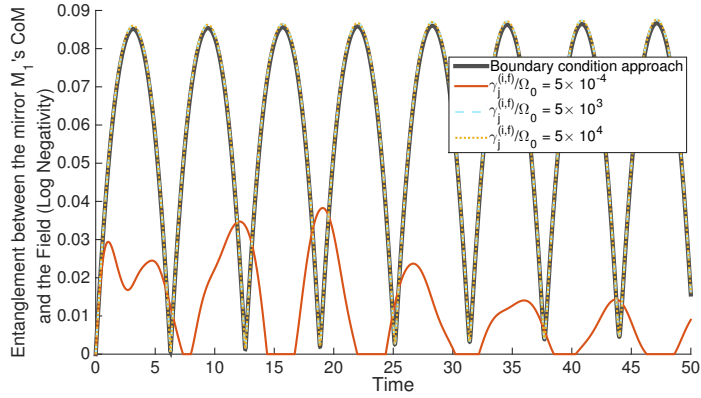


(b) Entanglement between the center of mass of mirror $\mathcal{M}_1$ and the field as a function of time for different damping rates for the mirrors' internal degrees of freedom.

Figure 4.4: Comparison of the entanglement dynamics from boundary condition approach and MOF model for the two mirror setup – the two approaches match in the limit of strongly damped *idf*s. The parameter values (in units $\hbar = c = k_B = 1$) were chosen as $\Omega_{1,2} = 100$, $\Omega_{P1} = 0.05$, $\Omega_{P2} = 0.2$ for the two internal degrees of freedom, $M_{1,2} = 1$ and $\mho_{1,2} = 1$ for the mechanical degrees of freedom, the field

102

### 4.1.2 Entanglement dynamics in the coupled MOFOM system

The coupled MOFOM system dynamics can be solved from (4.12)–(4.17) by finding the normal modes of the system and their time evolution. One can then obtain the 10x10 dimensional covariance matrix for the dynamical variables pertaining to the two mirrors and the field. We define the MOFOM covariance matrix $\mathcal{V}_{MOFOM}$ as

$$\mathcal{V}_{MOFOM} = \begin{pmatrix} \mathbf{V_{M_1M_1}} & \mathbf{V_{M_1M_2}} & \mathbf{V_{M_1F}} & \mathbf{V_{M_1O_1}} & \mathbf{V_{M_1O_2}} \\[6pt] \mathbf{V_{M_1M_2}^T} & \mathbf{V_{M_2M_2}} & \mathbf{V_{M_2F}} & \mathbf{V_{M_2O_1}} & \mathbf{V_{M_2O_2}} \\[6pt] \mathbf{V_{M_1F}^T} & \mathbf{V_{M_2F}^T} & \mathbf{V_{FF}} & \mathbf{V_{FO_1}} & \mathbf{V_{FO_2}} \\[6pt] \mathbf{V_{M_1O_1}^T} & \mathbf{V_{M_2O_1}^T} & \mathbf{V_{FO_1}^T} & \mathbf{V_{O_1O_1}} & \mathbf{V_{O_1O_2}} \\[6pt] \mathbf{V_{M_1O_2}^T} & \mathbf{V_{M_2O_2}^T} & \mathbf{V_{FO_2}^T} & \mathbf{V_{O_1O_2}^T} & \mathbf{V_{O_2O_2}} \end{pmatrix} \tag{4.28}$$

Again, the on-diagonal matrix $\mathbf{V_{kk}}$ stands for the sub-covariance matrix of the $k^{th}$ reduced subsystem, defined as $(\mathbf{V_{kk}})_{ij} \equiv \frac{1}{2}\left\langle \{X_i^{(k)}, X_j^{(k)}\} \right\rangle$, with $X_i^{(k)}$ and $X_j^{(k)}$ representing the i and j quadratures corresponding to the position and momentum variables of the $k^{th}$ reduced subsystem, more explicitly $\boldsymbol{X}^{(k)} \equiv \{\tilde{x}^{(k)}, \tilde{p}^{(k)}\}$. Here, $\{\mathcal{O}_1, \mathcal{O}_2\}$ denotes the anti-commutator between the operators $\mathcal{O}_1$ and $\mathcal{O}_2$. The off-diagonal sub-matrix $\mathbf{V_{kl}}$ consists of the correlations between the $k^{th}$ and the $l^{th}$ subsystems, such that $(\mathbf{V_{kl}})_{ij} \equiv \frac{1}{2}\left\langle \{X_i^{(k)}, X_j^{(l)}\} \right\rangle$, where the i and j quadrature components belong to different subsystems. The expectation values of the correlators are taken over the initial density operator of the five subsystems at $t = 0$, which we assume to be in a thermal state with a temperature determined by that of the corresponding bath. More explicitly, the initial density matrix of the MOFOM

system can be written as

$$\rho(0) = \rho_{M_1}^{T_1^{(m)}} \otimes \rho_{M_2}^{T_2^{(m)}} \otimes \rho_{O_1}^{T_1^{(i)}} \otimes \rho_{O_2}^{T_2^{(i)}} \otimes \rho_f^{T_f} \tag{4.29}$$

where the density matrix $\rho_k^{T_k}$ for subsystem $k$ corresponds to a thermal distribution with temperature $T_k$.

We now consider the part of the covariance matrix that represents the reduced covariance matrix for the two mechanical degrees of freedom

$$\mathcal{V}_{M_1 M_2} = \begin{pmatrix} \mathbf{V_{M_1 M_1}} & \mathbf{V_{M_1 M_2}} \\ \mathbf{V_{M_1 M_2}^T} & \mathbf{V_{M_2 M_2}} \end{pmatrix} \tag{4.30}$$

and find the logarithmic negativity $E_N^{M_1 M_2}$ using the positive partial transpose (PPT) criteria for determining separability (see Appendix A). It can also be proved (Appendix B) that calculating the correlators for any two subsystems after coarse-graining over the remaining degrees of freedom is equivalent to considering the correlation values as in the sub-covariance matrix. With this result we do not necessarily need to trace over the remaining subsystems to look at the entanglement between any two subsystems of interest.

Similarly to compare the entanglement between the case of a single mirror and the field in the presence of the second mirror with that from what we found earlier, we also consider the covariance matrices for the individual mirrors and the field

$$\mathcal{V}_{M_j F} = \begin{pmatrix} \mathbf{V_{M_j M_j}} & \mathbf{V_{M_j F}} \\ \mathbf{V_{M_j F}^T} & \mathbf{V_{FF}} \end{pmatrix} \tag{4.31}$$

Having found the reduced covariance matrix for the relevant subsystems that we wish to study the entanglement between, we now list the various parameters pertaining to the five subsystems and the assumptions made in table 4.1.

| Mechanical degrees of freedom | Internal degrees of freedom | Field |
|---|---|---|
| $\mho_{1,2}$ (Frequencies of the mechanical oscillators) | $\Omega_{1,2}$ (*idf* resonance frequencies) | $\omega$ (Frequency of the field mode) |
| $M_{1,2}$ (Mirror masses) | $\Omega_{P1,2}$ (*idf*-field coupling strengths) | $\Phi_0$ (Field amplitude) |
| $\Gamma_{1,2}$ (Mechanical damping rates) | $\gamma_{1,2}^{(f)}$, $\gamma_{1,2}^{(i)}$ (*idf* damping rates from interaction with the two baths) | $\Gamma_F$ (Field mode damping) |
| $T_{1,2}^{(m)}$ (Temperature of the mechanical baths) | $T_{1,2}^{(f)}$, $T_{1,2}^{(i)}$ (Field and *idf* bath temperatures) | $T_f$ (Field bath temperature) |

Table 4.1: Parameters pertaining to the five subsystems – the mirrors' *mdf*s, *idf*s and the single mode field $\Phi_\omega$. The separation between the two mirror CoM positions $d$ is an additional parameter. The assumptions restricting these parameters in our analysis are 1.) $\mho_j \ll \Omega_j$, for a slow-moving mirror, 2.) weak-coupling between the *idf*s and the field such that $\Omega_{P,j} \ll \Omega_j$, 3.) $\Delta_j \ll \Omega_j$ for the rotating-wave approximation, 4.) $|\Phi_0|^2 \ll \frac{M_j \mho_j^2 c}{\Omega_j^3 \epsilon_0}$ for weak-driving to ensure small amplitude of the mirror motion and 5.) Markovian noise and Ohmic dissipation for all subsystems.

In the previous section we considered the effect of changing the *idf* damping rates on the *mdf* $_1$-field and the *mdf* -*mdf* entanglement and found how in the limit of strongly damped internal degrees one recovers the boundary condition results.

It can also be seen from Fig. 4.4 that it takes a larger *idf* damping to reach the boundary condition limit for the mirror-mirror entanglement, meaning that while for a certain mirror the boundary condition approach might describe the optomechanical entanglement well, it could possibly give inaccurate results when considering the entanglement of the mirror motion with that of another mirror.

One could also ask how does the entanglement between a single mirror and the field in the presence of the second mirror compare with the case when there is no other mirror. We illustrate this comparison in Fig. 4.5, where we find that for the given set of parameter values the entanglement between the mirror and the field is smaller when a second identical mirror is present. We also note that as a function of the mirror separation the entanglement dynamics is periodic after a distance $\Delta d = 2\pi c/\omega$, coming from the free spectral range of the cavity. Also, from comparing Fig. 4.5(a) and Fig. 4.5(b) it can be seen that for larger *idf* -field detuning values there is a smaller entanglement and the distance dependence is less pronounced as well. This can be explained based on what we found in Fig. 4.2 and Fig. 4.3 as well, where we find that as one moves further away from *idf* -field resonance the dependence of the effective mirror-field couplings on the mirror separation $d$ becomes less prominent.
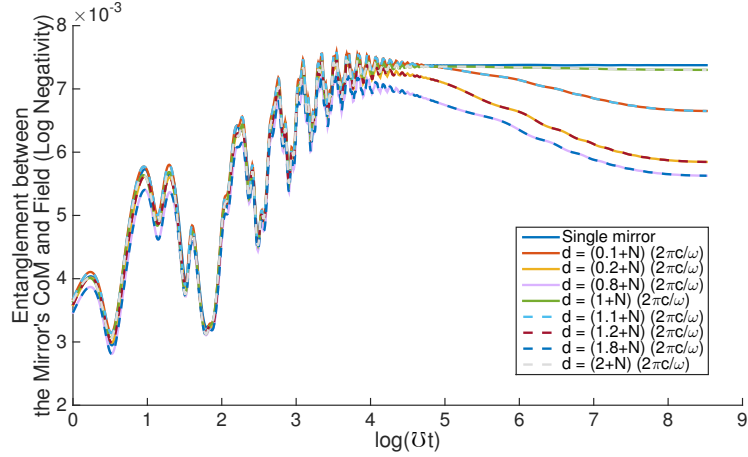
(a) Entanglement between the CoM of mirror $\mathcal{M}_1$ and the field for different values of the mirror separation, for an *idf*-field detuning of $\Delta_{1,2}/\mho = -5$
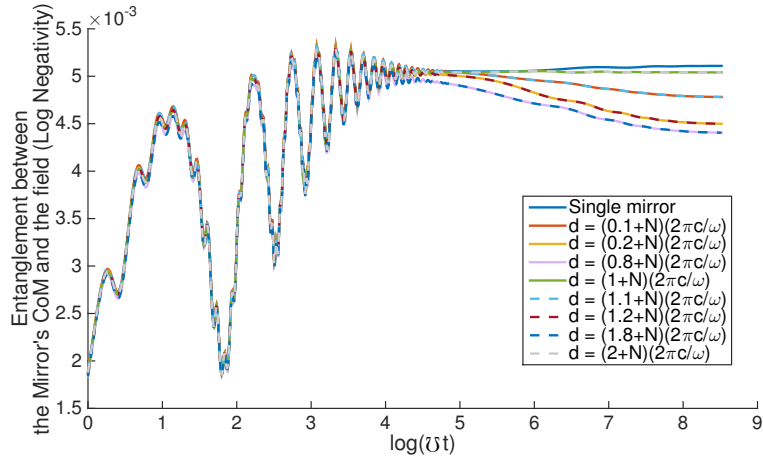


(b) Entanglement between the CoM of mirror $\mathcal{M}_1$ and the field for different values of the mirror separation, for an *idf*-field detuning of $\Delta_{1,2}/\mho = -10$

Figure 4.5: Comparison of the entanglement between a single mirror and the field with and without the second mirror's presence – we note that for the chosen parameter values there is a smaller mirror-field entanglement for the two-mirror setup as compared to the single mirror case, all the other parameters being identical. In units where $\hbar = c = k_B = 1$ and $e = \sqrt{4\pi\alpha}$, we have $M_{1,2} = 1$, $\mho_{1,2} = 1$, $\Gamma_{1,2} = 0.1$ and $T_{1,2}^{(m)} = 0.1$ for the two *mdf*s, $\Omega_{1,2} = 100$, $\Omega_{P1,P2} = 0.05$, $\gamma_{1,2}^{(i,f)} \approx 0.02$ and $T_{1,2}^{(i,f)} = 0.1$ for the *idf*s, and $\Phi_0 \approx 10^{-4}$ and $\Gamma_F = 10^{-3}$ for the field.

To study the entanglement between two mechanical degrees of freedom as a function of some additional parameters, we consider the realistic setup of two atoms interacting with common single mode cavity field in the following subsection.

### 4.1.3 Mechanical Entanglement between Two Atoms

Let us consider two atoms interacting with a single mode cavity field. Using the MOF model to describe the atom-field interaction for each of the atoms, we find the entanglement between the CoM motion of the two atoms. As in the previous chapter we use the typical parameter values from [95, 96]. As we showed in section 2.3.1, for the purposes of rough estimation our analysis from the MOF model can be easily extended from 1+1 to 3+1 D by replacing the vacuum permittivity $\epsilon_0 \to \mathcal{A}\epsilon_0$ where $\mathcal{A}$ is the cross-sectional area of the driving field, assuming that the longitudinal component of the field is negligibly small and that one can ignore scattering from the atomic dipole in the transverse directions.

We rewrite the original action as

$$
S = \int \mathrm{d}t \left[ \sum_{j=1,2} \left( \frac{1}{2} M_j \dot{\boldsymbol{R}_j}^2 - \frac{1}{2} M_j \mho_j^2 \boldsymbol{R_j}^2 \right) + \left( \frac{1}{2} m_j \dot{\boldsymbol{q}_j}^2 - \frac{1}{2} m_j \Omega_j^2 \boldsymbol{q_j}^2 \right) \right.
$$
$$
\left. + \int \mathrm{d}^3 r \frac{\epsilon_0}{2} \left\{ (\partial_t \boldsymbol{\Phi})^2 - c^2 \left( \boldsymbol{\nabla_r} \times \boldsymbol{\Phi} \right)^2 + \sum_{j=1,2} \lambda_j \dot{\boldsymbol{q}_j} \cdot \boldsymbol{\Phi} \delta^3 (\boldsymbol{r} - \boldsymbol{R_j}) \right\} \right]
$$

(4.32)

where $\boldsymbol{R_j}$ now refers to the CoM coordinates of the j$^{th}$ atom, $\boldsymbol{q_j}$ is the 3 dimensional *idf* amplitude of the mirror $\mathcal{M}_j$, that represents the motion of an electron within the j$^{th}$ atom and $\boldsymbol{\Phi}$ is the vector potential of the EM field. One can obtain the following equations of motion for the classical solutions of the coupled field and *idf* degrees of

freedom

$$\ddot{\bar{q}}_j + \Omega_j^2 \bar{q}_j = -\frac{\lambda_j}{m_j}\dot{\bar{\Phi}}\left(\bar{R}_j, t\right) \tag{4.33}$$

$$\epsilon_0 \left(\ddot{\bar{\Phi}}\left(r, t\right) - c^2\nabla_r^2\bar{\Phi}\left(r, t\right)\right) = \sum_{j=1,2}\lambda_j\dot{\bar{q}}_j\delta^3(r - \bar{R}_j) \tag{4.34}$$

Assuming that we have a driving field of the form $\boldsymbol{\Phi} = \boldsymbol{\Phi}_0\frac{\Omega_0}{\omega}f(x,y)g(z,t)$, with $f(x,y)$ as the transverse mode function of the field and the longitudinal part $g(z,t)$ similar to the 1+1 D plane wave ansatz given by

$$g(z,t) = e^{-i\omega t}\left[\Theta(-z)\left\{e^{ik_z z} + R_1\left(\omega\right)e^{-ik-zz}\right\}\right.$$

$$+\left(\Theta(z) - \Theta(z-d)\right)\left\{T_1\left(\omega\right)e^{ik_z z} + R_2\left(\omega\right)e^{-ik_z(z-d)}\right\}$$

$$\left.+\Theta(z-d)T_2\left(\omega\right)e^{ik_z(z-d)}\right] + H.C. \tag{4.35}$$

Here we have assumed that there is no scattering in the transverse direction and no diffraction effects for the field, such that the transverse mode function $f(x,y)$ is continuous across the position of the atoms $\{\bar{X}_{1,2}, \bar{Y}_{1,2}\}$ in the $x$-$y$ plane. We integrate the field equation of motion (4.34) around the position of the atoms $\bar{Z}_{1,2}$ in z and over the $x$-$y$ plane

$$\lambda_j\dot{\bar{q}}_j = \epsilon_0 c^2\boldsymbol{\Phi}_0\frac{\Omega_0}{\omega}\left(\int_{-\infty}^{\infty}\mathrm{d}x\int_{-\infty}^{\infty}\mathrm{d}y f(x,y)\right)\partial_z\left(g(z)\right)|_{\bar{Z}_j^-}^{\bar{Z}_j^+} \tag{4.36}$$

$$= -2i\epsilon_0 k_z c\boldsymbol{\Phi}_0\frac{\Omega_0}{\omega}\mathcal{A}\partial_z\left(g(z)\right)|_{\bar{Z}_j^-}^{\bar{Z}_j^+} \tag{4.37}$$

where in the last step we have replaced the integral over the transverse mode function $\mathcal{A} \equiv \left(\int_{-\infty}^{\infty}\mathrm{d}x\int_{-\infty}^{\infty}\mathrm{d}y f(x,y)\right)$. One could also solve for steady-state *idf* dynamics from (4.33) to find

$$\lambda\dot{\bar{q}}_j = \frac{-\omega^2\lambda_j^2}{m_j\left(\omega^2 - \Omega_j^2\right)}\frac{\Omega_0}{\omega}\boldsymbol{\Phi}_0 f(\bar{X}_j, \bar{Y}_j)g(\bar{Z}_j) \tag{4.38}$$

Further assuming that $\bar{X}_1 = \bar{X}_2$ and $\bar{Y}_1 = \bar{Y}_2$ such that the normalized mode function $f(\bar{X}_j, \bar{Y}_j) = 1$ at both the atomic CoM positions, from (4.37) and (4.38) one can obtain the reflection and transmission coefficients as before in (3.25)–(3.28) with the plasma frequencies $\Omega_{Pj}$ replaced by

$$\Omega_{Pj}^{(3D)} \equiv \frac{\lambda_j^2}{2m_j \epsilon_0 c \mathcal{A}} \tag{4.39}$$

.

As in section 2.3.1, we identify the CoM motion of the two atoms as the mechanical degrees of freedom, assuming that the atoms are in identical harmonic traps, such that we have for the *mdf* parameters – $M_1 = M_2 = 1.4 \times 10^{-25}$ kg, $\mho_1 = \mho_2 \approx 10$ kHz as the trap frequency, $\Gamma_1 = \Gamma_2 \approx 10 s^{-1}$ and temperatures for the mechanical bath as $T_{1,2}^{(m)} \sim 0.1$ mK. The internal degrees of freedom represent the electronic transitions between the atomic levels, which as before we assume to be linear as well with a frequency given by the transition frequency for the $5^2 S_{1/2} F = 3 \leftrightarrow 5^2 P_{3/2} F = 4$ transition, such that $\Omega_1/(2\pi c) = \Omega_2/(2\pi c) \approx \frac{1}{780 \times 10^{-9}}$m$^{-1}$. The damping rate for the *idfs* is given by the cavity modified damping $\gamma_{1,2}^{(f)} \approx 10$ MHz from the coupling of the electron to the field mode continuum. We note that there is no other bath for the electronic degrees of freedom in this case, thus $\gamma_{1,2}^{(i)} = 0$. For the field, we choose $\omega = \Omega_{1,2} + \Delta_a$, where $\Delta_a \approx 10$ MHz is the detuning of the cavity field with respect to the atomic resonance. The cavity damping rate for a typical $Q \approx 5 \times 10^5$ is $\Gamma_F \sim \frac{c}{QL} \approx 2.5$ MHz, given the cavity length of $L = 120\mu$m. We assume the input power to be $\mathcal{P} \approx 0.1$ pW and the beam cross sectional area $\mathcal{A} \approx 7 \times 10^{-10}$ m$^2$. We ensure that the power inside the cavity remains small enough

so that the higher lying levels in the harmonic oscillator model of the *idf* do not get populated and the linear approximation remains good.

Using these parameter values we find the effective coupling strength between the *idf*s and the field as $\alpha_{O_{1,2}F} \sim 0.1$ GHz, the effective *idf-mdf* couplings as $\alpha_{O_{1,2}M_{1,2}} \sim 0.1$ MHz and the effective *mdf-* field coupling to be $\alpha_{M_{1,2}F} \sim 100$ MHz. From Fig. 4.6 one can note that as expected moving away from the internal resonance of the atoms, one finds smaller motional entanglement. This can be understood from the fact that for a single atom a larger *idf*-field detuning leads to smaller *mdf*-field entanglement and knowing that the field is the only channel via which the entanglement between the two separate atomic CoMs can be transferred, one necessarily requires a large *mdf*-field entanglement for both the atoms to be able to observe a large entanglement between the motion of the two atoms. Furthermore, from Fig. 4.7 we note that the entanglement exists for very low temperatures of the mechanical bath $< 0.5mK$.
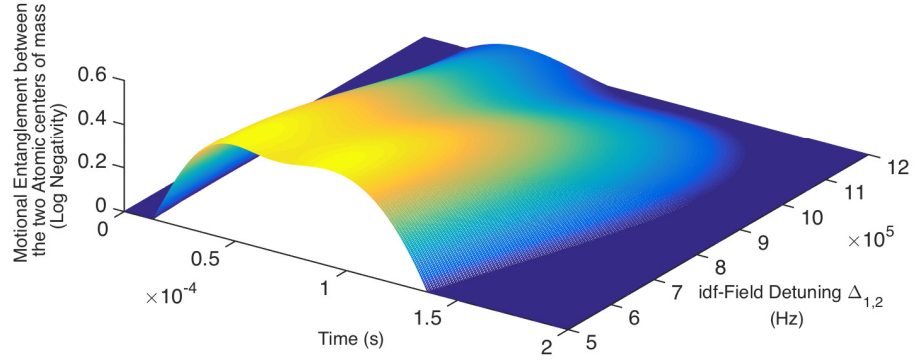
Figure 4.6: Entanglement between the motion of the two atoms as a function of the detuning of the field with respect to the atomic resonance frequency $\Omega$ and time. We fix all the other parameters as $Q = 5 \times 10^5$ for the quality factor of the cavity, $L = 120\mu$m for the cavity length, $\mathcal{A} \approx \pi(15\mu \text{ m})^2$ for the field cross sectional area, $\mathcal{P} = 0.01$ pW for the driving field power, $2\pi c/\Omega = 780$ nm for the $idf$ resonance, $m = m_e$ for the $idf$ mass, $\lambda = e$ for the $idf$-field coupling strength, $\gamma_f \approx 18$ MHz for the $idf$ damping, $M = 1.4 \times 10^{-25}$ kg for the atomic mass, $\mho = 10kHz$ for the trap frequency, $T_m = 0.1$ mK for the temperature of the mechanical and $T_i = T_f = 100$ K for the field and the $idf$ bath temperatures.
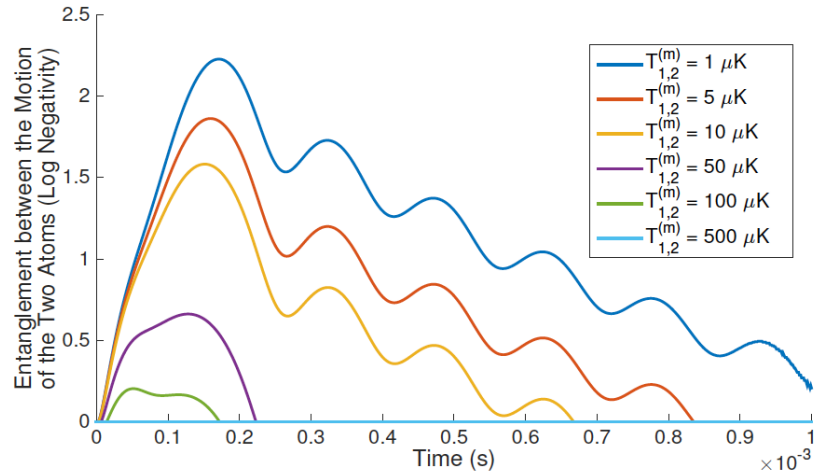
Figure 4.7: Entanglement between the atomic CoM motion and the field mode as a function of the temperature of the mechanical bath, all the other values being fixed as detailed in Fig. 4.6 and the field detuning set at 10 MHz. It can be seen that, as expected, as one goes to low enough temperatures, one can find long-lived entanglement between the two atoms.

Chapter 5:   Results and Discussion

The foremost theme of this study is to highlight the significance of the internal degrees of freedom of a mirror that play the role of the essential intermediary when it comes to the interaction between a quantum field and the mirror's mechanical motion. We illustrate how a microscopic model of quantum optomechanics, such as the MOF model proposed by Galley, Behunin and Hu [1] is a physically more complete and intuitive description for optomechanical interactions, in that not only can it agreeably reproduce the known optomechanical properties both in the classical and quantum regimes, it also elucidates new physical aspects which are not accounted for in the general description of optomechanical interactions via radiation pressure coupling. We extend the analysis in [1] to study the quantum dynamics of the coupled mirror and field system, identifying the parameter regimes where the role of the internal degrees of the mirror becomes important and make connections with relevant experimental setups. Specifically looking at the quantum entanglement between the mirror's mechanical motion and the field, we find that there is a significant and even a critical role played by the internal degree of freedom in certain parameter regimes as it can act as a means to coherently transfer correlations between the field and the mechanical degree of freedom. We also use the model to look at the

114

entanglement between the motion of two mirrors interacting with a common field via their internal degrees of freedom and implement our calculations to the case of atom-field and atom-atom interactions. We summarize the main findings of our work in the following section.

## 5.1 Summary of results

*Radiation pressure force* – When considering the classical CoM motion we find that formally the radiation pressure force acting on the mirror center of mass agrees with what one obtains from the boundary condition approach (equation (1.8) in section 1.4.1). This is true for both $q\Phi$ [1] and $\dot{q}\Phi$ couplings. Though while in the conventional approach the field is determined by the fixed boundary conditions, in the MOF model the coupled internal and external dynamics determine the value of the field at the CoM position at any given instant. This allows one to look at new physical effects that entail the coupled dynamics of the mirror's optical and mechanical degrees of freedom and can not be captured with the boundary condition approach.

*Optical properties* – We find that the MOF model can exhibit a variety of optical behavior (section 1.4.2). Depending on the optomechanical element in consideration one can phenomenologically determine the form of coupling and the parameters pertaining to the internal degree of freedom from the reflection spectrum (see Fig.1.1). For example, we use the $q\Phi$ coupling as in [1] to describe the optical behavior of metal with a Drude-Lorentz response, while the reflection spectrum of

a structure with a sharp internal resonance such as a photonic crystal or an atom is well modeled by the $\dot{q}\Phi$ *idf* -field coupling with appropriately chosen parameters. Similarly, considering the reflection properties for a system of two mirrors interacting with a common field via their internal degrees of freedom, we find that the reflection peaks at the internal resonance of the two mirrors. Additionally there is also an interference effect from the cavity formed between the two mirrors that depends on the mirror separation (see Fig. 3.2). As shown in Fig. 3.3, we also note that as expected for strong *idf* -field coupling, the distance dependence of the reflectivity coming from the interference effect is more pronounced. The reflection coefficients determine the effective coupling strengths between the fluctuations of the center of mass motion and the field.

*Corrections to the effective mirror-field coupling from the quantum fluctuations of the idf* – It can be seen from (1.36) and also (2.6) that the effective coupling between the mirror center of mass and the field has two contributions – that from the classical amplitude of the surface charge currents determined by the reflection coefficient and additionally a separate contribution from the quantum fluctuations of the *idf* . While the first part agrees with the boundary condition approach, the latter is not accounted for if one does not allow the *idf* to be a separate quantum degree of freedom. It can be seen that such a contribution from the fluctuation mediated mirror-field coupling becomes significant in the strong coupling regime.

*Radiation pressure shot noise* – We also observe that for an undamped *idf* the radiation pressure force is determined not only by the quantum fluctuations of the field but also those of the *idf* as suggested by (2.24). While in the steady state limit

116

the strength of these fluctuations is largely determined by the boundary conditions, in the early time limit the *idf* being an independent quantum degree of freedom its quantum fluctuations would influence the radiation pressure shot noise as well.

*Agreement with the boundary condition approach* – As shown in section 2.2, from (2.34)–(2.37) and (2.7)–(2.12) it can be seen that the dynamics from the MOF model reduce to those in the boundary condition approach in the appropriate limit, i.e., when the *idf* is coupled to both the field continuum and an internal bath and is in the over damped regime, or alternatively when the driving field is far detuned from the internal resonance. We illustrate the effect of damping in Fig. 2.2, where it can be seen that as the *idf* becomes overdamped there is a perfect agreement in the system dynamics (represented in terms of the mirror-field entanglement dynamics) between the boundary condition approach and the MOF model. This is expected since for fast enough internal dynamics the boundary conditions can describe the system adequately. Similarly when considering the entanglement between two mirrors as discussed in section 4.1.1, we find a perfect agreement between the dynamics in the MOF model with those found from the boundary condition considerations in the appropriate limit, that is, where the two internal degrees (1) couple weakly to the field and (2) are overdamped or the driving field is far-detuned with respect to the two internal resonances. This can be seen from comparing the equations of motion for the mirror CoM and the field from either approaches ((4.24)–(4.27) with (4.12)–(4.17)). Also, comparing the entanglement dynamics found from the boundary condition approach with those from the MOF model in Fig. 4.4 for different *idf* damping rates, we find that as expected both the mirror-mirror and the mirror-field

117

entanglements from the two approaches concur in the overdamped *idf* limit.

*Coherent transfer of excitations* – As illustrated in Fig.2.2, isolating the *idf* from the environment can provide an additional channel for coherent transfer of mirror-field correlations and for an undamped *idf* we observe much larger steady state entanglement. For example, in including the *idf* to the coupled quantum dynamics of the MOF system we allow for the possibility of the field photon to cause a Raman-scattering-like transition changing the internal state of the mirror in addition to the Rayleigh scattering like processes. A process wherein one can have a single excitation of the mirror's internal degree split into a field photon and a mirror phonon can be described by a two-mode squeezing Hamiltonian. Such an interaction causes the mirror center of mass to be entangled with the field [98]. This can specially be seen from Fig. 2.3 where if the field is red-detuned with respect to the internal resonance by the mechanical resonance frequency (such that $\omega + \mho = \Omega$), then one gets a larger steady state entanglement. This is much like a blue-detuned drive in a typical cavity optomechanics setup generating an entangled cavity photon and a phonon [63]. Such a dependence of the optomechanical interaction on the *idf*-field resonance leading to an enhanced mirror-field entanglement is something that can not be captured in the boundary condition treatment of optomechanical interactions where one does not allow for the *idf* to be a separate quantum degree of freedom.

*Entanglement between atomic CoM motion and field* – In section 2.3.1, showing that our approach can be readily extended to 3+1 D, we implement our calculations to the case of a single atom trapped in a cavity as in the experimental setup of

118

[95] to find the entanglement between the atom's center of mass motion and the field. Assuming that the atom's internal structure is given by a harmonic oscillator for weak enough driving and considering the electronic excitations as the *idf*, we find a very close agreement between the vacuum Rabi coupling found from the considerations of our model and that in [95]. We then study the entanglement between the atomic center of mass motion and the field as a function of the field detuning, temperature of the mechanical bath and cavity Q-factor (Fig. 2.3). As expected, the steady state entanglement increases as one decreases the *idf*-field detuning and the temperature (Fig. 2.3 (a) and (b)) and increases with increasing the cavity Q-factor. This is so because on increasing the Q-factor the field amplitude builds up inside the cavity leading to larger effective coupling between the atomic motion and the field. Although since we assume weak driving for the Lorentz atom model to be valid, our analysis is only true for small enough Q factors and detuning values such that the excitation probability for the atom remains small.

*Motional entanglement between two atoms* – As in the case of a single mirror, we also implement our analysis to study the entanglement between the motion of two atoms interacting with a common field. Similar to section 2.3.1, we use the same parameters in section 4.1.3 to look at the entanglement dynamics between the center of mass motion of the atoms as a function of the *idf*-field detuning and the temperature of the mechanical baths. Again, as for the case of atom-field optomechanical entanglement, the entanglement between the two atoms increases with decreasing the field detuning and the temperature. We note the motional entanglement is highly sensitive to the internal degrees' parameters of the two mirrors.

*Field frequency shift* – When looking at the quantized Hamiltonian of the coupled mirror and field system, we note that there is an additional shift to the field frequency from its second order interaction with the *idf* as seen from (1.36) and (2.2), a feature that is not accounted for in the boundary condition treatment. Such a diamagnetic term contribution can be significant in the strong coupling regimes, even leading to change in the radiation pressure force from attractive to repulsive as has been studied in [97].

## 5.2   Future directions

*Hybrid setups* –  The MOF model provides a common framework to study hybrid setups with disparate optomechanical elements such as atoms and larger mechanical oscillators. For example, it can be seen from section 1.4.2 that one can describe different kinds of mirrors using the MOF model in terms of their optical properties and based on our analysis in chapters 2 and 3 one can study the interaction between two different mirrors. Typically when considering the mechanical effects of light on atomic scale systems one does not include the backaction of the atomic motion on the field, while for the case of larger optomechanical elements the field configuration is determined strongly by the position of the mirror via the boundary conditions. On the other hand, while for atoms one acknowledges the role of the internal degrees of freedom, usually there is no consideration of the internal structure of a mirror for larger systems. Thus, albeit being quite simplistic, the MOF model can possibly provide a more general theory to include a range of

setups with atomistic systems and larger mirrors as limiting cases, both in terms of backreaction on the field and including the internal dynamics. In this work we have implemented our model to the case of atoms, as an extension it would be interesting to explore the possibility of describing larger systems which exhibit internal resonances and combine the two elements to study a hybrid setup.

*Fully dynamical description* – For relativistically moving mirrors, as in the case of dynamical Casimir effect [92], applying boundary conditions is an inadequate description of the dynamics since in the time scales over which internal degrees and the field reach a steady state thereby leading to an effective boundary condition, the mirror center of mass moves appreciably enough to affect their interaction with the field. In cases where the timescales of the mechanical motion and the field-internal degree of freedom interaction are close to each other, including the internal degree of freedom becomes relevant as the only means to capture the coupled dynamical interplay of the three subsystems. The role of the internal degrees of freedom in dynamical Casimir effect has not been studied in the literature yet and this could potentially be an important extension of our work.

*Backaction of the mechanics on the mirror-field interaction* – It has been noted in several works that the self-consistent backaction of an optomechanical element can lead to interesting effects such as modifications to the cooling limit [70, 71], access to strong single photon-mirror optomechanical coupling and collective long-ranged interactions in an array of atomic mirrors [72]. In our current analysis we restrict the center of mass motion to the Lamb-Dicke limit, assuming that the motion does not affect the optical properties of the mirror. In addition to the backaction, the

MOF model can also include the internal degrees of the mirror thereby leading to new physical effects and possibly a cooling scheme that exploits the backaction of the *idf* on the field.

*A microscopic model for Casimir forces* – For the case of two mirrors interacting with each other in the absence of a driving field, one can look at the corrections to the Casimir/Casimir-Polder forces. It can be seen from (3.30) that the MOF model allows one to take into account corrections that come from including the fluctuations of the center of mass motion. We expect that these corrections would become important for mirrors with a small enough mass. Such an effect that corresponds to processes such as the emission and absorption of a virtual phonon has not yet been studied in the literature and can be analyzed with the MOF model.

## 5.3   Conclusion

In conclusion, we see that including the internal degrees of freedom of a mirror naturally leads to a whole range of interesting physical features that one otherwise misses out when using conventional approach to optomechanics. We show that the MOF model allows us to go beyond the usual disjoint treatment of mirror-field interactions wherein one imposes boundary conditions on the field and treats the mechanical effects of the field arising from the radiation pressure force separately to attain a self-consistent depiction where we see both the radiation pressure (section 1.4.1) and the boundary conditions (section 1.4.2) emerge from a physically motivated microscopic interaction. Not only does a microscopic model like the

MOF model reproduce the known optomechanical properties and provide a more self-consistent approach of studying optomechanical interactions, more importantly it leads to qualitatively different physics, specifically in the quantum regime. For example we show that including a whole other quantum degree of freedom that provides a means to coherently transfer quantum correlations between the field and the mirror's mechanical motion can, in appropriate parameter regimes, lead to a larger optomechanical entanglement. We show that in the parameter regimes where the *idf* is isolated from the environment, or if one probes close to the internal resonance of the mirror, or for strong coupling, the role of the *idf* becomes more pronounced. From studying the mirror-field entanglement as a function of the various parameters of the model pertaining to the *idf* and otherwise, we find that the presence of the *idf* can influence the entanglement dynamics to a significant extent. We conclude that the internal degree of freedom being the quintessential mediator of interaction between the mirror center of mass and the field, the MOF model gives a physically more complete treatment of the mirror-field interactions.

# Appendix A:   Logarithmic negativity

After $t = 0$ the interaction is turned on and the three subsystems ($mdf$, $idf$ and the field) begin to interact with each other as the reduced density matrices for each of individual becomes a mixed state. The linearity of the interaction terms guarantees that the quantum state of the three harmonic oscillators that starts Gaussian remains Gaussian. Thus the dynamics of quantum entanglement can be studied by examining the behavior of the quantity $\Sigma$ [99] and the logarithmic negativity $E_{MF}$ [100]:

$$\Sigma \quad \equiv \quad \det\left[\mathcal{V}_{MF}{}^{PT} + \frac{i\hbar}{2}\mathcal{M}\right], \tag{A.1}$$

$$E_{MF} \quad \equiv \quad \max\left\{0, -\log_2 2c_-\right\}. \tag{A.2}$$

Here $\mathcal{M}$ is the symplectic matrix $\mathbf{1} \otimes (-i)\sigma_y$, $\mathcal{V}_{MF}$ is the partial transpose of the covariance matrix

$$\mathcal{V}_{MF} = \begin{pmatrix} \mathbf{V_{MM}} & \mathbf{V_{MF}} \\ \mathbf{V_{MF}^T} & \mathbf{V_{FF}} \end{pmatrix} \tag{A.3}$$

as defined in (2.41). $(c_+, c_-)$ is the symplectic spectrum of $\mathcal{V}_{MF}{}^{PT} + (i\hbar/2)\mathcal{M}$, given by

$$c_\pm \equiv \left[\frac{Z \pm \sqrt{Z^2 - 4\det\mathcal{V}_{MF}}}{2}\right]^{1/2} \tag{A.4}$$

124

with

$$Z = \det \mathbf{V}_{MM} + \det \mathbf{V}_{FF} - 2 \det \mathbf{V}_{MF}. \tag{A.5}$$

For the quantum oscillators in Gaussian state, $E_{MF} > 0$, $\Sigma < 0$, and $c_- < \hbar/2$, if and only if the quantum state of the two subsystems is entangled [101]. $E_{MF}$ is an entanglement monotone [102] whose value can indicate the degree of entanglement.

## Appendix B: With or Without

## A Trace, Of Doubt?

Here we consider the question of whether it is justified to use the joint covariance matrix of $N$ subsystems in order to deduce the entanglement between few, say two, of the constituent subsystems. For example, in chapter 3 we found the joint covariance matrix of the mirror CoM, *idf* and field and used it to calculate the log Negativity between the mirror CoM and the field, without explicitly tracing away the *idf*. We will show in the following that it is justified to do so.

Let us consider a density matrix $\hat{\rho}(0) = \hat{\rho}_1(0) \otimes \hat{\rho}_2(0) \otimes \ldots \hat{\rho}_N(0)$ of $N$ harmonic oscillators, initially in a separable state. Where in some basis we can express the reduced density matrices of the individual subsystems as

$$\hat{\rho}_k(0) = \sum_{i_k j_k} \alpha_{i_k j_k}^{(k)} |i_k\rangle \langle j_k| \tag{B.1}$$

Let us assume that the three systems begin to interact with each other at time $t = 0$ and evolve unitarily such that

$$\hat{\rho}(t) = \mathcal{U}\hat{\rho}(0)\mathcal{U}^\dagger \tag{B.2}$$

$$= \mathcal{U}\hat{\rho}_1(0) \otimes \hat{\rho}_2(0) \otimes \ldots \hat{\rho}_N(0)\mathcal{U}^\dagger \tag{B.3}$$

$$= \mathcal{U} \sum_{i_1 j_1} \alpha_{i_1 j_1}^{(1)} |i_1\rangle \langle j_1| \otimes \sum_{i_2 j_2} \alpha_{i_2 j_2}^{(2)} |i_2\rangle \langle j_2| \otimes \cdots \sum_{i_N j_N} \alpha_{i_N j_N}^{(N)} |i_N\rangle \langle j_N|\mathcal{U}^\dagger \tag{B.4}$$

Now, say the time evolved state is given as

$$\mathcal{U}|i_1\rangle|i_2\rangle\ldots|i_N\rangle = \sum_{m_1 m_2 \ldots m_N} \xi_{i_1 i_2 \ldots i_N}^{m_1 m_2 \ldots m_N}(t) |m_1\rangle|m_2\rangle\ldots|m_N\rangle \qquad (\text{B.5})$$

which gives

$$\hat{\rho}(t) = \sum_{i_1 i_2 \ldots i_n} \sum_{j_1 j_2 \ldots j_N} \sum_{m_1 m_2 \ldots m_N} \sum_{n_1 n_2 \ldots n_N} \alpha_{i_1 j_1}^{(1)} \alpha_{i_2 j_2}^{(2)} \ldots \alpha_{i_N j_N}^{(N)} \xi_{i_1 i_2 \ldots i_N}^{m_1 m_2 \ldots m_N}(t) \left(\xi_{j_1 j_2 \ldots j_N}^{n_1 n_2 \ldots n_N}(t)\right)^*$$

$$|m_1\rangle|m_2\rangle\ldots|m_N\rangle\langle n_1|\langle n_2|\ldots\langle n_N|$$

$$(\text{B.6})$$

Now, say, we wish to trace away all the subsystems but the first and the second, so that we can study their entanglement. Then, taking a trace over subsystems 3 to N, the reduced density matrix of system 1 and 2 at time $t$ becomes

$$\hat{\rho}_{12}(t) = \sum_{p_3 p_4 \ldots p_N} \langle p_3|\langle p_4|\ldots\langle p_N| \sum_{i_1 i_2 \ldots i_n} \sum_{j_1 j_2 \ldots j_N} \sum_{m_1 m_2 \ldots m_N} \sum_{n_1 n_2 \ldots n_N} \alpha_{i_1 j_1}^{(1)} \alpha_{i_2 j_2}^{(2)} \ldots \alpha_{i_N j_N}^{(N)}$$

$$\xi_{i_1 i_2 \ldots i_N}^{m_1 m_2 \ldots m_N}(t) \left(\xi_{j_1 j_2 \ldots j_N}^{n_1 n_2 \ldots n_N}(t)\right)^* |m_1\rangle|m_2\rangle\ldots|m_N\rangle\langle n_1|\langle n_2|\ldots\langle n_N||p_3\rangle|p_4\rangle\ldots|p_N\rangle$$

$$(\text{B.7})$$

$$\implies \hat{\rho}_{12}(t) = \sum_{p_3 p_4 \ldots p_N} \sum_{i_1 i_2 \ldots i_n} \sum_{j_1 j_2 \ldots j_N} \sum_{m_1 m_2 \ldots m_N} \sum_{n_1 n_2 \ldots n_N} \alpha_{i_1 j_1}^{(1)} \alpha_{i_2 j_2}^{(2)} \ldots \alpha_{i_N j_N}^{(N)}$$

$$\xi_{i_1 i_2 \ldots i_N}^{m_1 m_2 \ldots m_N}(t) \left(\xi_{j_1 j_2 \ldots j_N}^{n_1 n_2 \ldots n_N}(t)\right)^* \delta_{p_3 m_3}\delta_{p_3 n_3}\ldots\delta_{p_N m_N}\delta_{p_N n_N} |m_1\rangle|m_2\rangle\langle n_1|\langle n_2|$$

$$(\text{B.8})$$

Now summing over $m_3 \ldots m_N$ and $n_3 \ldots n_N$, gives us

$$\implies \hat{\rho}_{12}(t) = \sum_{p_3 p_4 \ldots p_N} \sum_{i_1 i_2 \ldots i_n} \sum_{j_1 j_2 \ldots j_N} \sum_{m_1 m_2} \sum_{n_1 n_2} \alpha_{i_1 j_1}^{(1)} \alpha_{i_2 j_2}^{(2)} \ldots \alpha_{i_N j_N}^{(N)}$$

$$\xi_{i_1 i_2 \ldots i_N}^{m_1 m_2 p_3 \ldots p_N}(t) \left(\xi_{j_1 j_2 \ldots j_N}^{n_1 n_2 p_3 \ldots p_N}(t)\right)^* |m_1\rangle|m_2\rangle\langle n_1|\langle n_2|$$

$$(\text{B.9})$$

Now, let us evaluate the expectation value of some operator $\hat{\mathcal{O}}_{12}$ defined on the joint

subspace of system 1 and 2. In the Schrödinger picture we have

$$\left\langle \hat{\mathcal{O}}_{12}\hat{\rho}_{12}(t)\right\rangle_{12} = \sum_{p_1 p_2} \langle p_1| \langle p_2| \sum_{p_3...p_N} \sum_{i_1 i_2...i_n} \sum_{j_1 j_2...j_N} \sum_{m_1 m_2} \sum_{n_1 n_2} \alpha^{(1)}_{i_1 j_1} \alpha^{(2)}_{i_2 j_2} \ldots \alpha^{(N)}_{i_N j_N}$$

$$\xi^{m_1 m_2 p_3...p_N}_{i_1 i_2...i_N}(t) \left(\xi^{n_1 n_2 p_3...p_N}_{j_1 j_2...j_N}(t)\right)^* |m_1\rangle |m_2\rangle \langle n_1| \langle n_2| \hat{\mathcal{O}}_{12} |p_1\rangle |p_2\rangle$$

$$\text{(B.10)}$$

$$\implies \left\langle \hat{\mathcal{O}}_{12}\hat{\rho}_{12}(t)\right\rangle_{12} = \sum_{p_1...p_N} \sum_{i_1 i_2...i_n} \sum_{j_1 j_2...j_N} \sum_{m_1 m_2} \sum_{n_1 n_2} \alpha^{(1)}_{i_1 j_1} \alpha^{(2)}_{i_2 j_2} \ldots \alpha^{(N)}_{i_N j_N}$$

$$\xi^{m_1 m_2 p_3...p_N}_{i_1 i_2...i_N}(t) \left(\xi^{n_1 n_2 p_3...p_N}_{j_1 j_2...j_N}(t)\right)^* \delta_{m_1 p_1} \delta_{m_2 p_2} \mathcal{O}^{n_1 n_2 p_1 p_2}_{12} \quad \text{(B.11)}$$

$$\implies \left\langle \hat{\mathcal{O}}_{12}\hat{\rho}_{12}(t)\right\rangle_{12} = \sum_{p_1...p_N} \sum_{i_1 i_2...i_n} \sum_{j_1 j_2...j_N} \sum_{n_1 n_2} \alpha^{(1)}_{i_1 j_1} \alpha^{(2)}_{i_2 j_2} \ldots \alpha^{(N)}_{i_N j_N}$$

$$\xi^{p_1...p_N}_{i_1 i_2...i_N}(t) \left(\xi^{n_1 n_2 p_3...p_N}_{j_1 j_2...j_N}(t)\right)^* \mathcal{O}^{n_1 n_2 p_1 p_2}_{12} \quad \text{(B.12)}$$

Now consider finding the expectation value of the operator $\hat{\mathcal{O}}_{12}$ without finding the

reduced density matrix of system 1 and 2, such that

$$\left\langle \hat{\mathcal{O}}_{12}\hat{\rho}(t)\right\rangle_{12...N} = \sum_{p_1...p_N} \langle p_1| \ldots \langle p_N| \sum_{i_1 i_2...i_n} \sum_{j_1 j_2...j_N} \sum_{m_1 m_2...m_N} \sum_{n_1 n_2...n_N} \alpha^{(1)}_{i_1 j_1} \alpha^{(2)}_{i_2 j_2} \ldots \alpha^{(N)}_{i_N j_N}$$

$$\xi^{m_1 m_2...m_N}_{i_1 i_2...i_N}(t) \left(\xi^{n_1 n_2...n_N}_{j_1 j_2...j_N}(t)\right)^* |m_1\rangle |m_2\rangle \ldots |m_N\rangle \langle n_1| \langle n_2| \ldots \langle n_N| \hat{\mathcal{O}}_{12} |p_1\rangle \ldots |p_N\rangle$$

$$\text{(B.13)}$$

$$\implies \left\langle \hat{\mathcal{O}}_{12}\hat{\rho}(t)\right\rangle_{12...N} = \sum_{p_1...p_N} \sum_{i_1 i_2...i_n} \sum_{j_1 j_2...j_N} \sum_{m_1 m_2...m_N} \sum_{n_1 n_2...n_N} \alpha^{(1)}_{i_1 j_1} \alpha^{(2)}_{i_2 j_2} \ldots \alpha^{(N)}_{i_N j_N}$$

$$\xi^{m_1 m_2...m_N}_{i_1 i_2...i_N}(t) \left(\xi^{n_1 n_2...n_N}_{j_1 j_2...j_N}(t)\right)^* \delta_{m_1 p_1} \ldots \delta_{m_N p_N} \left(\delta_{n_3 p_3} \ldots \delta_{n_N p_N}\right) \langle n_1| \langle n_2| \hat{\mathcal{O}}_{12} |p_1\rangle |p_2\rangle$$

$$\text{(B.14)}$$

$$\implies \left\langle \hat{\mathcal{O}}_{12}\hat{\rho}(t) \right\rangle_{12...N} = \sum_{p_1...p_N} \sum_{i_1 i_2...i_n} \sum_{j_1 j_2...j_N} \sum_{n_1 n_2} \alpha^{(1)}_{i_1 j_1} \alpha^{(2)}_{i_2 j_2} \ldots \alpha^{(N)}_{i_N j_N}$$

$$\xi^{p_1 p_2...p_N}_{i_1 i_2...i_N}(t) \left( \xi^{n_1 n_2 p_3...p_N}_{j_1 j_2...j_N}(t) \right)^* \mathcal{O}^{n_1 n_2 p_1 p_2}_{12} \tag{B.15}$$

Thus from comparing (B.12) and (B.14), we can see that to evaluate the expectation value of an operator in a certain subspace we do not need to trace over the remaining subsystems explicitly and all the influence from the interactions is accounted for consistently.

# Bibliography

[1] "Oscillator-field model of moving mirrors in quantum optomechanics", C. R. Galley, R. O. Behunin and B. L. Hu, Phys. Rev. A **87**, 043832 (2013).

[2] J. Kepler, De Cometis (1619).

[3] "A preliminary communication on the pressure of heat and light radiation", E. F. Nichols and G. F. Hull, Phys. Rev. **13**, 307 (1901) .

[4] "Untersuchungen über die Druckkräfte des Lichtes", P. Lebedew, Ann. Phys. **311**, 433 (1901).

[5] "Ponderomotive Effects of Electromagnetic Radiation", V. B. Braginsky and A. B. Manukin, Sov. Phys. JETP **25**, 653 (1967).

[6] "Investigation of Dissipative Ponderomotive Effects of Electromagnetic Radiation", V. B. Braginsky, A. B. Manukin and M. Y. Tikhonov, Sov. Phys. JETP **31**, 829 (1970).

[7] "Quantum singularities of a ponderomotive meter of electromagnetic energy", V. B. Braginsky Y. I. Vorontsov, and F. Ya. Khalili, Sov. Phys. JETP **46**, 705 (1977).

[8] R. Weiss, in *Sources of Gravitational Radiation*, edited by L. Smarr, (Cambridge Univ. Press, Cambridge, 1979).

[9] "Quantum-Mechanical Radiation-Pressure Fluctuations in an Interferometer", C. Caves, Phys. Rev. Lett. **45**, 75 (1980).

[10] "Optical Bistability and Mirror Confinement Induced by Radiation Pressure", A. Dorsel, J. D. McCullen, P. Meystre, E. Vignes and H. Walther, Phys. Rev. Lett. **51**, 1550 (1983).

[11] "Acceleration and Trapping of Particles by Radiation Pressure", A. Ashkin, Phys. Rev. Lett. **24**, 156 (1970).

[12] "Trapping of Atoms by Resonance Radiation Pressure", A. Ashkin, Phys. Rev. Lett. **40**, 729 (1978).

[13] "Cooling of gases by laser radiation", T. Hänsch and A. Schawlow, Opt. Comm. **13**, 68 (1975).

[14] "Proposed $10^{14}$ D$\nu < \nu$ Laser Fluorescence Spectroscopy on Tl+ Mono-Ion Oscillator III (side band cooling)", D. Wineland and H. Dehmelt, Bull. Am. Phys. Soc. **20**, 637 (1975).

[15] "Quantum ground state and single-phonon control of a mechanical resonator", A. D. O'Connell, M. Hofheinz, M. Ansmann, Radoslaw C. Bialczak, M. Lenander, Erik Lucero, M. Neeley, D. Sank, H. Wang, M. Weides, J. Wenner, John M. Martinis and A. N. Cleland, Nature **464**, 697 (2010).

[16] "Laser cooling of a nanomechanical oscillator into its quantum ground state", Jasper Chan, T. P. Mayer Alegre, Amir H. Safavi-Naeini, Jeff T. Hill, Alex Krause, Simon Gröblacher, Markus Aspelmeyer and Oskar Painter, Nature **478**, 89 (2011).

[17] "Cavity optomechanics", M. Aspelmeyer, T. J. Kippenberg and F. Marquardt, Rev. Mod. Phys. **86**, 1391 (2014).

[18] "A short walk through quantum optomechanics", P. Meystre, Annalen der Physik **525**, 215 (2013).

[19] "Trend: Optomechanics", Marquardt, F., and S. M. Girvin, Physics **2**, 40 (2009).

[20] Markus Aspelmeyer, Tobias J. Kippenberg, Florian Marquardt, *Cavity Optomechanics: Nano- and Micromechanical Resonators Interacting with Light*, Springer (2014).

[21] "Quantum-coherent coupling of a mechanical oscillator to an optical cavity mode", E. Verhagen, S. Delèglise, S. Weis, A. Schliesser and T. J. Kippenberg, Nature **482**, 63 (2012).

[22] "Squeezed light from a silicon micromechanical resonator", Amir H. Safavi-Naeini, Simon Gröblacher, Jeff T. Hill, Jasper Chan, Markus Aspelmeyer and Oskar Painter, Nature **500**, 185 (2013).

[23] "Non-classical light generated by quantum-noise-driven cavity optomechanics", Daniel W. C. Brooks, Thierry Botter, Sydney Schreppler, Thomas P. Purdy, Nathan Brahms and Dan M. Stamper-Kurn, Nature **488**, 476 (2012).

[24] "Coherent state transfer between itinerant microwave fields and a mechanical oscillator", T. A. Palomaki, J. W. Harlow, J. D. Teufel, R. W. Simmonds and K. W. Lehnert, Nature **495**, 210 (2013).

[25] "Entangling Mechanical Motion with Microwave Fields", T. A. Palomaki, J. D. Teufel, R. W. Simmonds and K. W. Lehnert, Science **342**, 710 (2013).

[26] "Quantum squeezing of motion in a mechanical resonator", E. E. Wollman, C. U. Lei, A. J. Weinstein, J. Suh, A. Kronwald, F. Marquardt, A. A. Clerk and K. C. Schwab, , arXiv:1507.01662 (2015).

[27] "A gravitational wave observatory operating beyond the quantum shot-noise limit", The LIGO Scientific Collaboration, Nat Phys **7**, 962 (2011).

[28] "Radiation-pressure cooling and optomechanical instability of a micromirror", O. Arcizet, P. F. Cohadon, T. Briant, M. Pinard and A. Heidmann, Nature **444**, 71 (2006).

[29] "Sub-kelvin optical cooling of a micromechanical resonator", D. Kleckner and D. Bouwmeester, Nature **444**, 75 (2006).

[30] "Radiation-pressure self-cooling of a micromirror in a cryogenic environment", S. Gröblacher, S. Gigan, H. R. Böhm, A. Zeilinger and M. Aspelmeyer, Europhysics Letters, **81**, 54003 (2008).

[31] "Observation of strong coupling between a micromechanical resonator and an optical cavity field", S. Gröblacher, K. Hammerer, M. R. Vanner and M. Aspelmeyer, Nature **460**, 724 (2009).

[32] "An All-Optical Trap for a Gram-Scale Mirror", T. Corbitt, Y. Chen, E. Innerhofer, H.Muller-Ebhardt, D.Ottaway, H. Rehbein, D. Sigg, S.Whitcomb, C.Wipf, and N.Mavalvala, Phys. Rev. Lett. **98**, 150802 (2007).

[33] "Modeling Dispersive Coupling and Losses of Localized Optical and Mechanical Modes in Optomechanical Crystals", M. Eichenfield, J. Chan, A. H. Safavi-Naeini, K. J. Vahala, and O. Painter, Opt. Express **17**, 20078 (2009).

[34] A. H. Safavi-Naeini and O. Painter, "Cavity optomechanics - nano- and micromechanical resonators interacting with light", (Springer, 2014) Chap. 10 Optomechanical Crystal Devices.

[35] "Fabrication and coupling to planar high-Q silica disk microcavities", T. J. Kippenberg, S. M. Spillane, D. K. Armani, and K. J. Vahala, Applied Physics Letters **83**, 797 (2003).

[36] "High Frequency GaAs Nano-Optomechanical Disk Resonator", L. Ding, C. Baker, P. Senellart, A. Lemaitre, S.Ducci, G. Leo, and I. Favero, Phys. Rev. Lett. **105**, 263903 (2010).

[37] "Synchronization of micromechanical oscillators using light", M. Zhang, G. S. Wiederhecker, S. Manipatruni, A. Barnard, P. McEuen, and M. Lipson, Phys. Rev. Lett. **109**, 233906 (2012).

[38] "Tunable optical coupler controlled by optical gradient forces", X. Sun, K. Y. Fong, C. Xiong, W. H. P. Pernice, and H. X. Tang, Opt. Express **19**, 22316 (2011).

[39] "Photonic Micro-Electromechanical Systems Vibrating at X-band (11-GHz) Rates", M. Tomes and T. Carmon, Phys. Rev. Lett. **102**, 113601 (2009).

[40] "Resolved-sideband and cryogenic cooling of an optomechanical resonator", Y.-S. Park and H. Wang, Nat Phys **5**, 489 (2009).

[41] A. Schliesser and T. J. Kippenberg, "Cavity optomechanics - nano- and micromechanical resonators interacting with light", (Springer, 2014) Chap. 6 Cavity Optomechanics with Whispering-Gallery-ModeMicroresonators.

[42] "Sideband cooling of micromechanical motion to the quantum ground state", J. D. Teufel, T. Donner, D. Li, J. W. Harlow, M. S. Allman, K. Cicak, A. J. Sirois, J. D. Whittaker, K.W. Lehnert, and R.W. Simmonds, Nature **475**, 359 (2011).

[43] "Back-action Evading Measurements of Nanomechanical Motion", J. B. Hertzberg, T. Rocheleau, T. Ndukum, M. Savva, A. A. Clerk, and K. C. Schwab, Nat. Phys. **6**, 213 (2010).

[44] K. W. Lehnert, "Cavity optomechanics - nano- and micromechanical resonators interacting with light", (Springer, 2014) Chap. 11 Introduction toMicrowave Cavity Optomechanics.

[45] "Cavity optomechanics with cold atoms", D. M. Stamper-Kurn, arXiv: 1204.4351v1 (2012).

[46] "Cavity optomechanics with a Bose-Einstein condensate", F. Brennecke, S. Ritter, T. Donner, T. Esslinger, Science **10**, 322, 235 (2008).

[47] "Role Reversal in a Bose-Condensed Optomechanical System", K. Zhang, P. Meystre, and W. Zhang, Phys. Rev. Lett. **108**, 240405 (2012).

[48] "Observation of quantum-measurement backaction with an ultracold atomic gas", K.W.Murch, K. L.Moore, S. Gupta, and D. M. Stamper-Kurn, Nat. Phys. **4**, 561 (2008).

[49] "Realization of an optomechanical interface between ultracold atoms and a membrane", S. Camerer, M. Korppi, A. Jöckel, D. Hunger, T. W. Hansch, and P. Treutlein, Phys. Rev. Lett. **107**, 223001 (2011).

[50] "Sympathetic cooling of a membrane oscillator in a hybrid mechanical-atomic system", Andreas Jöckel, Aline Faber, Tobias Kampschulte, Maria Korppi, Matthew T. Rakher and Philipp Treutlein, Nature Nanotechnology **10**, 55 (2015).

[51] "Tunable cavity optomechanics with ultracold Atoms", T. P. Purdy, D. W. C. Brooks, T. Botter, N. Brahms, Z.-Y. Ma, and D. M. Stamper-Kurn, Phys. Rev. Lett. **105**, 133602 (2010).

[52] "Quantum-state transfer between a Bose-Einstein condensate and an optomechanical mirror", S. Singh, H. Jing, E. M. Wright, and P. Meystre, Phys. Rev. A **86**, 021801 (2012).

[53] "Motion of atoms in a radiation trap", J. P. Gordon and A. Ashkin, Phys. Rev. A **21**,1606 (1980).

[54] "Dressed-atom approach to atomic motion in laser light: the dipole force revisited", J. Dalibard and C. Cohen-Tannoudji, J. Opt. Soc. Am. B **2**,1707 (1985).

[55] "Doppler Optomechanics of a Photonic Crystal", K. Karrai, I. Favero and C. Metzger, Phys. Rev. Lett., **100**, 240801 (2008).

[56] "Optical cavity cooling of mechanical modes of a semiconductor nanomembrane", K. Usami, A. Naesby, T. Bagci, B. Melholt Nielsen, J. Liu, S. Stobbe, P. Lodahl and E. S. Polzik, Nat. Phys. **8**, 168 (2012).

[57] "Exciton-mediated photothermal cooling in GaAs membranes", A. Xuereb, K. Usami, A. Naesby, E. S. Polzik and K. Hammerer, New J. Phys. **14**, 085024 (2012).

[58] "Optomechanical systems: Hot electrons but cool vibrations", A. Armour, Nat. Phys. **8**, 110 (2012).

[59] "Preparation of nonclassical states in cavities with a moving mirror", S. Bose, K. Jacobs, and P. L. Knight, Phys. Rev. A **56**, 4175 (1997).

[60] "Ponderomotive control of quantum macroscopic coherence", S. Mancini, V. I. Man'ko, and P. Tombesi, Phys. Rev. A **55**, 3042 (1997).

[61] "Scheme to probe the decoherence of a macroscopic object", S. Bose, K. Jacobs, and P. L. Knight, Phys. Rev. A **59**, 3204 (1999).

[62] "Creating and Probing Multipartite Macroscopic Entanglement with Light", M. Paternostro, D. Vitali, S. Gigan, M. S. Kim, C. Brukner, J. Eisert, and M. Aspelmeyer, Phys. Rev. Lett. **99**, 250401 (2007).

[63] "Optomechanical Entanglement between a Movable Mirror and a Cavity Field", D. Vitali, S. Gigan, A. Ferreira, H. R. Bohm, P. Tombesi, A. Guerreiro, V. Vedral, A. Zeilinger, and M. Aspelmeyer, Phys. Rev. Lett. **98**, 030405 (2007).

[64] "Universal quantum entanglement between an oscillator and continuous fields", H. Miao, S. Danilishin and Y. Chen, Phys. Rev. A **81**,052307 (2010).

[65] "Towards Quantum Superpositions of a Mirror", W. Marshall, C. Simon, R. Penrose, and D. Bouwmeester, Phys. Rev. Lett. **91**, 130401 (2003).

[66] "Reduction of a wave packet in quantum Brownian motion", W. G. Unruh and W. H. Zurek, Phys. Rev. D **4**, 1071 (1989).

[67] G. Barton and A. Calogeracos, Ann. Phys. **238**, 227 (1995). A. Calogeracos and G. Barton, Ann. Phys. **238**, 268 (1995).

[68] "Interaction between a moving mirror and radiation pressure: A Hamiltonian formulation", C. K. Law, Phys. Rev. A **51**, 2537 (1995).

[69] "Mechanical Response of Vacuum", R. Golestanian and M. Kardar, Phys. Rev. Lett. 78, 3421 (1997); "Path-integral approach to the dynamic Casimir effect with fluctuating boundaries", Phys. Rev. A 58, 1713 (1998).

[70] "Scattering theory of cooling and heating in optomechanical systems", André Xuereb, Peter Domokos, János Asbóth, Peter Horak and Tim Freegarde, Phys. Rev. A **79**, 053810 (2009).

[71] "Optomechanical coupling in a one-dimensional optical lattice", J. K. Asbóth, H. Ritsch and P. Domokos, Phys. Rev. A **77**, 063424 (2008).

[72] "Strong Coupling and Long-Range Collective Interactions in Optomechanical Arrays", A. Xuereb, C. Genes, A. Dantan, Phys. Rev. Lett. **109**, 223601 (2012).

[73] "Theoretical Analysis of Mechanical Displacement Measurement Using a Multiple Cavity Mode Transducer", J. M. Dobrindt and T. J. Kippenberg, Phys. Rev. Lett. **104**, 033901 (2010).

[74] R. O. Behunin, *Nonequilibrium Quantum Fluctuation Forces*, Doctoral Thesis, University of Maryland, College Park (2010).

[75] "The Lorentz Force and the Radiation Pressure of Light", T. Rothman and S. Boughn, Am. J. Phys. **77**, 122 (2009).

[76] "Moving atom-field interaction: Quantum motional decoherence and relaxation", S. Shresta and B. L. Hu, Phys. Rev. A **68**, 012110 (2003).

[77] "Moving atom-field interaction: Correction to the Casimir-Polder effect from coherent backaction", S. Shresta, B. L. Hu, and Nicholas G. Phillips, Phys. Rev. A **68**, 062101 (2003).

[78] "Stochastic theory of accelerated detectors in a quantum field", A. Raval, B. L. Hu, and J. Anglin, Phys. Rev. D **53**, 7003 (1996).

[79] "Does a Uniformly Accelerated Quantum Oscillator Radiate?", D. J. Raine, D. W. Sciama, P. G. Grove, Proc. R. Soc. Lond. A, **435**, 1893, 205-215 (1991).

[80] "Motion of a mirror under infinitely fluctuating quantum vacuum stress", Q. Wang and W. G. Unruh, Phys. Rev. D **89**, 085009 (2014).

[81] "Will small particles exhibit Brownian motion in the quantum vacuum?", G. Gour and L. Sriramkumar, Found. Phys. **29**, 1917 (1999).

[82] "Quantum fluctuations of mass for a mirror in vacuum", M. T. Jaekel and S. Reynaud, Phys. Lett. A **180**, 9 (1993).

[83] N. D. Birrell and P. C. W. Davies, *Quantum Fields in Curved Space* (Cambridge University Press, Cambridge, England, 1984).

[84] "Nonadiabatic optomechanical Hamiltonian of a moving dielectric membrane in a cavity", H. K. Cheung and C. K. Law, Phys. Rev. A **84**, 023812 (2011).

[85] N. W. Ashcroft and N. D. Mermin, *Solid State Physics* (Saunders, 1976).

[86] "Diamond photonic crystal slab: Leaky modes and modified photolumi-nescence emission of surface-deposited quantum dots", Lukáš Ondič, Oleg Babchenko, Marián Varga, Alexander Kromka, Jiří Čtyroký and Ivan Pelant, Sci. Rep. **2**, 914 (2012).

[87] "On the attraction between two perfectly conducting plates", H. B. G. Casimir, Proc. Kon. Nederland. Akad. Wetensch. **51**, 793 (1948).

[88] "Radiation pressure from the vacuum: Physical interpretation of the Casimir force", P. W. Milonni, R. J. Cook, and M. E. Goggin, Phys. Rev. A **38**, 1621 (1988).

[89] "*Colloquium*: Stimulating uncertainty: Amplifying the quantum vacuum with superconducting circuits", P. D. Nation, J. R. Johansson, M. P. Blencowe and F. Nori, (2012).

[90] "Quantum Theory of the Electromagnetic Field in a Variable-Length One-Dimensional Cavity", G. T. Moore, J. Math. Phys. **11**, 2679 (1970).

[91] "Radiation from a Moving Mirror in Two Dimensional Space-Time: Conformal Anomaly", S. A. Fulling and P. C. W. Davies, Proc. R. Soc. London, Ser. A **348**, 393 (1976).

[92] "Observation of the dynamical Casimir effect in a superconducting circuit", C.M. Wilson, G. Johansson, A. Pourkabirian, M. Simoen, J.R. Johansson, T. Duty, F. Nori and P. Delsing, Nature **479**, 376 (2011).

[93] "Observation of Radiation Pressure Shot Noise on a Macroscopic Object", T. P. Purdy, R. W. Peterson and C. A. Regal, Science **339**, 801 (2013).

[94] "Macroscopic quantum mechanics: theory and experimental concepts of op-tomechanics", Y. Chen, J. Phys. B **46**, 104001 (2013).

[95] "Cavity cooling of a single atom", P. Maunz, T. Puppe, I. Schuster, N. Syassen, P. W. H. Pinkse and G. Rempe, Nature, **428**, 50 (2004).

[96] P. Maunz, *Cavity cooling and spectroscopy of a bound atom-cavity system*, Doctoral Thesis, Max-Planck-Institut für Quantenoptik (2005).

[97] "Casimir forces on atoms in optical cavities", A. M. Alhambra, A. Kempf, and E. Martin-Martinez, Phys. Rev. A **89**, 033835 (2014).

[98] "Quantum mechanical pure states with gaussian wave functions", B. L. Schumaker, Phys. Rep. **135**, 317 (1986).

[99] "Disentanglement of two harmonic oscillators in relativistic motion", S.-Y. Lin, C.-H. Chou and B. L. Hu, Phys. Rev. D **78**, 125025 (2008).

[100] "Computable measure of entanglement", G. Vidal and R. F. Werner, Phys. Rev. A **65**, 032314 (2002).

[101] "Peres-Horodecki Separability Criterion for Continuous Variable Systems", R. Simon, Phys. Rev. Lett. **84**, 2726 (2000); "Inseparability Criterion for Continuous Variable Systems", L.-M. Duan, G. Giedke, J. I. Cirac, and P. Zoller, Phys. Rev. Lett. **84**, 2722 (2000).

[102] "Logarithmic Negativity: A Full Entanglement Monotone That is not Convex", M. B. Plenio, Phys. Rev. Lett. **95**, 090503 (2005).

[103] "Casimir force between partially transmitting mirrors", M. T. Jaekel and S. Reynaud, Journal de Physique I, **1** 1395 (1991).

[104] "Accelerated detector-quantum field correlations: From vacuum fluctuations to radiation flux", S.-Y. Lin and B. L. Hu, Phys. Rev. D **73**, 124018 (2006)

[105] "Temporal and spatial dependence of quantum entanglement from a field theory perspective", S.-Y. Lin and B. L. Hu, Phys. Rev. D **79**, 085020 (2009)

[106] "Models of wave-function collapse, underlying theories, and experimental tests", Angelo Bassi, Kinjalk Lochan, Seema Satin, Tejinder P. Singh, and Hendrik Ulbricht, Rev. Mod. Phys. **85**, 471 (2013).

[107] "Entangled mechanical oscillators", J. D. Jost, J. P. Home, J. M. Amini, D. Hanneke, R. Ozeri, C. Langer, J. J. Bollinger, D. Leibfried and D. J. Wineland, Nature, **459**, 683 (2009).

[108] "Steady State Entanglement in the Mechanical Vibrations of Two Dielectric Membranes", Michael J. Hartmann and Martin B. Plenio, Phys. Rev. Lett. **101**, 200503 (2008).

[109] "Entangling Macroscopic Oscillators Exploiting Radiation Pressure", Stefano Mancini, Vittrio Giovannetti, David Vitali and Paolo Tombesi, Phys. Rev. Lett. **88**, 120401 (2002).